UNIVERSITÀ DEGLI STUDI ROMA TRE

Variational approaches for electron-phonon interaction in strongly-correlated systems

Thesis submitted for the degree of

Doctor Philosophiæ

Ph. D. in Physics - XIX cycle

Supervisors:

Prof. *Roberto Raimondi*

Dr. *Massimo Capone*

Prof. *Claudio Castellani*

Candidate:

Paolo Barone

October 2006

Contents

Chapter 1

Introduction

In this work we will report our progress in developing variational approaches to the problem of electron-phonon (e-ph) interaction in strongly correlated systems, i.e. in those systems where screening is not effective enough and electrons experience a relevant residual short-range Coulomb repulsion. In this introductory chapter we discuss briefly the experimental findings that motivated our research and the reason why we believe that a variational scheme can prove useful to the understanding of the problem.

Generally speaking the interplay between lattice and electronic dynamics is always present in solids. Nevertheless in many materials, especially in conventional metals, electron screening is sufficiently effective, and electronic correlation effects are strongly suppressed; thus phonons substantially interact with almost independent quasiparticles and the e-ph coupling can be treated perturbativly in many relevant cases. This approach proved to be accurate for instance in the description of the temperature dependence of resistivity[1] or, most notably, in the identification of the pairing mechanism of conventional low-temperature superconductors. The latter is a combination of two effects: an overscreening effect due to the phonons, which mediate an effective attractive interaction between low-energy electrons, and the presence of a Fermi surface, which is ultimately responsible (through Pauli's exclusion principle) for the formation of stable Cooper pairs [2]. The observation that the attraction takes place only at small frequencies suggests that superconductivity should occur at very low temperatures, as also the experience suggested until 1986, when superconductivity with a high critical temperature T_c (HTSC) was observed in doped lanthanium-copper oxides[3]. These compounds turned out to belong to a whole class of materials (usually called cuprates) that display a rich and complex phenomenology, including also antiferromagnetic order and unconventional metallic properties, which could not be explained in the theoretical framework at disposal at that time. As it will be detailed below, cuprates are strongly correlated systems, i.e. systems in which the strenght of electron-electron (e-e) interactions is comparable to or larger than the kinetic energy and where physical properties can not be accounted for in a quasiparticle (Fermi-liquid) picture. On the other hand, even though their polar character (testified by different values of low- and high-frequency dielectric constants[4]) suggested a strong coupling

to lattice dynamics,[1] the e-ph interaction was initially ruled out as a possible mechanism for the high-temperature superconducting pairing. In fact a number of experiments seemed to contrast with the common wisdom concerning convential e-ph-induced superconductivity and led many people to consider different physical mechanisms; nonetheless it is worth reminding that the interpretation of those experimental findings was based on standard e-ph theory, not including the possibility of new effects due to the presence of strong e-e correlation. In recent years improvements in sample manipulations and experimental techniques, especially in Angle-Resolved Photoemission Spectroscopy (ARPES)[7], have revived the interest in the e-ph role in cuprates, since phonon signatures have been observed in many physical quantities, as we will detail in the following. Due to the strongly-correlated character of cuprates, interpretation of these findings require the development of a theory which is able to treat the simultaneous contributions of strong e-e interaction and non-negligible coupling with the lattice. A complete theory of this sort has not been formulated yet, and whether the e-ph coupling is relevant or not for the high-temperature superconductivity is therefore still an open question.

The issue of competing e-e and e-ph interactions is of much broader interest. Other transition metal oxides, such as the colossal magnetoresistive manganites[8] or the nickelates[9], display a rich phenomenology which is thought to be related to their complex lattice dynamics combined with other interaction mechanisms involving spin, charge and orbital degrees of freedom. Furthermore, in 1991 it was realized that fullerens (the large C_{60} molecules discovered in 1985 by Kroto[10]) could be arranged in alkali-doped compounds (fullerides) which display superconductivity at critical temperatures which are second only to the high T_c typical of cuprates[11]. In these systems many energy scales are similar (characteristic phonon energy $\omega_{ph} \lesssim$ bandwidth $W <$ electronic correlation U) and estimates of e-ph interaction suggest that they are in an intermediate coupling regime; this means on one hand that Migdal's theorem[12], which is usually considered in standard treatment of e-ph coupling, is not valid, and on the other hand that correlation effects should be duly taken into account. Indeed Capone *et al.*[13] showed in their analysis of a model for the fullerides that short-range Coulomb repulsion in combination with Jahn-Teller phonons can even enhance, for some value of the coupling constants, the superconducting pairing; this was rather unexpected and suggests that a whole new field in which competing different interactions are simultaneously active have to be investigated in order to understand properly fundamental effects.

Let us briefly mention at last the possible connections with the recently developed field of mesoscopics. During the last years, in fact, consistent improvements in microfabrication techniques have allowed to realize almost nanoscopic devices as quantum dots or ultrasmall metallic grains; such systems, besides their technological relevance, are proving to be an

[1] Actually Bednorz himself admitted in his Nobel lecture[5] that the search for high-T_c superconductivity in cuprates had followed the idea proposed by Chakraverty that polaron formation, due to strong e-ph coupling, could enhance superconducting pairing.[6]

excellent test field to directly probe and study the nature of electron correlations due to the unprecedented ability to resolve discrete energy levels[14]. Furthermore, when these microscopic devices are built up with single molecules or with organic compounds, molecular vibrations and their coupling to conducting electrons need to be included and are thought to compete in non-trivial ways with correlation-induced effects as the Coulomb-blockade or the Kondo effect[15]. Again, we believe that any contribution to the development of a general theoretical framework for the interplay of comparable e-e and e-ph interactions is nowadays extremely promising if not necessary.

It is beyond the scope of this thesis to review all the experimental details concerning materials that are often very different from each other. For this reason in the next section we will just give some recent result concerning the high-T_c superconductive cuprates and the possible relevance of the interplay between electronic correlations and lattice degrees of freedom in these systems; the last section of this introductory chapter will be devoted to some theoretical remarks.

1.1 Role of strong correlation and electron-phonon coupling in superconducting cuprates

Since their discovery in 1986 cuprates revealed a very rich phenomenology strongly dependent on temperature and chemical doping, as it can be seen in the schematic phase diagram for hole-doped compounds in Fig. 1.1. The undoped parent compounds are insulators with anti-

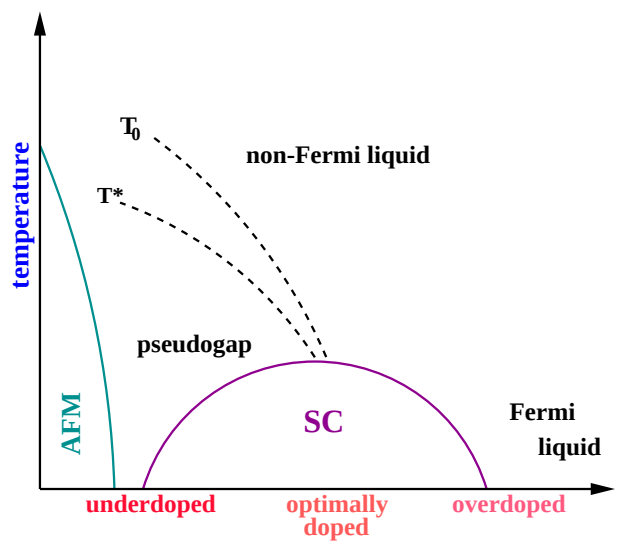

Figure 1.1: Schematic phase diagram of hole-doped cuprates; the antiferromagnetic phase is spread over a wider range for the electron-doped case, whereas the superconducting dome is smaller.

ferromagnetic order at low temperature; by introducing a finite ($\sim 5\%$) density of vacancies

a metallic character is observed in the normal state above T_c which however is found to be at odd with conventional Fermi-liquid metals up to relatively high ($\sim 15\%$) values of doping. At low temperatures antiferromagnetism is replaced by a superconductivity dome (the highest T_c defines the so-called optimally doped compounds). Despite the early experimental evidence for Cooper pairs in the superconducting phase of cuprates [5, 16], several differences have been observed with respect to convential superconductors, e.g. the $d-$wave rather than $s-$wave symmetry[17] of the pairing. Most notable is the pseudogap, i.e. a depression in the single-particle excitation spectrum with the same $d-$wave symmetry of the superconducting gap, observed in underdoped compounds above T_c[18].

The strongly correlated character of cuprates is a well-established fact. It is widely believed that the relevant physics occurs along the conducting planes made of copper and oxygen present in all the HTSC cuprates, while the 'out-of-plane' atoms serves essentially as a charge reservoir. In the undoped compounds copper has a valence +2, corresponding to a $3d^9$ electronic configuration which is splitted by the crystal field in five non-degenerate orbitals: the highest-energy one, which undergoes a hybridization with the $2p$ orbitals of neighbouring oxygens, is half-filled, hence, according to band theory, one should expect these compounds to have metallic character. The observed antiferromagnetic insulating phase can be understood only considering a residual short-range Coulomb repulsion experienced by electrons on Cu sites, which splits the $3d$ band in a completely filled lower band and in an empty upper band with an energy gap of the order of some eV[20]. This kind of physics is well captured in the most famous Hubbard model[21], where tight-binding electrons with hopping parameter t interact locally through a repulsive term U which makes the simultaneous presence of two electrons on a site energetically unfavourable. As reviewed in Ref. [19], the Hubbard interaction allows for the understanding of many experimental results, e.g. the transfer of spectral weight from high to low energy upon doping[20].

On the other hand a number of experiments testifies for a non negligible coupling with phonon modes. In the very beginning of the HTSC affaire, phonons were ruled out because it was thought that, in order to give the observed high T_c, the coupling strenght should have been such that structural instabilities could not be avoided[23]; furthermore in optimally-doped samples only a small isotope effect on the critical temperature was observed upon oxygen substitution[24], while above T_c the resistivity showed a linear behaviour with increasing temperature[25], in contrast with the common understanding of phonon contribution to the temperature dependence of resistivity[1]; both effects suggested a weak, if any, coupling with crystal degrees of freedom. Actually the situation is more complex and again depends crucially on doping; isotope coefficients on T_c are indeed small at optimal doping, but tend to increase as doping is reduced[26], in a region of the phase diagram where correlation effects are expected to play an important role. More interesting is the quite large isotope effect observed also in optimally-doped samples on the zero-temperature in-plane magnetic penetration depth, which can be connected to an isotope effect on the supercarrier effective mass[27], an effect absent in the Bardeen-Cooper-Schrieffer theory[28] for conventional superconduc-

tors. Direct observation of substantial phonon softening upon entering in the superconducting phase has been also made possible by neutron scattering measurements[29] suggesting, togheter with the appearence of Fano resonances in many phonon Raman spectra[30], a strong e-ph coupling.

The most striking and unusual signatures of possible e-ph interaction come however by ARPES measurements (for a recent review, see [7]). The energy-momentum dispersion curves along the nodal direction, i.e. where the superconducting gap is zero, show in fact an abrubt slope change in all HTSC cuprates. This kink has been observed in various hole-doped samples in a very similar energy-scale range (50-70 meV) even for systems with different gap energy, it is present above and below T_c and it covers the entire doping range, even if it is stronger in underdoped samples[31]. The origin of such a kink can be ascribed to a coupling between electrons and some bosonic mode, which is likely of phonon origin (magnetic resonance should be ruled out, being observed only in certain materials and below T_c). Actually a $O^{18} - O^{16}$ exchange experiment has been carried out in order to test the idea of e-ph coupling , and a strong isotope effect has been reported in nodal dispersion (see Fig. 1.2). From the conventional e-ph coupling one should have expected a small shift of phonon energy due to isotope exchange, while keeping most of the dispersion intact. Surprisingly, the low-energy dispersion is almost left unchanged by isotope substitution, while major effects appear for energies higher than the energy scale of the kink.

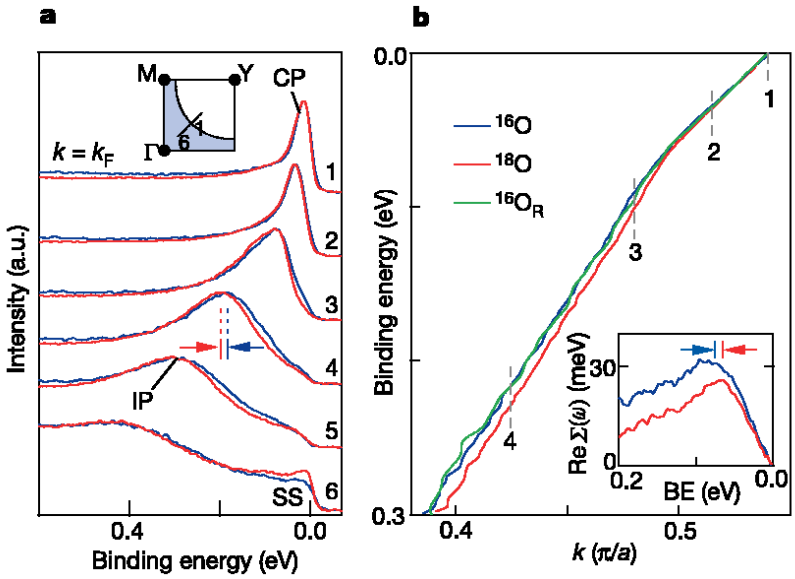

Figure 1.2: Isotope-induced in optimally doped $Bi_2Sr_2CaCu_2O_{8+\delta}$ in the superconducting phase[32]. In panel **a** raw Energy Dispersion Curves along the nodal direction, as sketched in the inset. Panel **b** shows the isotope effect in the nodal dispersion; low energy dispersion is nearly isotope-independent, as opposite to the high energy one. The effect is reversible by isotope re-substitution.

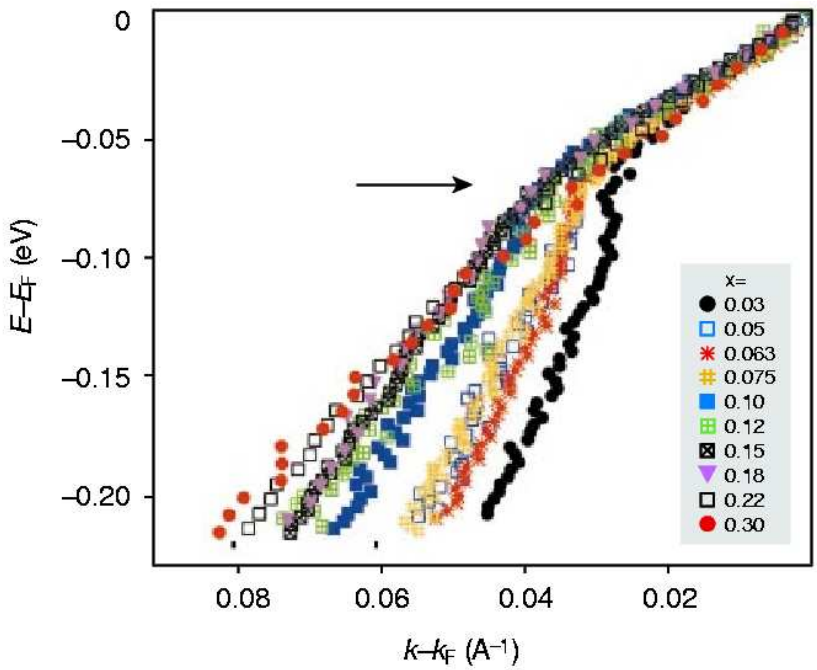

Figure 1.3: Doping dependence of the nodal electron dynamics in $La_{2-x}Sr_xCuO_4$[33]. The arrow indicates the position of kink that separates the high-energy and low-energy parts with different slopes.

Actually, this dichotomy between low and high energy features has been observed over the entire doping range, as depicted in Fig. 1.3, with an 'universal nodal Fermi velocity' behaviour for binding energies smaller than the energy scale of the kink, and strongly doping-dependent high-energy velocities, that can be extracted with a fitting procedure from the dispersion and are found to increase with decreasing hole concentration[33]. These findings cannot be explained by conventional theories for e-ph and e-e interaction. From the point of view of phonons, in a picture where e-ph coupling changes with doping but the 'bare band' does not, one should have expected an opposite dependence on doping, namely high energy features almost untouched and low energy ones strongly doping dependent. On the other hand, by considering e-e interaction, which gets stronger approaching the Mott insulator with decreasing doping, the expected effect should have been a depressed effective mass and enhanced velocity upon increasing doping, effect which is not seen in the low energy sector and that is exactly the opposite of the high energy findings in cuprates. These anomalies indicate potential deviations from standard theories and suggest a possible complex interplay between electron-phonon and electron-electron interaction which should be carefully addressed.

Another set of experimental measurements for undoped and slightly doped samples suggests that this interplay, including also the presence of correlation-induced antiferromagnetism, could play an important role. As it is well-known, the relevant model for the dynamics of charge carriers in an antiferromagnetic background is the $t-J$ model, which can

be viewed as an expansion for large U of the already mentioned Hubbard model, where mobility scale t is renormalized to scale $J \sim t^2/U$[34]. Although measured dispersions along the nodal direction in many parent compounds show agreement with the calculated ones[35], a few puzzles remain in the interpretation of ARPES data[36] when e-ph coupling is not considered, that can be resumed in Fig. 1.4. First, the width of the sharpest peak (A in fig 1.4) near $(\pi/2, \pi/2)$ has a width ($\sim 300\, meV$) that is comparable with the entire occupied bandwidth, much broader than that obtained from $t - J$ calculations and too much broad to be considered as a quasiparticle peak. Second, the experimentally exctracted chemical potential μ is located at $\sim$ 0.45 eV above the peak A, which then cannot be considered a quasiparticle peak. Actually Mishchenko and Nagaosa[37] showed that this problem can

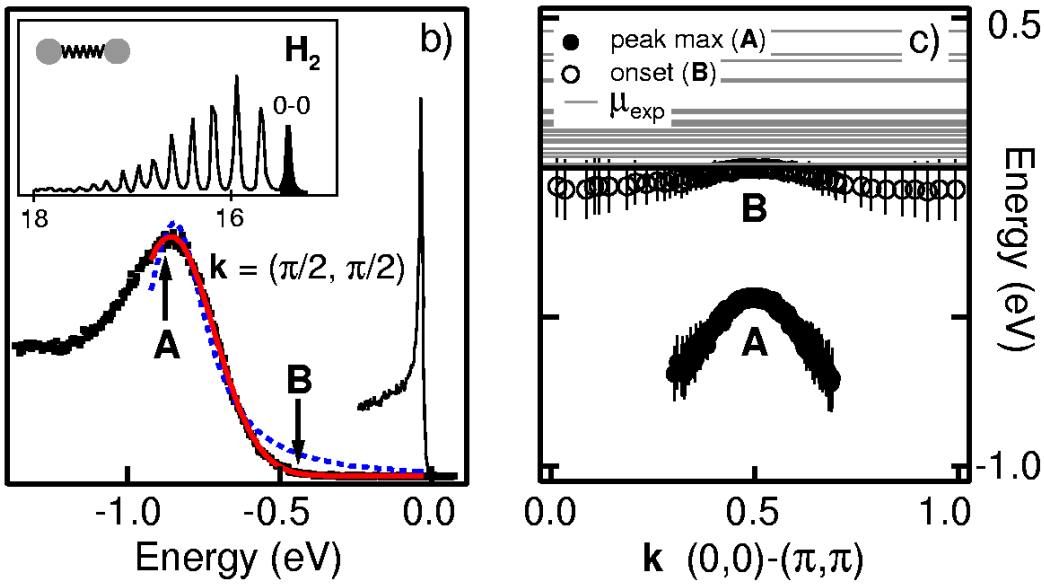

Figure 1.4: Photoemission spectrum of $Ca_2CuO_2Cl_2$ at $\mathbf{k} = (\pi/2, \pi/2)$. A and B denote the peak maximum and the onset of spectral weight, respectively. Comparison with Sr_2RuO_4 is shown in thin black, while the inset shows photoemission spectra from H_2. In panel **c** dispersion of A and B along $(0,0) - (\pi,\pi)$ is shown, togheter wit experimental values for μ.[36]

be resolved by considering the polaron effect, induced by strong e-ph coupling, in the $t - J$ model, as confirmed also by Rösch and Gunnarson[38]. In their analysis they showed that the quasiparticle peak has a vanishingly small residue Z and is then hidden in the tail of spectral intensity (B in Fig.1.4), while feature A is simply incoherent weight associated to 'shake-off' excitations whose center of mass corresponds to the motion of a hole in the background of frozen lattice configuration; this means, as shown in Fig. 1.5, that the dispersion of the hole remains that of the non-interacting limit, i.e. of the $t - J$ model without phonons, while the line-width broadens.

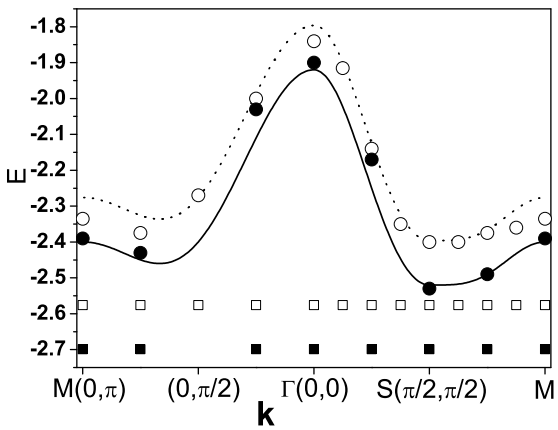

Figure 1.5: Dispersion of resonance energies in the $t-J$ model with e-ph coupling at $J/t = 0.3$ from Ref. [37] . Open and filled squared represent the lowest polaron resonance, which shows no momentum dependence, at two different values of the coupling, while the open and filled circles indicate the broad resonance; the solid curves are dispersions of a hole in the pure $t - J$ model.

1.2 Theoretical remarks on e-e and e-ph interactions

The problems of electron correlation and electron-phonon interaction in solid state physics represent a theoretical challenge even when considered separately, as the huge amount of works devoted to them since the half of the past century testifies. The main difficulty lies in their many-body character which can lead to collective behaviour not ascribible to the constituents of the solid (electrons or phonons) but to their mutual interactions. Analytical solutions are thus allowed only in some limiting cases where interactions are treated perturbatively. For example, when considering a solid in which the effective Coulomb repulsion between electrons is sizeably reduced by screening effects, the system of weakly-interacting particles can be safely mapped onto a gas of non-interacting quasiparticles with characteristic long life-time, and the e-e interaction is included as a small renormalization of the free parameters. Alternatively, one can start from the insulating atomic limit where each electron is tightly bound to an ion and introduce electronic motion as a perturbation. When no small parameter can be identified for such a perturbative approach, one has to resort to more complicated many-body techniques. On the other hand, even the problem of a single electron on a lattice in the presence of a sizeable e-ph coupling is already a many-body problem: the difficulty consists in describing the dressing of the electron by a coherent multiphonon cloud which moves coherently with it so as to form a quasiparticle, the polaron. Finally, when considering e-e and e-ph interactions as comparable, their interplay can lead to absolutely non-trivial outcomes; in this case one has to face an additional difficulty, which arises from the competition between the repulsive and instantaneous nature of the electronic correlation and the retarded and attractive effective interaction experienced by electrons due to the coupling

with lattice dynamics.

Many numerical methods have been developed in the context of strong correlation[39] and of polaronic physics[40], such as, among others, finite-clusters Exact Diagonalization (ED), Quantum Montecarlo (QMC), Numerical Renormalization Group (NRG), Density Matrix Renormalization Group (DMRG) and the semianalytic Dynamical Mean-Field Theory (DMFT), which have enormously contribute to the understanding of the phenomena involved. Nonetheless it is not unfair to say that the wealth of available analytical results has helped, with their more transparent physical insight, in the interpretation of numerical results. We believe, then, that the development of an approximate non-perturbative approach beside more accurate numerical techniques can be highly desirable in order to get an overall physical understanding of the problem. From this point of view variational approaches show some advantage, even though they can be safely applied only to get ground-state properties. The strength and the weakness of a variational approach lies generally in the choice of an appropriate trial wavefunction. This is a weakness because the chosen wavefunction can not contain all the relevant physics, leading to approximate or even wrong results. But it is also a strenght because it allows for a rather direct check of physical intuition.

In this thesis we discuss mainly two variational approaches for the electron-phonon coupling in the presence of strong correlation which were developed combining different methods, which are variational in nature, coming from the field of strongly correlated systems and of polaronic physics.

In **Chapter 2** we introduce the Hubbard-Holstein model, where e-e and e-ph interactions are introduced in the most transparent way, and discuss the main physical properties of the Hubbard and Holstein models taken separately; this discussion will allow us to identify the physical ingredients that must be included in a suitable theoretical description of the electron-phonon problem in strongly correlated systems, and will give us the chance to introduce the technical machinery we exploited in the development of our variational approaches.

Chapter 3 is devoted to the description of a variational approach based on an unitary transformation thanks to which phonons are ruled out from the outset and an effective model for correlated electrons is derived, where proper renormalizations of electronic parameters account for e-ph coupling effects. Our findings in the paramagnetic sector of the model are discussed and compared with available results.

Chapter 4 explores some limitations of the variational approach described in the previous chapter and paves the way to **Chapter 5**, where we present a proper generalization of the Gutzwiller technique able to describe simultaneously electronic and phononic ground-state properties. Results provided by both approaches are compared and eventually commented in the **Conclusions**.

Chapter 2

The Hubbard-Holstein model

2.1 General remarks on the choice of the model

The reference model for a strongly correlated system is the single-band Hubbard model[21] already mentioned in the introduction. The Hamiltonian is made by a tight-binding term, that favours electronic delocalization, and by a local term which accounts for the on-site Coulomb repulsion experienced by electrons with opposite spins, thus imposing a constraint on the electron motion. As it will be clarified in the next sections, the presence of these two competing terms in the Hubbard model accounts for the basic mechanism of the correlation-driven metal-insulator transition as initially proposed by Peierls[41] and Mott[42].

On the other hand, lattice dynamics and its interaction with electrons can be included in many different ways (cfr. Ref. [43]) according to the kind of physics one wants to describe. Throughout this work we will be concerned with perhaps the simplest electron-phonon model, where only Einsten dispersionless modes are considered to interact locally with the on-site electronic density. This model is generally referred to as the Holstein molecular crystal model[44] and it was originally proposed in order to study the so-called "self-trapping" localization of an electron in the short-range polarization field induced by the electron itself, as Landau initially suggested in 1933[45]. In fact, it captures the competition between the energy gain coming from the itineracy of electrons and that coming from the potential energy due to the electron-induced local deformations of the lattice.

The combination of these models is thought to be suitable for the understanding of the interplay between electronic correlation and electron-phonon interaction. The resulting model, usually called the Hubbard-Holstein model, represents clearly an oversimplified description of both e-e and e-ph interactions, but retains what are thought to be the relevant ingredients of a system in which electrons experience simultaneously an instantaneous short-range repulsion and a phonon-mediated retarded attraction. Actually, in spite of its formal simplicity, it is not exactly solvable even in one dimension and it displays a very rich phase diagram even when considering the paramagnetic phase without symmetry breaking. This is due to the interplay of different energy scales (electron mobility, electronic correlation, phonon charac-

teristic frequency, e-ph coupling) and to the associated large parameter space (that includes also the electron density and the temperature).

The experimental findings discussed in the introductory chapter has motivated in recent years a detailed study of the Hubbard-Holstein model. Many works have been devoted to the analysis of the renormalization of e-ph vertex function in the presence of strong correlation; this problem was addressed both by analytical tools (slave-boson approaches[46, 48, 49], Hubbard $X-$operators[47] and flow-equation approach[50]) and numerical QMC technique[51], revealing a strong momentum-dependent renormalization of the vertex function when large momenta are transferred, which could explain the lack of phonon features in transport properties observed in cuprates, and an enhancement of the phonon-mediated e-e attraction at low transferred momenta which could lead to $d-$wave superconductivity or charge instabilities. The possibility for a phase separation induced by the coexistence of strong e-e and e-ph couplings has indeed been investigated[52, 53, 54], and ground-state properties have been extensively studied in the paramagnetic sector, mainly exploiting numerical techniques. Among these, DMFT studies have provided detailed phase diagrams[55, 56] and informations about phonon-induced renormalization of the electron properties close to the Mott transition both in the half-filled regime[57, 58] and for small values of electron doping[59, 60]. Approximate approaches also have been proposed in order to analyze spectral properties of the Hubbard-Holstein model, based on a variational scheme[61] or on the Coherent Potential Approximation (CPA) relevant for large values of the e-e repulsion in the Mott insulating phase[62]. Very recently Sangiovanni *et al.*[63] have carried out a DMFT analysis in the antiferromagnetic sector, relevant for real correlated systems such the cuprates, which shows that antiferromagnetic correlations strongly enhance phonon-induced effects on the electron Green's function with respect to the paramagnetic phase, even though the e-ph interaction is moderately suppressed by the Coulomb interaction.

In summary, the Hubbard-Holstein model represents the simplest possible way to the study of non-trivial effects arising from the interplay between electron-electron interaction and electron-phonon coupling and it is expected to retain the relevant physics of real materials. Furthermore, thanks to the simple and intuitive way in which the competing interaction mechanisms are introduced and to the huge amount of accurate numerical results to compare with, it proves to be an excellent playground for the development of the variational approaches to be discussed. In the remainder of the chapter we will discuss in detail some properties of the e-e and e-ph interaction taken separately, introducing the reader to some early approach from which our following work will develop.

2.2 The e-e interaction in the Hubbard model

As mentioned in the previous section, the Hamiltonian of the Hubbard model consists of two terms, a tight-binding term H_t and a local repulsive term H_U, which in second quantization

read:

$$H_t = -t \sum_{\langle i,j \rangle, \sigma} c^\dagger_{i\sigma} c_{j\sigma}, \tag{2.1}$$

$$H_U = U \sum_i n_{i\uparrow} n_{i\downarrow}, \tag{2.2}$$

where $c_{i\sigma}$ ($c^\dagger_{i\sigma}$) is the annihilation(creation) operator at site i for spin-σ electrons, and $n_{i,\sigma} = c^\dagger_{i\sigma} c_{i\sigma}$ is the corresponding density operator. t represents the nearest-neighbour hopping, while the positive U is the on-site Hubbard repulsion. The hopping term accounts for the mobility of the tight-binding electrons, but it is useful to introduce the half-bandwidth D, whose expression in terms of t depends on dimensionality and on the lattice considered, as the scale for the electronic kinetic energy. On the other hand, the Hubbard U accounts for the energy an electron has to pay when it hops to an already occupied neighbouring site. Along the original proposals of Peierls[41] and Mott[42], one expects that when the repulsion is large with respect to the hopping amplitude (or, alternatively, to the kinetic energy scale of electrons) the system can turn insulating. Actually this locking effect is possible only when there are as many electrons as available lattice sites; when this condition is realized the system is said to be half filled, and the insulating phase is made of a collection of singly-occupied sites, no matter the spin state (paramagnetic Mott insulator). The relevant parameters are then:

- ► $n = \left\langle \frac{1}{L} \sum_{i\sigma} n_{i\sigma} \right\rangle$ - mean electron density per site;
- ► $u = \frac{U}{D}$ - degree of correlation.

It is worth noticing that, when considering the Hubbard model with nearest-neighbour hopping only in any bipartite lattice, the half-filling ground state is found to be insulating with antiferromagnetic order as soon as the repulsion U is different from zero[64]. The mechanism behind this transition is different from the Mott proposal and it was originally introduced by Slater[65] who proposed that a metal-insulator transition can be associated to an effective doubling of the unit cell due to antiferromagnetic ordering. Therefore the metal-insulator Mott transition can be hidden by antiferromagnetic correlations, unless a frustrating mechanism for antiferromagnetic ordering is included.

In any case, the Hubbard model represents a many-body problem which needs non-perturbative approaches to be solved. Actually the exact solution has been found only in one dimension[66], and a full description of the Mott transition has been attained only recently by means of the Dynamical Mean-Field Theory[39]. Early approaches were based on perturbative expansion around the limiting weak- and strong-coupling cases, and they necessarily lacked a complete understanding of the phenomenon, even though they described in a quite satisfactory way how the transition is reached from the two sides, thus giving access to important physical insight.

The first strong-coupling approach was proposed by Hubbard himself[21]. Starting from the insulating side, he introduced an effective band picture by which the density of states (DOS) of the insulator consists in two bands of width W centered at $\pm U/2$; the lower band is associated to holes, whereas the upper is associated to doubly-occupied sites, with a gap between them of the order of $U-W$. Decreasing the strength of the repulsion, the gap shrinks and it eventually closes when $U \approx W$. This closure of the gap signals the metal-insulator transition, as the two bands merge to give rise to a metal.

On the other hand, a scheme which approaches the metal-insulator transition from the metallic side was introduced by Brinkman and Rice[67] in 1970. They exploited the fact that

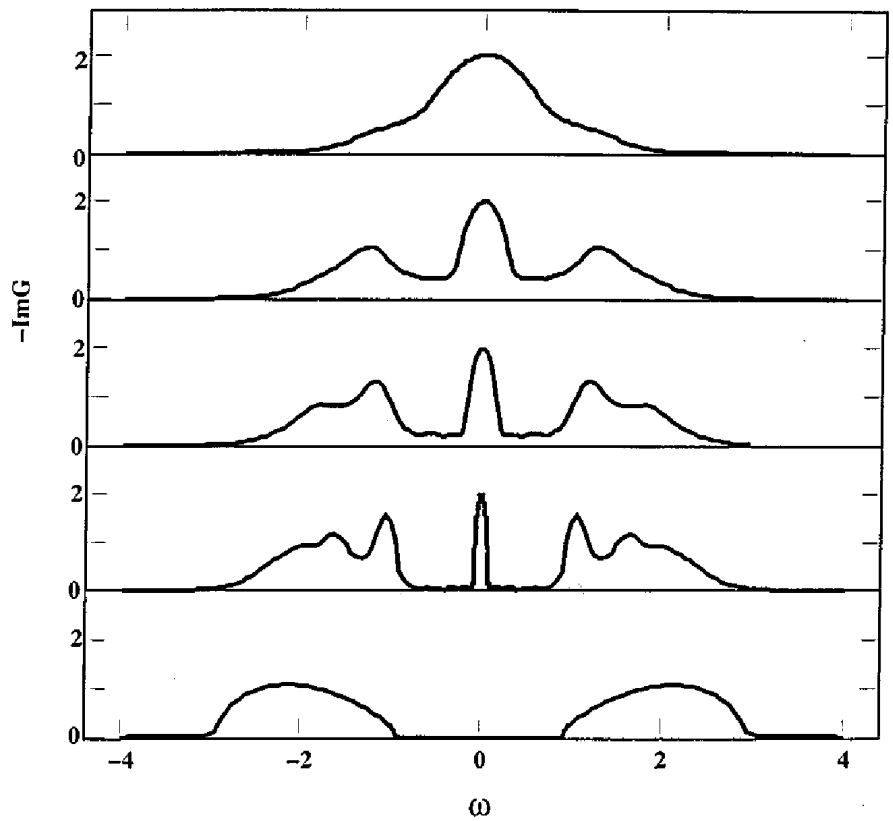

Figure 2.1: Density of states of the Hubbard model as computed in DMFT[39]. From top to bottom: evolution of the DOS for metallic solutions with increasing U, with the development of quasiparticle peak and high-energy incoherent bands, and characteristic DOS of the insulating phase (last panel).

the Hubbard term only acts when two electrons occupy the same site. By using the so-called Gutzwiller approximation[68] they showed that it is possible to project out these doubly-occupied states and to describe the metallic phase in terms of a Fermi liquid renormalized by U through the mean value of double occupancy $d = (1/L)\langle n_{i\uparrow} n_{i\downarrow}\rangle$. In the paramagnetic phase, due to the higher energy cost associated to the double occupancy, d decreases as U is increased

up to a critical value U_{BR} where d vanishes. The metal-insulator transition is associated in this approach by the divergence of the electronic effective mass $m^*/m \propto (U_{BR} - U)^{-1}$.

Thanks to Dynamical Mean-Field Theory, these two apparently different pictures were finally unified[39]. The essential idea of DMFT is to replace a lattice model by a single-site quantum impurity model embedded in an effective medium to be determined self-consistently. In this sense it can be viewed as a generalization to quantum many-body problems of classical mean-field theory, where the main difference lies in the fact that, even if spatial fluctuations are frozen as in the classic case, local quantum fluctuations (i.e. temporal fluctuations between the possible quantum states at a given lattice site) are fully taken into account. Therefore DMFT provides a unique nonperturbative framework which allows to treat metallic and insulating properties of the model on the same footing, unlike the earlier approaches previously sketched which move from the insulating or metallic side of the transition. Moving from the insulating side of the paramagnetic half-filled phase, the DMFT-computed DOS of the Hubbard model displays two high-energy features of width $\approx W = 2D$ centered at $\pm U/2$, which correspond to the lower and upper bands proposed by Hubbard; decreasing the strength of the repulsion, the gap between them shrinks and eventually closes when $U = U_{c1}$. On the

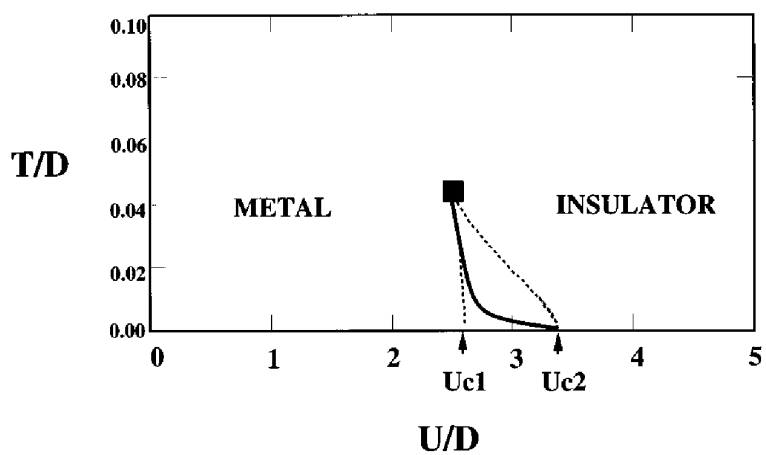

Figure 2.2: Phase diagram in the $U-T$ space for the single-band Hubbard model[39]. Dotted lines enclose a region in which metallic and insulating solutions coexist, solid line represents the first-order metal-insulator transition, which ends in two second-order critical points.

other hand, starting from the non-interacting limit and increasing U, a quasiparticle peak develops at low energies whose weight Z is related, in the DMFT framework, to the inverse of the effective mass; Z decreases as the Hubbard term strength increases, and the spectral weight lost by the coherent quasiparticle peak is transferred in two incoherent bands which develop at high energy. This metallic solution disappears at a critical value U_{c2}, when Z vanishes, i.e. when the effective mass diverges, and all the spectral weight has been conveyed in the incoherent Hubbard bands. Since U_{c1} is found to be smaller than U_{c2}, the metallic and insulating solutions coexist for $U_{c1} < U < U_{c2}$ and the stable phase must be determined

by comparing the corresponding energies. At $T = 0$ the metallic phase displays the lowest energy, hence the transition occurs for $U = U_{c2}$ and it is found to be second-order. At finite temperature a coexistence region is observed which ends up in a second-order critical point at a temperature which is approximatively 1/50 of the bandwidth W; the Mott transition occurs in this region and it is of first order, while above the critical temperature the metallic solution evolves smoothly in an insulating one.

In the next two sections we will describe in some detail the Gutzwiller variational approach and the more sophisticated slave-boson method which, as it will be detailed below, is equivalent to the first when considered at the mean-field level. Our following inclusion of the electron-phonon coupling in correlated systems will move from these approaches that were originally proposed and developed in the context of strongly-correlated physics.

2.2.1 The Gutzwiller approach

In his seminal work[68], Gutzwiller proposed a variational trial wavefunction where atomic configurations with large deviations from the average occupancy could be reduced with respect to a Hartree-Fock reference state, depending on the value of a variational parameter. To be more explicit, one starts from the non-interacting Slater determinant and variationally projects out doubly occupied sites, whose average number is expected to decrease by increasing the on-site repulsion U. Due to its many-body character, the evaluation of expectation values over the Gutzwiller wavefunction is still a complicated problem. Gutwiller himself introduced an approximate scheme to compute expectation values for the single-band Hubbard model, the so-called Gutzwiller approximation (GA)[68] that will be sketched below in the more physically transparent formulation given by Ogawa[69] (see also [70]); only in the late eighties anaylitical techniques were introduced that allow for exact computation in the one-dimensional case[71, 72] and in the limit of infinite dimensions[73]. For the latter case the Gutzwiller approximation coincides with the exact average over the Gutzwiller wavefunction.

Let's start from the uncorrelated ground-state of the Hamiltonian H_t in the paramagnetic sector, the Fermi sea given by:

$$|\Psi_0\rangle = \prod_{|k|<k_F} c^\dagger_{k\uparrow} c^\dagger_{k\downarrow} |0\rangle. \tag{2.3}$$

The trial wavefunction introduced by Gutzwiller is:

$$|\Psi_{GW}\rangle = \prod_i \big(1 - (1-g) n_{i\uparrow} n_{i\downarrow}\big) |\Psi_0\rangle = g^{\hat{D}} |\Psi_0\rangle, \tag{2.4}$$

where the $\hat{D}$ operator counts the number of doubly-occupied lattice sites and g is a variational parameter to be determined by minimization of the ground-state energy:

$$E_G = \frac{\langle \Psi_{GW} | H_t | \Psi_{GW}\rangle + \langle \Psi_{GW} |\ H_U | \Psi_{GW}\rangle}{\langle \Psi_{GW} | \Psi_{GW}\rangle}. \tag{2.5}$$

Let $L, N_\uparrow, N_\downarrow, D$ be the number of lattice points, up spins, down spins and doubly occupied sites respectively, and $n_\sigma = N_\sigma/L, d = D/L$. Being the number of doubly-occupied sites

the relevant quantity in this approach, one can express in a general way the Fermi sea as a combination of electronic configurations labelled by D:

$$|\Psi_0\rangle = \sum_D \sum_{\{j_d\}} A_{j_D} |\psi_{j_D}\rangle, \tag{2.6}$$

where $|\psi_{j_D}\rangle$ is a generic Fock state with a given number D of doubly-occupied sites, A_{j_D} is the related coefficient and the sums run over all the allowed values for D and over all the Fock states with given D. The Gutzwiller approximation consists now in neglecting the dependence of the matrix elements on spin configurations and spatial correlations, such that the motion of up-spin is essentially independent from the down-spin behaviour and viceversa: this allows to recast the problem of computing expectation values in a combinatorial way. The norm of the trial wavefunction reads

$$\langle \Psi_{GW} | \Psi_{GW} \rangle = \sum_D g^{2D} \, \overline{|A_{j_D}|^2}, \tag{2.7}$$

where $\overline{|A_{j_D}|^2} = N_D(L, N_\uparrow, N_\downarrow)\, P(L, N_\uparrow)\, P(L, N_\downarrow)$. is given simply by the product of N_D, the number of different spin configurations for D doubly-occupied sites with given $L, N_\uparrow, N_\downarrow$,

$$N_D(L, N_\uparrow, N_\downarrow) = \frac{L!}{(N_\uparrow - D)!\,(N_\downarrow - D)!\,D!\,(L - N_\uparrow - N_\downarrow + D)!}, \tag{2.8}$$

and $P(L, N_\sigma)$, the probability for a configuration of σ spins to occur (which are all equal and independent because spatial correlations are neglected):

$$P(L, N_\sigma) = \frac{1}{\binom{L}{N_\sigma}} \simeq n_\sigma^{N_\sigma} \, (1 - n_\sigma)^{L - N_\sigma}. \tag{2.9}$$

The expectation values of H_t, H_U are computed in the same spirit. Let's focus on the first one when only a spin-up particle is involved. Then one singles out two lattice sites between which the hopping process is supposed to occur and neglects what happens in the remaining lattice (no spatial correlations). There are four possible processes, sketched in Fig.2.3. Two of these correspond to the motion of an empty or a doubly-occupied site (Fig.2.3(a)) where the hopping process does not change the number D, whereas in fig 2.3(b) the empty and doubly-occupied site annihilate each other or are created, respectively. In the latter case D is changed by one, and the total interaction energy UD is modified. The environment of these processes is constituted by the remainder of the lattice (with $L-2$ sites) and the number N_D of spin configurations depends on the number of spins which are hopping between the selected sites. For example, in the first process in which only a spin-up particle is involved, one has $N_D(L-2, N_\uparrow - 1, N_\downarrow)$ and a matrix element equal to g^{2D} since the number of doubly-occupied sites of the total configuration is D in both initial and final state. Finally, the probability for finding any up-spin configuration in the environment is $P(L-2, N_\uparrow - 1)$, while one gets $P(L, N_\downarrow)$ because the down-spin configuration is left untouched. Extending this procedure to the four hopping processes one obtains:

$$\langle H_t \rangle = -q_\uparrow |\varepsilon_\uparrow| - q_\downarrow |\varepsilon_\downarrow|, \tag{2.10}$$

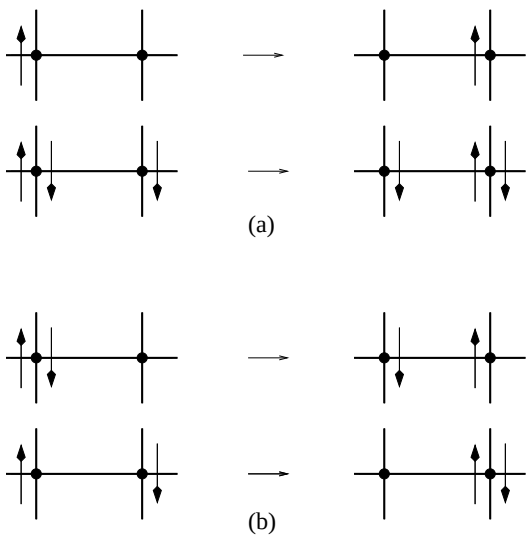

Figure 2.3: The four possible hopping processes for a spin-up particle in the Hubbard model. Processes (a) leave the number of doubly-occupied sites unchanged; processes (b) represent the 'polarization' of a medium of singly-occupied sites in terms of empty and doubly-occupied sites, changing D by one.

where $|\varepsilon_\sigma|$ is the average energy of σ-electrons in the uncorrelated case,

$$\varepsilon_\sigma = \frac{1}{L}\left\langle \Psi_0 \right| - t \sum_{\langle i,j\rangle,\sigma} c^\dagger_{i\sigma} c_{j\sigma} \left| \Psi_0 \right\rangle = \sum_{|k|<k_F} \varepsilon(k) < 0, \tag{2.11}$$

and q_σ's are renormalization parameters given by:

$$\begin{aligned} q_\sigma \;=\; & \sum_D g^{2D} \left[N_D(L-2, N_\sigma - 1, N_{-\sigma}) \,+\, g^2\, N_D(L-2, N_\sigma - 1, N_{-\sigma} - 2) \right. \\ & \left. +\, 2g\, N_D(L-2, N_\sigma - 1, N_{-\sigma} - 1) \right] \, P(L-2, N_\sigma - 1)\, P(L, N_{-\sigma}). \end{aligned} \tag{2.12}$$

Analogously the expectation value for the Hubbard term turns out to be:

$$\langle H_U \rangle = L \sum_D g^{2D+2}\, N_D(L-1, N_\uparrow - 1, N_\downarrow - 1)\, P(L, N_\uparrow)\, P(L, N_\downarrow). \tag{2.13}$$

In the thermodynamic limit only the largest terms in the sums are retained[69], and a somewhat tedious calculation allows to express the variational parameter g by the more physical $d = D/L$. The ground-state energy is at last:

$$\frac{E_G}{L} = -q_\uparrow(d, n_\uparrow, n_\downarrow)|\varepsilon_\uparrow| - q_\downarrow(d, n_\uparrow, n_\downarrow)|\varepsilon_\downarrow| + Ud, \tag{2.14}$$

with

$$q_\sigma = \frac{\left[\sqrt{(n_\sigma - d)\,(1 - n_\sigma - n_{-\sigma} + d)} \,+\, \sqrt{d\,(n_{-\sigma} - d)}\right]^2}{n_\sigma\,(1 - n_\sigma)}. \tag{2.15}$$

One can easily see that $q_\sigma = 1$ in the noninteracting paramagnetic system, where $n_\uparrow = n_\downarrow = n/2$ and $d = n^2/4$, and that that it decreases as soon the interaction is switched on; therefore the Gutzwiller approach, while treating the correlation term exactly, provides an effective description of the kinetic energy term, calculating its reduction due to the decrease of the doubly-occupied sites that follows from the presence of the on-site repulsive interaction, which makes hopping energetically unfavorable. To be more quantitative, we can choose the half-filling ($n = 1$) paramagnetic ($q_\uparrow = q_\downarrow \equiv q, \varepsilon_\uparrow = \varepsilon_\downarrow \equiv \varepsilon_0/2$) case, as proposed by Brinkman and Rice[67], and recast Eq.(2.15) in terms of d only:

$$q = 8\,d\,(1 - 2\,d). \tag{2.16}$$

By replacing it in the variational energy Eq.(2.14) and minimizing with respect to d, we find:

$$d = \frac{1}{4}\left[1 - \frac{U}{U_c}\right], \tag{2.17}$$

$$q = 1 - \left[\frac{U}{U_c}\right]^2, \tag{2.18}$$

$$\frac{E_G}{L} = -|\varepsilon_0|\left[1 - \frac{U}{U_c}\right]^2, \tag{2.19}$$

where $U_c = U_{BR} = 8|\varepsilon_0|$. The first of these formulas highlights the decrease of the number of doubly-occupied sites as U is increased, with a corresponding reduction of the kinetic energy. Furthermore they show that a critical U_c exists at which all the sites of the lattice are singly occupied ($d = 0$ and the number of electrons and lattice points coincide) by particles which are stuck to their sites ($q = 0$, hence the kinetic energy vanishes): this is the Gutzwiller picture of the paramagnetic Mott insulator. At the same time the energy vanishes smoothly, that means that the transition is second order; an undesired consequence of this finding is that the insulating phase cannot be described in the Gutzwiller approach, being all relevant quantities equal to zero. At last, as it will be clearer in the next section, the renormalization factor q can be identified with the inverse effective mass[67]; therefore in the present approach the Mott metal-insulator transition is driven by the divergence of m^*/m.

As the given formulation due to Ogawa[69] shows, the strongest approximation made by Gutzwiller is the neglect of spatial correlations and consequently of spin configurations in the evaluation of energy expectation values. In fact, while spin configurations with the same number of doubly-occupied sites all have the same expectation value for the interaction term, their expectation value for the kinetic energy will generally be different; therefore, while the first term is treated exactly, the kinetic term is approximated in a way which includes all possible hopping processes but neglects the environment where these hoppings take place.

Recently Bünemann and coworkers[74] have introduced an alternative formulation of the Gutzwiller variational technique which allow to extend the class of trial wavefunctions to multiband models and general on-site interactions (see also [75]). In this framework expectation values can be computed within a general graph formalism that allows for exact evaluations in infinite dimensions and for a controlled expansion in 1/d[76]. Because spatial

correlations become irrelevant when d$=\infty$, it is not surprising that the Gutzwiller approximation described above does not introduce any further approximation on the Gutzwiller wavefunction. As this formulation will prove useful in order to include e-ph coupling, here we will briefly sketch it.

For the trial wavefunction we use a general expression similar to Eq.(2.4),

$$|\Psi_{GW}\rangle = \prod_i \mathcal{P}_i |\Psi_0\rangle, \tag{2.20}$$

where $|\Psi_0\rangle$ is the Fermi sea and the Gutzwiller projector $g^{\hat{D}}$ is substituted with a general projection operator,

$$\mathcal{P}_i = \sum_l \lambda_l \, \hat{m}_{i;l} = \sum_l \lambda_l \, |l_i\rangle\langle l_i|, \tag{2.21}$$

where $\hat{m}_{i;l} = |l_i\rangle\langle l_i|$ projects the uncorrelated state on local configurations with given l electrons; λ_l, the relative weights for such states, have to be determined variationally. To be specific, in the single-band Hubbard model one has only $l = 0, 1, 2$, that means zero, one spin-up or spin-down and two electrons on a site i. As shown in Refs.[74, 76], there is a certain arbitrariness in the choice of the variational parameters λ's, related to the fact that any transformation acting on $|\Psi_0\rangle$ and involving operators of which $|\Psi_0\rangle$ is an eigenstate amounts simply to a multiplicative factor. This allows one to impose, without losing generality, the normalization condition

$$\langle\Psi_0|\mathcal{P}_i^2|\Psi_0\rangle = 1, \tag{2.22}$$

as well as an additional constraint on the single-particle density matrix,

$$\langle\Psi_0|\mathcal{P}_i c_{i\sigma}^\dagger c_{i\sigma'} \mathcal{P}_i|\Psi_0\rangle = \langle\Psi_0|c_{i\sigma}^\dagger c_{i\sigma'}|\Psi_0\rangle = \delta_{\sigma,\sigma'} \, \frac{n}{2}, \tag{2.23}$$

where the last equality stems from our choice of a paramagnetic uncorrelated $|\Psi_0\rangle$. The physical meaning of the variational parameters emerges by exploiting the fact that $P(l) = \langle\hat{m}_l\rangle = \lambda_l^2 P_0(l)$, from which [74]:

$$\lambda_l^2 = \frac{P(l)}{P_0(l)}, \tag{2.24}$$

where $P_0(l)$ and $P(l)$ represent the occupation probabilities of the $l-$electron configuration in the uncorrelated $|\Psi_0\rangle$ and correlated $|\Psi_{GW}\rangle$ wavefunctions. This allows one to recast the constraints Eqs.(2.22),(2.23) as:

$$P(0) + P(1) + P(2) = 1, \tag{2.25}$$

$$P(1) + 2P(2) = n. \tag{2.26}$$

Therefore, in this representation the correlated probability distribution is the variational quantity which has to be optimized.

When considering the infinite-dimensions limit, the on-site interaction is still well defined but the hopping parameter must be rescaled as $t = t'/\sqrt{\mathrm{d}}$ in order to obtain a finite kinetic energy and therefore a nontrivial model[73]. This scaling simplifies the computation

of expectation values as it turns out that the lowest order within a perturbation expansion in the parameters $(1-\lambda_l)$ is exact when d$=\infty$. In fact one can adopt a graph formalism to evaluate such expectation values, with lines representing the noninteracting one-particle density matrix

$$\mathbf{P}^0_\sigma(i,j) = \langle\Psi_0|c^\dagger_{i\sigma}\, c_{j\sigma}|\Psi_0\rangle, \tag{2.27}$$

and vertices representing the expansion parameters[73, 76]. In analogy with the diagrammatic representation of Green's functions, one may therefore define a "self-energy" as the sum of all one-particle irreducible diagrams where at least four lines meet at every internal vertex. This property comes from the absence of trivial loops at any vertex, due to the subtraction of Hartree contributions in the perturbative expansion of $\mathcal{P}_i$, that has been shown to lead to Eqs. (2.22),(2.23) (cfr. Refs. [76, 74]). We notice now that on a d-dimensional lattice, the scaling of the hopping parameter implies that for d $\gg 1$ $\mathbf{P}^0_\sigma(i,j) \simeq o\,((\sqrt{1/d})^\nu)$, where $\nu = |i-j| = \sum_{l=1}^{d} |i_l - j_l|$ is the so-called "Manhattan" metric which counts the number of nearest-neighbour steps from site i to site j on a d-dimensional lattice. Since there are always at least three separate paths from one vertex to another in the self-energy, this vanishes completely in infinite dimensions, and the Gutzwiller approximation, based on the neglect of spatial correlations, is found to give the exact result. In particular one finds that the expectation value of the hopping term reduces to:

$$\langle H_t\rangle = \sum_{\langle i,j\rangle,\sigma} \langle\Psi_0|\mathcal{P}_i\, c^\dagger_{i\sigma}\mathcal{P}_i\mathcal{P}_j c_{j\sigma}\mathcal{P}_j, |\Psi_0\rangle \tag{2.28}$$

as no contributions come from sites different than those involved in the hopping processes. Therefore creation of a spin-up particle on an empty site, for example, will generate in the present formalism a renormalization factor proportional to $\sqrt{P(1)P(0)}$.

One obtains then for the average variational energy per site in the paramagnetic sector (for technical details see [74]):

$$\frac{E_G}{L} = -q|\varepsilon| + U\,P(2), \tag{2.29}$$

$$q = \frac{2}{n(2-n)}\Big[\sqrt{P(1)P(0)} + \sqrt{P(2)P(1)}\Big]^2, \tag{2.30}$$

that has to be minimized taking into account the constraints Eqs. (2.25), (2.26). By identifying $P(2)$ with d, one is able to express the variational energy as a function of d and n only, and the result obtained in the GA framework is exactly recovered. To be more explicit, by putting $n=1$, one immediatly gets $P(0)=P(2)=d$, $P(1)=1-2d$ and $q = 8\,d\,(1-2d)$, which corresponds to the Brinkmann-Rice findings previously discussed.

2.2.2 The slave-boson technique

The slave-boson method is a very powerful tool developed in the context of strongly-correlated systems. In its original formulation it was meant to tackle the problem of a magnetic impurity

in a metallic environment, and consisted in replacing the on-site infinite correlation of the impurity (Anderson model) with a local constraint which was handled by standard field-theoretical methods[77, 78, 79]. Several slave-boson representations were thereafter proposed and applied to lattice systems such as the Hubbard or the related t-J models[80, 81, 82]. The basic idea of a slave-boson approach is to introduce some auxiliary fields which allow to decouple the correlation term and to keep track of the "backflow" of spin and density excitations of the medium that is expected when an electron hops in a strongly-correlated system. In the Kotliar-Ruckenstein proposal[80], this task is accomplished by introducing four projection operators that measure the occupation numbers in each of the four possible states available for hopping, in the same spirit of the Gutzwiller variational wavefunction. Actually, as we will see in the following, the results of the Gutzwiller approach can be obtained as a mean-field approximation in the framework of slave bosons.

Kotliar and Ruckenstein introduced four auxiliary fields, $e_i, p_{i\sigma}, d_i$, whose occupation numbers $e_i^\dagger e_i, p_{i\sigma}^\dagger p_{i\sigma}, d_i^\dagger d_i$ represent the projectors on the four possible electronic states on site i, namely empty, singly- and doubly-occupied configuration. They proposed the following correspondence between the initial representation of fermions $\{c_{i\sigma}\}$ and the new enlarged representation $\{\tilde{c}_{i\sigma}\} \otimes \{e_i, p_{i\sigma}, d_i\}$:

$$\begin{array}{lcl}
|0\rangle = |\tilde{0}\rangle & \mapsto & |1\rangle = e_i^\dagger\,|\tilde{0}\rangle \\
|\uparrow\rangle = c_{i\uparrow}^\dagger\,|\tilde{0}\rangle & \mapsto & |2\rangle = p_{i\uparrow}^\dagger\,\tilde{c}_{i\uparrow}^\dagger\,|\tilde{0}\rangle \\
|\downarrow\rangle = c_{i\downarrow}^\dagger\,|\tilde{0}\rangle & \mapsto & |3\rangle = p_{i\downarrow}^\dagger\,\tilde{c}_{i\downarrow}^\dagger\,|\tilde{0}\rangle \\
|\uparrow\downarrow\rangle = c_{i\uparrow}^\dagger\,c_{i\downarrow}^\dagger\,|\tilde{0}\rangle & \mapsto & |4\rangle = d_i^\dagger\,\tilde{c}_{i\uparrow}^\dagger\,\tilde{c}_{i\downarrow}^\dagger\,|\tilde{0}\rangle
\end{array}$$

with $|\tilde{0}\rangle$ the vacuum state in the enlarged Hilbert space.

In order to get rid of the unphysical states that the new representation introduces, one imposes the following constraints in the enlarged Fock space:

$$1 = \sum_\sigma p_{i\sigma}^\dagger p_{i\sigma} + d_i^\dagger d_i + e_i^\dagger e_i \quad \forall i, \tag{2.31}$$

$$0 = \tilde{c}_{i\sigma}^\dagger \tilde{c}_{i\sigma} - p_{i\sigma}^\dagger p_{i\sigma} - d_i^\dagger d_i \quad \forall i, \sigma. \tag{2.32}$$

The first constraint, Eq.(2.31), guarantees that the operators we introduced satisfy the algebra of projectors or equivalently, in terms of the bosonic slave particles, that no more and no less than one boson can sit on a given site; the second constraint Eq.(2.32), on the other hand, equates the two ways of counting the fermion occupancy of a given spin.

Let's see now how the processes of annihilation and creation of an electron can be described in the new representation. Consider for example a spin-up particle; because of Pauli's exclusion principle it can be created only on an empty or a spin-down singly-occupied site. In the first case one has to annihilate the 'empty' boson and to create a spin-up boson, while the fermionic character should be built in by the pseudofermion operator, $c_{i\uparrow}^\dagger \mapsto \tilde{c}_{i\uparrow}^\dagger\, p_{i\uparrow}^\dagger e_i$. Analogously, in the second case one gets $c_{i\uparrow}^\dagger \mapsto \tilde{c}_{i\uparrow}^\dagger\, d_i^\dagger p_{i\downarrow}$, as the boson which labels the

single spin-down state must be replaced by the boson that labels the doubly-occupied one. Therefore the following relations are found

$$c^\dagger_{i\sigma} \;\mapsto\; \tilde{c}^\dagger_{i\sigma}\,(\,p^\dagger_{i\sigma}\,e_i \,+\, d^\dagger_i\,p_{i,-\sigma}\,) \,=\, \tilde{c}^\dagger_{i\sigma}\,z^\dagger_{i\sigma}, \tag{2.33}$$

$$c_{i\sigma} \;\mapsto\; \tilde{c}_{i\sigma}\,(\,e^\dagger_i\,p_{i\sigma} \,+\, p^\dagger_{i,-\sigma}\,d_i\,) \,=\, \tilde{c}_{i\sigma}\,z_{i\sigma}, \tag{2.34}$$

which allow to recast the Hubbard Hamiltonian as:

$$H = -t \sum_{\langle i,j\rangle,\sigma} \tilde{c}^\dagger_{i\sigma}\tilde{c}_{j\sigma}\,z^\dagger_{i\sigma}\,z_{j\sigma} + U\sum_i d^\dagger_i d_i\,. \tag{2.35}$$

It is easily checked that as long as the constraints Eqs.(2.31),(2.32) are satisfied, the orginal Hamiltonian has the same matrix elements of Eq. (2.35) when computed in the physical subspace. Electrons are now decoupled and their interaction is expressed in terms of slave-boson operators. Furthermore the hopping operators $z^\dagger_{i\sigma}z_{j\sigma}$ just introduced keep track exactly of the four possible processes shown in Fig.2.3. Before going further, let us remark that the choice of $z^\dagger_{i\sigma}$ is not unique, and one can replace it by any combination $U_{i\sigma}z^\dagger_{i\sigma}V_{i\sigma}$ which leads to the same spectrum of the original Hamiltonian as long as the constraints are satisfied[1]. No approximations have been made until this point.

In order to calculate physical observables one can consider the partition function Z expressed as a functional integral over coherent states of Fermi and Bose fields. Since the constraints are preserved under time evolution[80], they can be enforced at each site by time-independent Lagrange multipliers. One gets:

$$\mathcal{Z} = \int \mathcal{D}\tilde{c}\,\mathcal{D}e\,\mathcal{D}p_\sigma\,\mathcal{D}d\prod_{i\sigma} d\lambda^{(1)}_i d\lambda^{(2)}_{i\sigma}\,\exp\Big[-\int_0^\beta \mathcal{L}(\tau)\,d\tau\Big], \tag{2.36}$$

where the Lagrangian $\mathcal{L}(\tau)$ is

$$\begin{aligned}\mathcal{L}(\tau) \;=\; & \sum_{\langle i,j\rangle\sigma} \tilde{c}^\dagger_{i\sigma}\Big[\big(\partial_\tau - \mu + \lambda^{(2)}_{i\sigma}\delta_{i,j}\big) \,-\, z^\dagger_{i\sigma}\,z_{j\sigma}t\Big]\tilde{c}_{j\sigma} \,+\, \sum_i e^\dagger_i\big(\partial_\tau + \lambda^{(1)}_i\big)e_i \,+ \\ & \sum_{i\sigma} p^\dagger_{i\sigma}\big(\partial_\tau + \lambda^{(1)}_i - \lambda^{(2)}_{i\sigma}\big)p_{i\sigma} \,+\, \sum_i d^\dagger_i\big(\partial_\tau + \lambda^{(1)}_i - \sum_\sigma \lambda^{(2)}_{i\sigma} + U\big)d_i\,,\end{aligned} \tag{2.37}$$

and $\lambda^{(1)}_i, \lambda^{(2)}_{i\sigma}$ are the Lagrange multipliers enforcing the constraints Eqs. (2.31),(2.32) respectively.

The Fermi fields enter quadratically in the above expression for $\mathcal{L}$, hence they can be exactly integrated. This is not true for the Bose fields, which couple in a very complicated manner in the kinetic term. The usual approach to this problem is the saddle-point approximation in which all Bose fields and Lagrange multipliers are taken to be independent of space and time. The original strongly-correlated system is then mapped onto an effective model

[1] As discussed in Ref. [82], this implies that $U_{i\sigma}$ and $V_{i\sigma}$ should be diagonal operators such as $U_{i\sigma} = 1$ in the (0) and $(-\sigma)$ configurations, and $V_{i\sigma} = 1$ in (σ) and $(\uparrow\downarrow)$.

of free quasiparticle with mass renormalized by $1/q = 1/z_0^2$. Of course, the saddle-point values of the slave bosons and of the Lagrange multipliers must be evaluated variationally by minimization of the free-energy functional, which in the paramagnetic sector reads:

$$\begin{aligned} f &= -\frac{2}{\beta}\sum_{k,i\omega_n} \ln(-i\omega_n + q\varepsilon_k) + U d_0^2 - \mu\, n + \\ &\quad \lambda_0^{(1)}(e_0^2 + 2p_0^2 + d^2 - 1) + \lambda_0^{(2)}(n - 2p_0^2 - 2d_0^2). \end{aligned} \tag{2.38}$$

Let us notice that, due to the fact that in the saddle-point approximation the constraints are only satisfied on average, the choice of a proper expression for the $z_{i\sigma}$ is crucial. Kotliar and Ruckenstein proposed to replace $z_{i\sigma}$ with

$$z_{i\sigma}^{(KR)} = \frac{1}{\sqrt{1 - d_i^\dagger d_i - p_{i\sigma}^\dagger p_{i\sigma}}}\; z_{i\sigma}\; \frac{1}{\sqrt{1 - e_i^\dagger e_i - p_{i,-\sigma}^\dagger p_{i,-\sigma}}}, \tag{2.39}$$

that leads to the correct result at mean-field level when $U = 0$[80]. Actually this choice allows to obtain the Gutzwiller variational results discussed in the previous chapter; by looking at the ground-state energy of the model, which corresponds to the zero-temperature limit of the free energy Eq.(2.38) with the saddle-point value of $z_{i\sigma}^{(KR)}$, one finds that it corresponds exactly to Eqs. (2.14),(2.15) when considering the paramagnetic phase ($n_\uparrow = n_\downarrow = n/2$) and to Eqs. (2.29),(2.30) upon substituting $P(0) = e_0^2$, $P(1) = 2p_0^2$, $P(2) = d_0^2$.

The slave-boson framework, nevertheless, allows for some step ahead with respect to the Gutzwiller approach, even at the mean-field level. Thanks to the integral functional formulation, one is able to compute dynamical quantities over the saddle-point action obtained from Eq.(2.37) by replacing in it all the Bose fields and the Lagrange multipliers with their mean-field values. For example the (local) Green function for the physical electron reads:

$$\mathcal{G}_{ii}(\tau) = \langle T_\tau c_i(\tau) c_i^\dagger(0)\rangle = z_0^2 \big\langle T_\tau \tilde{c}_i(\tau)\tilde{c}_i^\dagger(0)\big\rangle_{\mathcal{L}_0}, \tag{2.40}$$

where T_τ is the finite-temperature time-ordering operator in the Matsubara formalism; the last expectation value must be computed over the saddle-point lagrangian $\mathcal{L}_0$. Due to the quadratic dependence of $\mathcal{L}_0$ on the Fermi fields, one immediately gets:

$$\mathcal{G}_{ii}(i\omega_n) = \sum_k \frac{z_0^2}{i\omega_n - z_0^2\,\xi_k}, \tag{2.41}$$

where $\xi_k = \varepsilon_k - \mu^{(0)}$ is the free-electron dispersion renormalized to the chemical potential of the uncorrelated system[2]. Therefore it appears clearly from Eq.(2.41) that in the present approach the quasiparticle residue and the inverse of the effective mass are the same and that they are both equal to $z_0^2 \equiv q$. Then, whereas Brinkmann and Rice were able to characterize the Mott metal-insulator transition with the divergence (vanishing) of m^* (q) and

[2]This is due to the relation between the true chemical potential of the system and the uncorrelated one; when working at fixed density one finds that $\mu - \lambda_0^{(2)} = z_0^2\mu^{(0)}$ at the mean-field level.

suggested that the low-energy peak in the density of states should shrink with increasing U and eventually vanish at the MIT, the slave-boson framework suggests also that the spectral weight of the coherent low-energy peak is not normalized to one, and that it is progressively lost when approaching the transition for being transferred to high-energy incoherent features. As mentioned before, this is actually what was observed in the DMFT analysis of the Hubbard model. In the present context these incoherent features are likely to appear with the inclusion of quantum fluctuations around the saddle point at all orders. However, inclusion of fluctuations appears to be a difficult task even at the lowest order. Nevertheless, in the insulating phase at half filling some simplification holds which allowed Raimondi and Castellani[83] to include gaussian fluctuations of the slave bosons. In a few words, they found that the relevant physics of the Mott insulator is captured by the fluctuations of empty and doubly-occupied sites only; these fluctuations give rise to two bosonic levels $\omega_{1,q}, \omega_{2,q}$ from which one can build the incoherent Hubbard bands divided by a gap that appears to be proportional to $U(1-U_c/U)^{1/2}$. This last result allows to reconcile the insulating description due to Hubbard with the weak-coupling scenario proposed by Brinkmann and Rice; in fact it shows that the gap closes exactly when $U = U_c$, i.e. at the same critical value at which the effective mass of the correlated metal diverges. We notice however that this is slightly different from the picture obtained in the DMFT framework, where the more accurate description of the electron dynamics shows that the gap characteristic of the insulating phase has already developed when the system undergoes the metal-insulator transition (cfr. Fig. 2.1 and the discussion in Sec. 2.2).

2.3 The e-ph interaction in the Holstein model

As already mentioned, the Holstein model provides a simple picture in which the effects of the coupling between electrons and lattice deformations can be analyzed. Its Hamiltonian reads:

$$H = H_t + H^0_{ph} + H_{e-ph}, \tag{2.42}$$

where

$$H^0_{ph} = \sum_i \left(\frac{P_i^2}{2M} + \frac{K}{2} X_i^2 \right), \tag{2.43}$$

$$H_{e-ph} = g' \sum_i n_i X_i, \tag{2.44}$$

where X_i, P_i are the local ionic displacements and conjugate momenta and $n_i = n_{i\uparrow} + n_{i\downarrow}$ is the total electron density on given site i; M, K are respectively the mass and the spring constant of the harmonic oscillators which mimic the small oscillations of ions and are connected by the relation $K = M\,\omega_0^2$. H_t is the already introduced hopping term for tight-binding electrons, while g' is a dimensionless coupling constant. It is useful to write the above Hamiltonian in its second-quantization form, by introducing the annihilation and creation phonon operators

a_i, $a_i^\dagger$ which are related to the lattice displacement and momentum by $X_i = (a_i^\dagger + a_i)/\sqrt{2M\omega_0}$ and $iP_i = (a_i - a_i^\dagger)\sqrt{M\omega_0/2}$. Then one gets

$$H_{ph}^0 = \sum_i \omega_0 \, a_i^\dagger a_i, \tag{2.45}$$

$$H_{e-ph} = g \sum_i n_i \, (a_i^\dagger + a_i), \tag{2.46}$$

where a dimensionful coupling constant has been introduced that includes the physical characteristics of the ions, namely $g = g'/\sqrt{2M\omega_0}$. In order to get a flavour of the physical content of this model one can look at the phonon-mediated electronic properties by eliminating the phononic degree of freedom, which enter quadratically in the Hamiltonian and can be exactly integrated out. One finds that they mediate an effective retarded density-density interaction:

$$V_{eff}(\omega) = -g^2 \, \frac{\omega_0}{\omega_0^2 - \omega^2}, \tag{2.47}$$

which acts between electrons with opposite as well as parallel spins. Hence the e-ph coupling affects the electronic properties renormalizing the energy levels of electrons and inducing an attractive interaction between them. Both effects depend crucially on the value of ω_0, the characteristic energy of ion oscillations, which appears as a relevant parameter of the model. We can introduce then:

- $\gamma = \dfrac{\omega_0}{D}$ - adiabaticity parameter (ratio of of phonons and electrons characteristic energies);
- $\lambda = \dfrac{2\,g^2}{\omega_0 \, D}$ - dimensionless e-ph coupling constant.

We notice that in standard Migdal-Eliashberg theory the e-ph coupling is defined in a slightly different way, namely as $\hat{\lambda} = 2N_0 g^2/\omega_0$, where N_0 is the electron density of state at the Fermi level. Nonetheless, in analogy with the definition of u, it is useful to measure the strenght of e-ph coupling as the ratio between polaronic binding energy and band energy. Actually, by recasting the effective phonon-mediated density-density interaction as:

$$V_{eff}(\omega) = -\frac{\lambda D}{2} \, \frac{\omega_0^2}{\omega_0^2 - \omega^2}. \tag{2.48}$$

one immediatly sees that, in the antiadiabatic limit $\gamma \to \infty$, i.e. when electron motion is slow with respect to the lattice dynamics, λ accounts both for the electronic energy gain (due to polaron formation) and for the attractive interaction between electrons with opposite spins. In this limit the system display the same physical properties of the attractive Hubbard model[84] with $u = -\lambda$. In particular it is known that increasing the electron-electron interaction the attractive Hubbard model displays a metal-insulator transition similar to the one we have described in the previous section, except for the fact that in this case the localized state is characterized by the presence of local pairs of electrons with opposite spins and by the absence of singly-occupied states[85].

The opposite limit $\gamma \to 0$, usually referred to as the adiabatic limit, implies that lattice dynamics is slow with respect to the typical kinetic energy of electrons. This means that the kinetic-energy term of the phonons is negligible, hence phonons become static fields; the electronic problem can then be solved by considering fixed phonon coordinates, as in the Born-Oppenheimer approximation, and then averaging over the X_i. In the limit of strong coupling a possible approach is to neglect the hopping term and to look for the minima of the adiabatic potential experienced by the electrons:

$$V_{sc}(X_i) = \frac{1}{2} K X_i^2 + g' n_i X_i, \tag{2.49}$$

that can be conveniently recast in terms of a dimensionless $x_i = \sqrt{M\omega_0}\, X_i$:

$$V_{sc}(x_i) = \frac{\omega_0}{2}\left(x_i + \sqrt{2}\frac{g}{\omega_0} n_i\right)^2 - \frac{\lambda D}{2} n_i. \tag{2.50}$$

Eq.(2.50) provides many insights in the properties of the model. First of all, it allows to connect the electron occupation of the lattice site with its distortion, showing also that the energy lowering of the corresponding electron level is given by $-\lambda D/2$. The displacement of the local oscillator is measured by another parameter which will prove to be relevant in the description of the polaron physics and that will emerge naturally in the atomic limit discussed in Section 2.3.2:

- $\alpha = \dfrac{g}{\omega_0}$ - measure of the lattice displacement[3].

This parameter can be conveniently expressed in terms of the previously introduced parameters as $\alpha^2 = \lambda/2\gamma$. If one requires, then, that this adiabatic potential is deep enough to bind the electron in the first place, the self-consistency of this strong-coupling approach is guaranteed and leads to a phase in which electron delocalization is suppressed. In the adiabatic limit, therefore, one recovers a transition, or at least a crossover, to a localized state as in the opposite antiadiabatic limit; in this case, however, the system displays a possible polarization due to the finite distortion of the lattice sites and the localization stems from the e-ph coupling itself rather than from a phonon-induced attraction.

We have briefly anticipated that the expected effects of the e-ph coupling in the Holstein model are (i) to induce local deformations of the lattice correlated to the presence of a charge and (ii) a crossover or transition to a localized phase. Nonetheless it is a very hard task to put this scenario in rigorous terms, even when considering the simplified limit of a single electron in the lattice (zero-density limit)[44, 86], in which the residual e-e interaction mediated by the phonons is absent. The crucial point is that the hopping of the electron is followed by a coherent propagation of the lattice deformation induced by the electron himself. In

[3]To be rigorous, we notice that in the exact adiabatic limit $\omega_0 = 0$ the parameter α is ill-defined; this is related to the fact that in this limit one should consider the classical lattice displacement X_i rather than the dimensionless operator x_i. Keeping fixed K and letting $M \to \infty$ one gets $g'/K \equiv \sqrt{\lambda D/K}$ as the proper measure of lattice displacement in the considered limit.

terms of phonons, it means that the electron is dressed by a multi-phonon cloud which moves coherently with it so as to form a quasiparticle, the polaron. While in the weak-coupling limit this effect can be incorporated in an enhanced effective mass for the quasiparticle[12], at intermediate and strong couplings multiple-phonon contributions begin to be important even neglecting vertex corrections[87] and the many-body character of the problem manifests, requiring more accurate non-perturbative approaches. Furthermore, the retarded character of the e-ph coupling, depending on the value of the adiabaticity parameter, leads to non-trivial space-time-dependent interaction between the polaronic charge carrier and the lattice deformation associated to it[43, 88].

When considering the finite-density case, a further complication comes from the residual attractive interaction experienced by polarons. Superconducting (SC) and charge-density-wave (CDW) instabilities are expected in this case[89, 90, 91], but we will focus only on the paramagnetic phase, whose understanding is required in order to include Hubbard repulsion, since the presence of sizeable U is expected to frustrate the establishing of SC and to some extent of CDW phases. As for the Hubbard model, Dynamical Mean-Field Theory has proved a fundamental tool in the analysis of the Holstein model in the exact adiabatic limit[92] and for finite γ[93, 94, 95]. In these works the two aspects of polaron formation, connected to the polarization of the system, and of the transition to a localized phase have been analyzed in the half-filling regime of the model. The first phenomenon can be addressed by looking at the mean square displacement $\langle X^2 \rangle$ of the oscillator or equivalently at the probability distribution function of the phonon field $P(X)$; the second one, on the other hand, can be connected to the vanishing of the density of states at Fermi level, which corresponds, as discussed for the Mott transition in the Hubbard model, to the vanishing of the quasiparticle weight. When $\gamma \to 0$, Millis and coworkers[92] found that three regimes may be distinguished at zero temperature:

i) at weak coupling the mean square displacement of the oscillator coordinate from its non-interacting reference position vanishes, and electron spectral function assumes the non-interacting form with small corrections that are correctly captured by perturbation theory;

ii) at intermediate coupling the mean square displacement of the oscillator is nonvanishing and the probability distribution function of the phonon field develops a bimodal shape; the quasiparticle weight is strongly reduced but still finite (polaron formation);

iii) at strong coupling the quasiparticle weight vanishes, the associated low-energy peak disappears and a gap develops in the spectral function; polarons are bound to form incoherent local pairs, called bipolarons.

When relaxing the adiabatic limit introducing zero-temperature quantum fluctuations one observes that the same picture, with a polaronic crossover followed by a bipolaronic transition, holds at small values of γ, but for larger values of the adiabaticity parameter the transition to

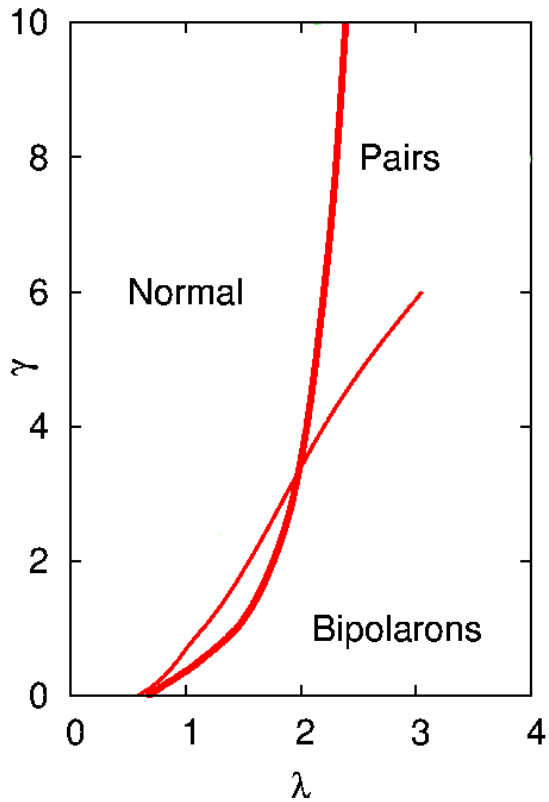

Figure 2.4: Phase diagram in the $\lambda - \gamma$ plane for the half-filled Holstein model as computed in DMFT[95]. The bold line is the locus where the quasiparticle weight vanishes, thus signalling the transition to a localized pair-phase; the thin line is the polaron crossover.

a localized state is found to occur before polarons could develop. This effect can be explained by considering that in the antiadiabatic limit one needs an infinite value for λ in order to get a finite α, which measures the lattice distortion induced by the e-ph coupling; on the other hand the metal to (pair-)insulating transition is expected to be controlled by the energetic balance between kinetic energy and the Hubbard-like attractive interaction mediated by phonons, which in this limit is weakly dependent on the phonon frequency as highlighted by Eq.2.48. Actually, as seen in Fig.2.4, while λ_{pol} which signals the polaron formation is almost linear with increasing γ, λ_{pair} tends to saturate to its antiadiabatic value. The same scenario appears when considering finite temperatures[96], where it is shown that the two phenomena of phonon-field polarization and of electron pairing occur for fairly similar couplings in the adiabatic limit and tend to coincide only when T is of the order of ω_0, i.e. when phonons begin to behave classically.

Another difference between adiabatic and antiadiabatic regimes can be extrapolated by looking at the electronic spectral function. In the antiadiabatic limit, where the Holstein model maps onto the attractive Hubbard model, the density of states evolves while ap-

proaching the pair-insulating phase as in the repulsive Hubbard model (see Fig.2.1), and low-energy features are clearly separated by the high-energy ones before the transition occurs. This energy separation at intermediate couplings vanishes approaching the adiabatic limit, and the effect of e-ph coupling can be seen only in a small window centered at the Fermi level[93]. The evolution of the electronic spectral function with the strength of e-ph coupling is shown in Fig. 2.5 well deep in the adiabatic regime (left panel, with $\omega_0 = 0.1D$) and for two larger values of the adiabaticity parameter (right panel). The physical origin of these unusual phonon signatures can be understood in a weak-coupling perturbative approach, which will therefore be discussed in the next section. In the following we will briefly discuss the strong-coupling regime moving from the atomic limit, that will allow us to put in rigorous terms some concept we have anticipated about polaron formation.

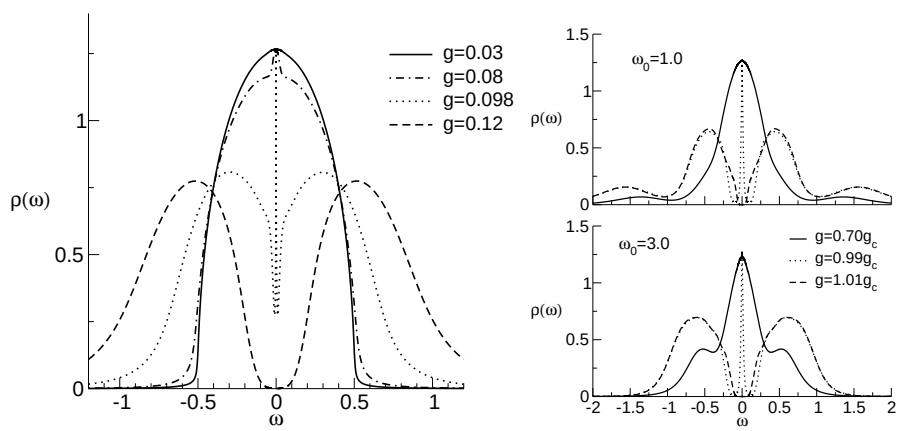

Figure 2.5: Electronic spectral density for the half-filled Holstein model from Ref. [93]; on the left the $\omega_0 = 0.05W$ results are shown for different values of the bare coupling constant g ($W = 2D$ is the electronic bandwidth), while on the right the evolution with g of the spectral function is reported for larger values of ω_0.

2.3.1 Weak-coupling perturbation theory

In this section we will sketch some results obtained in weak-coupling perturbation theory, which is the basis of the standard Migdal-Eliashberg (ME) theory for e-ph coupling in metals[97]. According to Migdal's theorem, in the adiabatic limit of small ω_0/ε_F, where ε_F is the Fermi energy of the metal, the effects of e-ph interaction on the electronic properties can be properly described in a field-theory framework without taking account of vertex corrections. The question of the reliability of ME theory in the Holstein model has been addressed by several authors[98, 99, 100], and it will not be discussed here, but it has been shown that Migdal's theorem holds only for weak and moderate couplings in the adiabatic limit, while it breaks down for vanishingly small g in the opposite limit. Nevertheless some qualitative features emerge from second-order perturbation theory that clarify the influence

of the adiabaticity parameter in determining the physical regimes of the system.

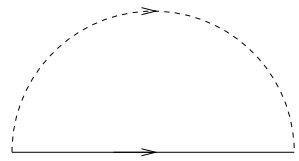

Figure 2.6: Second-order contribution to the electron self-energy in the presence of Holstein e-ph coupling. Solid line is the noninteracting Green function for electron, dotted line is the free phonon propagator.

Let's consider the electron self-energy in the presence of a Holstein-like coupling. The lowest-order term in the perturbation expansion neglecting vertex corrections is the second-order one, depicted in Fig. 2.6, which at finite temperatures gives:

$$\Sigma_2(\mathbf{p},\omega_n) = -g^2 T \sum_{\Omega_m} \sum_{\mathbf{q}} \mathcal{D}(\mathbf{q},\Omega_m)\, \mathcal{G}(\mathbf{p}-\mathbf{q},\omega_n-\Omega_m), \tag{2.51}$$

where $\mathcal{G}$ and $\mathcal{D}$ are the noninteracting Green functions for the electrons and for the phonons respectively. Eq. (2.51) can be handled by standard field-theory methods leading to the following $\mathbf{p}-$independent expression for the $T=0$ retarded self-energy:

$$\Sigma_2^R(\omega) = g^2 N_0 \left\{ \int_0^D d\xi \, \frac{1}{\omega-\omega_0-\xi+i0^+} + \int_{-D}^0 d\xi \, \frac{1}{\omega+\omega_0-\xi+i0^+} \right\}, \tag{2.52}$$

where for the sake of simplicity we have considered a half-filled system with a flat band of half width D, related to the density of state by $1 = 2DN_0$. Spectral properties of the system can be inferred by considering the spectral function $A(\omega)$, which is related to the retarded sel-energy according to:

$$A(\omega) = \frac{N_0}{\pi} \int_{-D}^{D} d\xi \, \frac{|Im[\Sigma_2^R]|}{(\omega-\xi-Re[\Sigma_2^R])^2 + (Im[\Sigma_2^R])^2}. \tag{2.53}$$

After performing the integral, the real part of Σ_2^R reads:

$$Re[\Sigma_2^R(\omega)] = -g^2\, N_0 \left\{ \ln\left|\frac{\omega-\omega_0-D}{\omega-\omega_0}\right| - \ln\left|\frac{\omega+\omega_0+D}{\omega+\omega_0}\right| \right\}, \tag{2.54}$$

while for the imaginary part one gets:

$$Im[\Sigma_2^R(\omega)] = -g^2\, N_0\, \pi \left\{ \int_0^D d\xi\, \delta(\omega-\omega_0-\xi) + \int_{-D}^0 d\xi\, \delta(\omega+\omega_0-\xi) \right\}. \tag{2.55}$$

As expected, the behaviour of the self-energy depends on the balance between two relevant energy scales, a phononic one (ω_0) and an electronic one (D). The ME result is recovered in the adiabatic limit when $\omega_0 \ll D$; then one can take the infinite$-D$ limit in 2.54, obtaining:

$$Re[\Sigma_2^R(\omega)] = -g^2\, N_0\, \ln\left|\frac{\omega+\omega_0}{\omega-\omega_0}\right|, \tag{2.56}$$

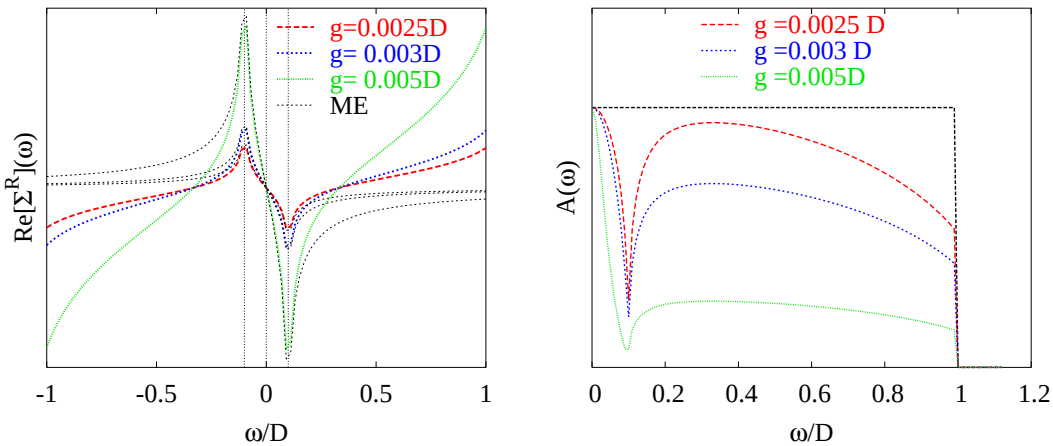

Figure 2.7: Frequency dependence of the real part of the retarded electronic self-energy of the Holstein model for a finite flat band at $\gamma = 0.1$ (left panel) and at different values of the bare coupling constant g; ME result correctly reproduce the almost linear dependence on ω in a window $\sim 2\omega_0/D$ wide but it lacks finite-band effects for higher energies. In the right panel the corresponding spectral function evolving from the flat uncorrelated band is shown.

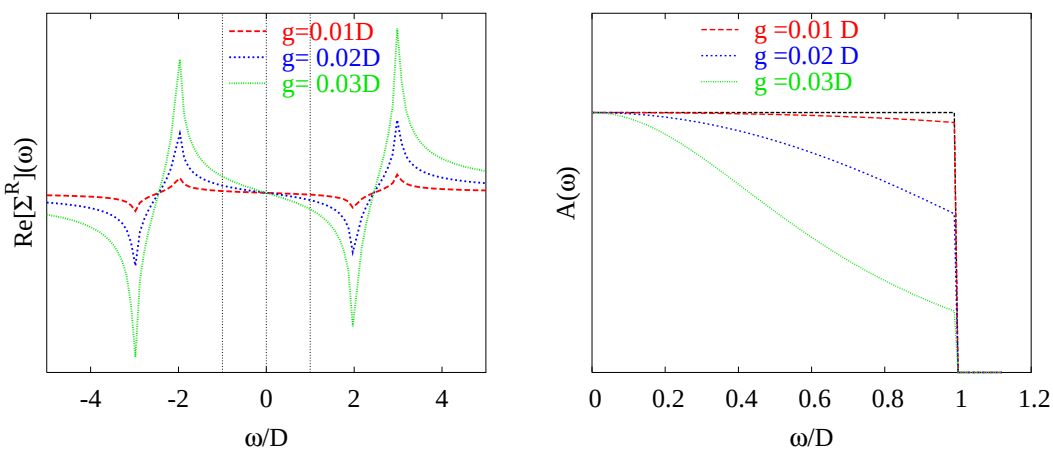

Figure 2.8: Evolution with g of the real part of the retarded electronic self-energy at $\gamma = 2$ (left) and corresponding spectral function (right). Inside the band the behaviour of $Re[\Sigma_2^R(\omega)]$ is almost linear with ω. for all couplings.

which can be expanded for $\omega < \omega_0$ as

$$Re[\Sigma_2^R(\omega)] \approx -N_0 \frac{2g^2}{\omega_0} \omega = -\hat{\lambda}\omega. \tag{2.57}$$

where we have defined the standard e-ph coupling as $\hat{\lambda} = 2N_0 g^2/\omega_0$. Due to the fact that the phonon energy falls in the electronic energy range (which in this limit is infinite!), ω_0 clearly

divides the frequency range in two regions in which the real part of the self-energy behaves differently; actually it is easy to see that for $\omega > \omega_0$ Eq.(2.56) can be expanded as

$$Re[\Sigma_2^R(\omega)] \approx -N_0 \frac{2g^2}{\omega_0} \frac{\omega_0^2}{\omega} = -\hat{\lambda}\frac{\omega_0^2}{\omega}. \tag{2.58}$$

Furthermore one can observe that the imaginary part of Σ_2^R is equal to zero for $|\omega| < \omega_0$, which implies that a quasiparticle picture holds in this energy range, while incoherent contributions become relevant for $|\omega| > \omega_0$ where $Im[\Sigma_2^R]$ turns out to be a constant, namely $-\pi g^2 N_0 \mathrm{sgn}\omega$[87]. The physical meaning of this different behaviour may be understood naïvely by considering that when $|\omega| < \omega_0$ no phonons can be created and electrons interact via virtual processes in a Hubbard-like fashion. This phenomenon is reflected in the electronic spectral density which, when considering small values of the coupling, shows quasiparticle-like signatures of e-ph interaction (namely a shrinking of the peak with depletion of spectral width) only in a window that is approximatively $2\omega_0$ wide around the Fermi surface, as seen in the right panel of Fig.2.7 (see also Ref. [100]), while incoherent contributions emerge when $|\omega| > \omega_0$.

On the other hand, in the opposite antiadiabatic limit the only relevant energy scale is ω_0. By expanding Eq.(2.54) one obtains, for all energies in the band:

$$Re[\Sigma_2^R(\omega)] \approx -\frac{g^2}{\omega_0^2}\omega = -\alpha^2\omega. \tag{2.59}$$

In this regime, then, the control parameter for the e-ph coupling should be α rather than λ as in the adiabatic limit, as already pointed out in [86, 101]. We notice that in this case one expects that the whole electronic band is renormalized in a quasiparticle fashion, since $Im[\Sigma_2^R] = 0$ for all energies in the band.

Thanks to its local nature, the real part of Σ_2^R can be connected straightforwardly to a physical quantity, the effective mass, according to:

$$\frac{m^*}{m} = 1 - \frac{\partial Re[\Sigma_2^R(\omega)]}{\partial\omega}\Big|_{\omega=0}. \tag{2.60}$$

In the simplified case that we are considering here, where the electronic band is flat, the effective mass can be computed exactly for any value of ω_0, D, and one gets:

$$\frac{m^*}{m} = 1 + N_0 \frac{2g^2}{\omega_0} \frac{1}{1+\frac{\omega_0}{D}} = 1 + N_0 \frac{\lambda D}{1+\gamma}. \tag{2.61}$$

From this expression one recovers the ME result $m^*/m = 1+\lambda D N_0$, that is correct only when condition $\omega_0 \ll D$ is strictly fulfilled, and the antiadiabatic weak-coupling result $m^*/m = 1+\alpha^2$ in the opposite limit; it also suggests that finite bands effects must be included when the case of nonadiabatic regimes is analyzed, and that the value of the phonon frequency can prove to be relevant. Actually this will be the case when including the Hubbard term in the Holstein model[60].

2.3.2 Atomic limit and Lang-Firsov transformation

The atomic limit allows to put in rigorous terms the concept of polaron formation. Neglecting hopping processes, one can look for the unitary transformation $\hat{U}$ that diagonalizes the Hamiltonian $H_{at} = H^0_{ph} + H_{e-ph}$. Lang and Firsov[102] found that this unitary transformation reads:

$$\hat{U} = e^S = e^{\alpha \sum_\sigma n_\sigma (a - a^\dagger)}, \tag{2.62}$$

which allows to exactly decouple the interaction term obtaining:

$$\hat{U}^\dagger H_{at} \hat{U} = \tilde{H}_{at} = \omega_0 a^\dagger a - \frac{g^2}{\omega_0} \sum_\sigma n_\sigma - 2\frac{g^2}{\omega_0} n_\uparrow n_\downarrow, \tag{2.63}$$

where the electron level (here fixed to zero) is shifted by an amount $g^2/\omega_0 = \lambda D/2$ and an attractive term $2g^2/\omega_0 = \lambda D$ is induced by the e-ph coupling, consistently with Eq.(2.48). Electron operators c_σ are transformed by the Lang-Firsov transformation into operators which describe a new charged object rigidly tied to the site displacements:

$$\tilde{c}^\dagger_\sigma = c^\dagger_\sigma \mathrm{X}^+, \tag{2.64}$$

$$\tilde{c}_\sigma = c_\sigma \mathrm{X}^-, \tag{2.65}$$

$$\mathrm{X}^\pm = e^{\pm\alpha (a - a^\dagger)}, \tag{2.66}$$

that is the polaron. When considering only one electron in the atomic site, then, $\lambda D/2$ represents the ground-state polaronic energy, and excited states are given by creation of extra phonons.

From the point of view of phonons, the effect of e-ph coupling is to induce a finite distortion of the site. Keeping in mind that $(a - a^\dagger)$ is proportional to the momentum operator of the phononic field, the Lang-Firsov transformation can be viewed as a translation of the free harmonic oscillator centered in the atomic site; the corresponding ground state for the phonons is:

$$|\phi(X - X_0)\rangle \equiv \mathrm{X}^+|0\rangle = \sum_m e^{-\frac{\alpha^2}{2}} \frac{\alpha^m}{\sqrt{m!}} |m\rangle, \tag{2.67}$$

where states $|m\rangle$ denotes the $m-$th excited states of the noninteracting harmonic oscillator and $X_0 = \sqrt{2}\alpha$ is the new equilibrium position of the atom.

From the point of view of the electron, it is useful to compute the spectral function or, equivalently, the retarded Green function of the single-electron problem:

$$G^R_e(t) = -\theta(t) \big\langle e^{i\tilde{H}t}\, c\, \mathrm{X}^-\, e^{-i\tilde{H}t}\, c^\dagger\, \mathrm{X}^+ \big\rangle. \tag{2.68}$$

Here the difficulty arise from the presence of the X operators, but for the zero-temperature case we are discussing the computation can be done by disentangling of operators[103] and

one gets:

$$G_e^R(\omega) = e^{-\alpha^2} \sum_{m=0}^{\infty} \frac{\alpha^{2m}}{m!} \frac{1}{\omega + \frac{g^2}{\omega_0} - m\omega_0 + i0^+}, \tag{2.69}$$

$$A(\omega) = e^{-\alpha^2} \sum_{m=0}^{\infty} \frac{\alpha^{2m}}{m!} \delta(\omega + \frac{g^2}{\omega_0} - m\omega_0). \tag{2.70}$$

Therefore the spectral function appears as a Poisson distribution of $\delta-$peaks separated by the phonon frequency ω_0, which however must not be confused with excited states: they describe the probability of the electron having a given energy ω *in the ground state of the polaron.* It is readily seen that the most probable state, where the spectral weight is maximum, occurs when $\bar{m} \sim \alpha^2$, hence the parameter α is not only a measure of the atomic distortion but also of the number of phonons involved in the polaron formation. On the other hand, from Eq. (2.70) one finds that the noninteracting level of the electron is shifted by an amount $-g^2/\omega_0$, but its spectral weight is reduced to $\exp[-\alpha^2]$, while the maximum of the spectral weight corresponds approximatively to the noninteracting energy $-g^2/\omega_0 + \bar{m}\omega_0 = 0$. Roughly speaking, the energy gain for the electron is converted in a cloud of excited phononic states.

When relaxing the atomic limit, hence including hopping processes in H_{at}, in the Lang-Firsov framework, one has to deal with the composite nature of the polaron we have just discussed. The hopping term, in fact, is transformed in

$$-t\, c_{i\sigma}^\dagger c_{j\sigma} \rightarrow -t\, \mathrm{X}_i^+ \mathrm{X}_j^- c_{i\sigma}^\dagger c_{j\sigma}, \tag{2.71}$$

which represents the hopping of the polaron. Therefore we pay the disappearence of the e-ph coupling with a more complicated kinetic term, and some approximation is required in order to handle the transformed Hamiltonian. Holstein proposed to average the lattice model over the free phonon variables, thus obtaining an effective model with the hopping constant renormalized to $t\langle 0|\mathrm{X}_i^+ \mathrm{X}_j^- |0\rangle = t\, \exp[-\alpha^2]$[44]. This approximation implies that the number of phonons in the phonon cloud surrounding each charge carrier remains largely unchanged during the transfer of a polaron from a site to the next; putting it in other words, emission and absorption of phonons during the hopping processes is neglected. The only reasonable regime in which this approximation is expected to hold is the antiadiabatic limit, where local lattice deformations can be considered to adapt themeselves almost instantaneously to the slowly-in-time varying positions of the electrons. Actually Ranninger and Thibblin[88] carefully analyzed a two-site toy model with Holstein coupling and found that the shape of the ground-state phonon wavefunction strongly deviates from the displaced oscillator when relaxing the condition of large γ; this is due to retardation effects between the motion of the electron and that of the displaced environment created by the electron itself, effects that the Holstein approximation neglects.

Within the Holstein approximation polarons are well defined quasiparticles with renormalized hopping, while electrons lose almost all of their coherence. Anyway one can evaluate the retarded Green function and the spectral function for the electrons in the same spirit of

the atomic limit with one particle; for a many-polarons system where a repulsive interaction was suitably introduced in order to compensate the phonon-induced e-e attraction ($U = \lambda D$) Alexandrov and Ranninger found[104]:

$$G_e^R(\mathbf{k},\omega) = \frac{e^{-\alpha^2}}{\omega + \frac{g^2}{\omega_0} - \varepsilon^*_{\mathbf{k}} + i0^+} + e^{-\alpha^2} \sum_{m=1}^{\infty} \frac{\alpha^{2m}}{m!} \frac{1}{L} \sum_{\mathbf{q}} \left[\frac{f(\varepsilon^*_{\mathbf{q}})}{\omega + \frac{g^2}{\omega_0} - \varepsilon^*_{\mathbf{q}} + m\omega_0 + i0^+} + \frac{1 - f(\varepsilon^*_{\mathbf{q}})}{\omega + \frac{g^2}{\omega_0} - \varepsilon^*_{\mathbf{q}} - m\omega_0 + i0^+} \right], \tag{2.72}$$

where $\varepsilon^*_{\mathbf{k}} = e^{-\alpha^2}\varepsilon_{\mathbf{k}}$. This solution shows a coherent low-energy quasiparticle band describing a polaron of effective mass

$$\frac{m^*}{m} = e^{\alpha^2}, \tag{2.73}$$

located around the polaron energy $\lambda D/2$, togheter with an incoherent structure at higher energies which comes from the possibility of changing the number of phonons in the phonon cloud during the excitation of the electron. This picture is valid only in the large-phonon-frequency limit, and it is consistent with the weak-coupling perturbative analysis discussed in the previous section, which provided a first-order expansion in power of α^2 of the effective mass Eq.(2.73).

Chapter 3

Variational slave-boson approach

3.1 Introducing the method

As discussed in the previous chapter, the Hubbard-Holstein model provides an excellent playground which allows to study the interplay of electron correlation and electron-phonon coupling. A close look at the main effects of the two interaction mechanisms taken separately suggests an absolutely non-trivial competition when they are considered togheter. For instance, it is well known that both e-e and e-ph interactions induce an increase of the effective mass of the free carriers; nevertheless it has been shown in the previous chapter that the coupling with the lattice dynamics mediates an attractive retarded interaction between electrons, which opposes the Coulomb repulsion responsible for the enhanced effective mass of the correlated quasiparticles. This screening effect depends crucially on the adiabaticity regime, making it hard to predict on intuitive grounds the ultimate behaviour of the charge carriers. A rich and complicated phase diagram is then expected even in the absence of broken-symmetry phases and neglecting temperature effects. Let us recall the full Hamiltonian we will consider throughout this chapter:

$$H = -t \sum_{\langle i,j \rangle, \sigma} c^{\dagger}_{i\sigma} \, c_{j\sigma} \; + U \sum_{i} n_{i\uparrow} n_{i\downarrow} + \omega_0 \sum_{i} a^{\dagger}_{i} \, a_i + g \sum_{i} (a^{\dagger}_{i} + a_i) \, n_i . \tag{3.1}$$

Its physics will be controlled by three of the following four parameters:

- $u = \dfrac{U}{D}$ - degree of electron correlation;
- $\gamma = \dfrac{\omega_0}{D}$ - adiabaticity parameter;
- $\alpha = \dfrac{g}{\omega_0}$ - measure of the lattice displacement;
- $\lambda = \dfrac{2\, g^2}{\omega_0 \, D}$ - e-ph coupling constant;

to which the averaged electron density per site n must be added.

Generally speaking, one could wonder how the electron properties are modified by the presence of the e-ph interaction, or equivalently analyze the modifications induced by the correlated electrons on the lattice dynamics, i.e. on the phonons. In this chapter we will focus mainly on the first aspect of the problem. Our procedure will consist then in deriving an effective correlated model for electrons in which phonon-induced effects are described by renormalization of electronic energy scales, namely hopping and Hubbard terms: this effective Hubbard model can be then analyzed by standard methods developed in the context of strongly-correlated systems, such as the slave-boson technique.

As detailed in the previous chapter, the simplest approach at our disposal which allows to capture polaronic physics in the Holstein model is the Lang-Firsov transformation (LFT)[102]. By means of the unitary transformation $e^S = \exp[\,\alpha \sum_i n_i\,(a_i - a_i^\dagger)]$ the Hubbard-Holstein model maps onto a polaronic model where the e-ph coupling vanishes and the Hubbard term is reduced by the attractive phonon-mediated interaction equal to $-\lambda D$; the transformed hopping term describes the mobility of the polarons, whose composite nature is captured by the operators $c_{i\sigma}^\dagger \mathrm{X}_i^+$, where $\mathrm{X}_i^\pm = \exp[\pm\,\alpha\,(a_i - a_i^\dagger)]$ account for the phonon creation and annihilation following hopping processes. In order to get rid of the lattice degrees of freedom thus obtaining an effective model for the electrons one can follow Holstein's suggestion[44] and average the transformed Hamiltonian over the noninteracting phononic vacuum; as already pointed out, this approximation is expected to give reliable results only in the antiadiabatic limit, where phonons adapt themselves almost instantaneously to the electronic configuration, hence preserving the number of phonons during hopping processes, and emission or absorption of phonons can be safely neglected. For the same reason, being retardation effects almost absent, the phonon-mediated e-e attraction is actually instantaneous and fully subtracts from the Hubbard repulsion.

Relaxing the antiadiabatic limit, one should expect a less severe renormalization both of the kinetic [105] and of the interaction term, due to the retardation effects between the motion of electrons and that of the displaced environment created by electrons themselves. These effects can be addressed in a variational LFT fashion [61, 106, 107]; even if many other variational approaches have been developed in the context of e-ph interaction (for a review about the variational approach to the Holstein model see [108] or [109]), the method we are going to discuss is more suitable for the analysis of phonon effects on the correlated physics of the Hubbard model.

3.1.1 Effective polaron-correlated model

We introduce a generalized Lang-Firsov transformation $U = e^S$, where

$$S = \alpha \sum_i \left[n + f_i\,(n_i - n)\right]\,(a_i - a_i^\dagger). \tag{3.2}$$

The presence of $n = \langle n_i \rangle$ in the transformation allows us to get rid from the outset of the trivial uniform displacement of the lattice due to phonons coupling with the average

electron density; therefore f_i are variational parameters whose minimization is expected to measure the coupling between phonon displacements and density fluctuations for any value of the adiabaticity parameter. Transformation (3.2) in general implies that electrons are not exactly decoupled from phonons and a residual e-ph interaction should be considered togheter with the complicated polaronic hopping term. We can get rid of this complication in the standard Holstein way and average the transformed Hamiltonian over $|0\rangle$, the vacuum state of the transformed phonons, obtaining an effective Hubbard-like model for electronic degrees of freedom only:

$$\begin{aligned} H_{eff} &= -t \sum_{\langle i,j\rangle,\sigma} e^{-\frac{\alpha^2}{2}(f_i^2+f_j^2)}\, c^\dagger_{i\sigma}\, c_{j\sigma} + \sum_i n_{i\uparrow} n_{i\downarrow} \left[U - 2\alpha^2\omega_0\,(2f_i - f_i^2)\,\right] \\ &\quad +2\alpha^2\omega_0 \sum_i \left[n\,(1-f_i)^2 \left(\frac{n}{2} - n_i\right) + f_i\, n_i \left(\frac{f_i}{2} - f_i\right)\right], \end{aligned} \tag{3.3}$$

with hopping, interaction and chemical potential renormalizations controlled by the variational parameters f_i.

We expect f_i to approach one in the antiadiabatic regime, where the standard LFT and Holstein approximation applies, and to decrease with decreasing γ when the adiabatic regime is approached and sizeable lattice distortions are expected only for large values of the e-ph coupling. To make this point clearer let us consider the $\mathrm{X}_i^\pm$ operators, which following the transformation (3.2) read:

$$\mathrm{X}_i^\pm = e^{\pm f_i\,\alpha\,(a\ -a^\dagger)}. \tag{3.4}$$

The ground state for the phonon is then given by $|\phi(X_i - X_{0i})\rangle \equiv \mathrm{X}_i^+|0\rangle$ which correspond to a displaced harmonic oscillator centered in $X_{0i} = \sqrt{2}\, f_i\, \alpha$. From this point of view, then, the variational parameters control the distortion of the lattice sites (hence the polaron formation) *but retain the antiadiabatic oscillator-like shape of the phononic wavefunctions.* Furthermore, emission and absorption of phonons as electrons move in the lattice are still neglected as in the Holstein approximation. Nonetheless, the retardation effects expected for finite values of the adiabaticity parameter are partially captured by our effective model Eq.(3.3). In fact when $f_i < 1$ the phonon-induced attractive term is reduced from its antiadiabatic value, as one should have predicted on the basis of Eq. (2.48). On the other hand the polaronic effective mass is made lighter by the factor f_i^2 multiplying α^2 in the exponential; keeping in mind that $\alpha^2 \sim \bar{m}$, the mean number of phonons involved in polaron formation, this means that in the present representation the charge carriers when hopping from one site to another are followed by a multiphonon cloud which is made up of a minor number of phonons with respect to the antiadiabatic limit, reflecting the fact that lattice deformations can not follow instantaneously electronic motion.

Rude as it is, this approximation will prove useful to describe the influence of e-ph coupling on the physics of correlated electrons, as it will be detailed in the following section where the paramagnetic phase of the effective model given by Eq. 3.3 is analysed.

3.1.2 Slave-boson mean field

Apart from the phonon-induced renormalizations of electron parameters, the Hamiltonian (3.3) represents a Hubbard-like model that can be solved by means of standard strong-correlation methods. We adopt here the Kotliar-Ruckenstein slave-boson approach[80] already described in the previous chapter; for each site we introduce four bosons $e_i, d_i, p_{i\sigma}$, representing the four possible states on site i (zero, two and one σ electron state), and a fermionic operator $\tilde{c}_{i\sigma}$ which is connected to the original electron operator by the relation $c_{i\sigma} = z_{i\sigma}\tilde{c}_{i\sigma}$, where

$$z_{i\sigma} = \frac{\left(e_i^\dagger p_{i\sigma} + p_{i\bar{\sigma}}^\dagger d_i\right)}{\sqrt{1 - d_i^\dagger d_i - p_{i\sigma}^\dagger p_{i\sigma}}\sqrt{1 - e_i^\dagger e_i - p_{i\bar{\sigma}}^\dagger p_{i\bar{\sigma}}}}. \tag{3.5}$$

The equivalence with the original Hilbert space is guaranteed by the constraints

$$\begin{aligned} 1 &= \sum_\sigma p_{i\sigma}^\dagger p_{i\sigma} + d_i^\dagger d_i + e_i^\dagger e_i \qquad (\forall i), \\ 0 &= c_{i\sigma}^\dagger c_{i\sigma} - p_{i\sigma}^\dagger p_{i\sigma} - d_i^\dagger d_i \qquad (\forall i, \sigma), \end{aligned}$$

which can be enforced introducing three Lagrange multipliers $\lambda_i^{(1)}, \lambda_{i\sigma}^{(2)}$ for each site i.

The mean-field solution at a given value of density n in the paramagnetic homogeneous phase is obtained by taking the saddle-point value for the Bose fields ($\langle e_i \rangle = e_0, \langle d_i \rangle = d_0, \langle p_{i\sigma} \rangle = p_0$) and assuming translation invariance, so that $f_i = f$ and $\lambda_i^{(1)} = \lambda_0^{(1)}, \lambda_{i\sigma}^{(2)} = \lambda_0^{(2)}$. Following closely Ref. [82], we minimize the resulting variational energy with respect to the Lagrange multipliers and use the constraints to get

$$E_0 = -|\varepsilon|\, q\, e^{-\alpha^2 f^2} + d_0^2 \left[U + 2\alpha^2\omega_0(f^2 - 2f)\right] - \alpha^2\omega_0(1-\delta)\left[1 - \delta(1-f)^2\right], \tag{3.6}$$

where we have put $n = 1-\delta$ and ε is the kinetic energy per site in the uncorrelated case. This is the only quantity that depends on the dimensionality and the topology of the lattice. In what follows we will consider an infinite-coordination Bethe lattice, which displays a semi-circular density of state with half width D; this particular choice allows for a direct comparison with other methods such the DMFT, that is known to give exact results in the limit of infinite dimensions, or the Gutzwiller approach, that will be described in the next section and where exact computation of expectation values is greatly simplified in the forementioned limit. By introducing the standard notation $x = e_0 + d_0$[110], one can express the saddle-point bosons as

$$d_0^2 = \frac{(x^2 - \delta)^2}{4x^2}, \tag{3.7}$$

$$e_0^2 = \frac{(x^2 + \delta)^2}{4x^2}, \tag{3.8}$$

$$p_0^2 = \frac{2x^2 - x^4 - \delta^2}{4x^2}, \tag{3.9}$$

and $q = z_0^2$, i.e. the reduction of the kinetic energy due to the electronic correlation, as

$$q = \frac{2x^2 - x^4 - \delta^2}{1 - \delta^2}. \tag{3.10}$$

In the absence of e-ph coupling, when $\alpha = 0$, Eq. (3.6) reduces to the well-known Gutzwiller energy for the pure Hubbard model (cfr. Eq. (2.14) or (2.29) in the previous chapter). On the other hand, taking the limit $f = 1$, one recovers the standard Lang-Firsov result, being the kinetic energy exponentially renormalized with the electron energy level and the Hubbard term shifted respectively by $-\alpha^2\omega_0$ and $-2\alpha^2\omega_0$.

In order to determine the mean-field solutions we minimize (3.6) with respect to the remaining variational parameters x^2 and f. One gets:

$$8\,\frac{1 - x^2}{1 - \delta^2}|\varepsilon|\, e^{-\alpha^2 f^2} = \left[U + 2\alpha^2\omega_0(f^2 - 2f)\right]\frac{x^4 - \delta^2}{x^4}, \tag{3.11}$$

$$q|\varepsilon|\, f\, e^{-\alpha^2 f^2} = \omega_0(1 - f)\left[\frac{(x^2 - \delta)^2}{2x^2} + \delta(1 - \delta)\right]. \tag{3.12}$$

For small doping δ the kinetic energy can be expanded around the half-filling value $|\varepsilon_0|$ as $|\varepsilon| = |\varepsilon_0|(1 - a\delta^2)$ (with a depending on the specific shape of the uncorrelated band: for a semicircular DOS one gets $|\varepsilon_0| = 4/3\pi \approx 0.4244D$ and $a = 3\pi^2/32 \approx 0.9253$) and the mean-field equation (3.11) can be conveniently rewritten as:

$$(1 - x^2)\,\frac{x^4}{x^4 - \delta^2} = \bar{u}\,\frac{1 - \delta^2}{1 - a\delta^2}\,, \tag{3.13}$$

where

$$\bar{u} = e^{\alpha^2 f^2}\left[\frac{U}{U_c} + \frac{\lambda D}{U_c}(f^2 - 2f)\right], \tag{3.14}$$

in which $U_c = 8|\varepsilon_0| \approx 3.3953D$ is the Brinkmann-Rice critical value for the Mott transition on the infinite-coordination Bethe lattice in the absence of phonons. Eq. (3.13) coincides with the result for the Hubbard model once U/U_c is replaced by $\bar{u}$ (cfr. Eq.(8) of Ref. [82]). This finding is easily interpreted in terms of renormalized interaction $U_{eff} = U + 2(f^2 - 2f)\alpha^2\omega_0$ and renormalized kinetic energy $\varepsilon_{eff} = \varepsilon e^{-\alpha^2 f^2}$, showing that in the present approach the value of the parameter f determines to what extent the electronic properties are affected by phonons. From a technical point of view, being Eq. (3.12) a transcendental equation, it can be useful to separate the exponential from the algebraic dependence on f, obtaining:

$$f = \left[1 + \frac{2\,|\varepsilon_0|}{\gamma\, D}\,\frac{1 - a\delta^2}{1 - \delta^2}\,\frac{x^2\,(2x^2 - x^4 - \delta^2)}{x^4 + \delta^2(1 - 2x^2)}\,e^{-\alpha^2 f^2}\right]^{-1}. \tag{3.15}$$

This form, as we shall see in the next section, is more suitable for a graphical analysis.

Eqs. (3.13),(3.15) are the mean-field equations one needs to consider in order to analyse the influence of e-ph coupling on the correlated physics of the model. In the next section we will discuss their solution in the simple limit of large Hubbard repulsion, that allow us to put on solid ground our analysis of the physical properties of the model at half-filling and in the doped correlated metal.

3.2 Limit of large U: polaronic transition

It is well known that the ground state of the half-filled paramagnetic phase of the Hubbard model in the limit of large U and in the presence of a frustrating mechanism for the AF phase is a Mott insulator, characterized in the present framework by having one electron on each site of the lattice, being double occupation not allowed ($d = 0$). In order to get nontrivial information about the strongly-correlated properties of the system, one needs to restore a metallic behaviour by introducing some vacancies $\delta \neq 0$. In the limit of infinite repulsion the solution of the mean-field equation (3.13) at finite values of the doping reads simply $x^2 = e_0^2 = \delta$; therefore it is reasonable to assume that $x^2 = \delta/\zeta$ in the presence of large but finite $U \gg U_c$[82, 110]. Expanding the mean-field equations to second order in δ, one finds

$$\zeta = \sqrt{1 - \frac{1}{\bar{u}}}, \tag{3.16}$$

that again coincides with the expression for the pure Hubbard model with renormalized parameters depending on f, and a self-consistent equation for the variational parameter:

$$f = \frac{1}{1 + C\frac{2\,|\epsilon_0|}{\gamma D} e^{-\alpha^2 f^2}}, \tag{3.17}$$

being $C = C(f; u, \gamma, \lambda) = 2\bar{u}/(2\bar{u} - 1)$ a coefficient which does not depend on x^2. In the limit $\bar{u} \gg 1$ (which is equivalent to $U/U_c \gg 1$ if λ is not too large) the prefactor C goes to 1, thus simplifying the analysis of Eq.(3.17).

It is useful to compare the behavior of Eq. (3.17) with the mean-field theory of the ferromagnetic transition. We will see that f, γ and λ play similar role to the magnetization, temperature and magnetic field, respectively. The mean-field equation has the form $f = h(f)$ and can be solved graphically just like the Curie-Weiss equation, as shown in Fig. 3.1. $h(f)$ varies from 0 to 1, so that f takes physically meaningful values. $h(0)$ is different from zero for any finite value of γ and $h(1) < 1$. Therefore $h(f)$ intersects the straight line in at least one point. The function $h(f)$ has an inflection point controlled by the value of the parameter γ. For small γ the inflection point is at small f, so that $h(f)$ crosses f in three points, while for larger γ only one intersection survives as the inflection point moves toward large f. γ clearly plays a role similar to the temperature, with a critical value γ_c which separates the two regimes. The critical point $(f_c, \gamma_c, \lambda_c)$ may be evaluated analytically by imposing

$$f_c = h(f_c; \lambda_c, \gamma_c), \tag{3.18}$$

$$1 = \frac{d}{df} h(f_c; \lambda_c, \gamma_c), \tag{3.19}$$

$$0 = \frac{d^2}{df^2} h(f_c; \lambda_c, \gamma_c), \tag{3.20}$$

which in the limit $C = 1$ give the critical values $f_c = \frac{2}{3}$, $\gamma_c = e^{-\frac{3}{2}} U_c/2 \simeq 0.3788$, and $\lambda_c = \frac{27}{4}\gamma_c \simeq 2.557$. When three solutions exist, we find two locally stable solutions f_- and

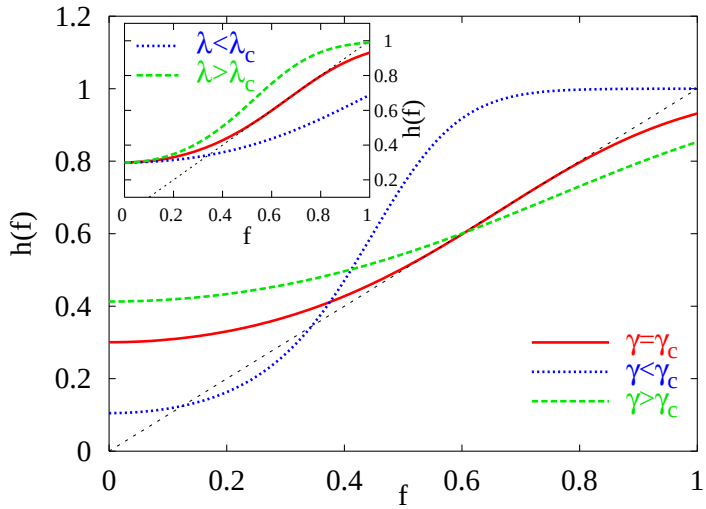

Figure 3.1: Graphical analysis for the self-consistent equation Eq. (3.17). Keeping fixed $\lambda = \lambda_c$, the different behaviour of $h(f)$ is displayed for three characteristic values of the adiabaticity parameter, namely $\gamma \lesseqgtr \gamma_c$; intersections with the bisector mark the graphical solution. In the inset the same plot is shown keeping γ fixed and varying the value of λ.

f_+, shown in Fig. 3.2, that are associated to weaker and stronger polaronic formation. As we pointed out before, in fact, a small value for f implies a little distortion of the lattice with respect to the atomic limit, whereas $f \approx 1$ signals full polaron formation with strong renormalizations of electronic parameters. The two solutions correspond to negative and positive magnetization in the ferromagnetic terminology. Notice that the variational nature of our treatment of phonon degrees of freedom implies that only the lowest energy state is a valid result of our approach, even if the equations allow for more solutions. The parameter λ (or more precisely the deviation from λ_c) acts as a magnetic field in determining the existence of the two potential solutions and which one is the ground state. For small (large) λ only $f_-(f_+)$ exists, and the energies of the two solutions cross in a first order line $\lambda_c(\gamma)$, ending in a critical point.

To summarize, when λ is large, lowering the "temperature" going from the anti-adiabatic to the adiabatic regime does not imply a dramatic change in the value of f; quantum lattice fluctuations are not able to damp the finite distortion due to the strong coupling with electrons, consistently with our discussion of the pure Holstein model. For small λ, on the other hand, f changes from $f \approx 1 - 1/\gamma$ to $f \approx \gamma$ moving from large to small γ. By looking at the evolution with the e-ph coupling, in the antiadiabatic (large "temperature") regime, we have a single solution smoothly evolving with the "magnetic field" λ that, from the point of view of phonons, describes a polaron crossover which becomes steeper as the critical γ_c is reached from above. This crossover becomes a first-order transition in the adiabatic regime and, according to what we have just said, should be interpreted as a polaronic transition. This is a little unexpected result, since it has been shown (at least for the single-polaron problem)

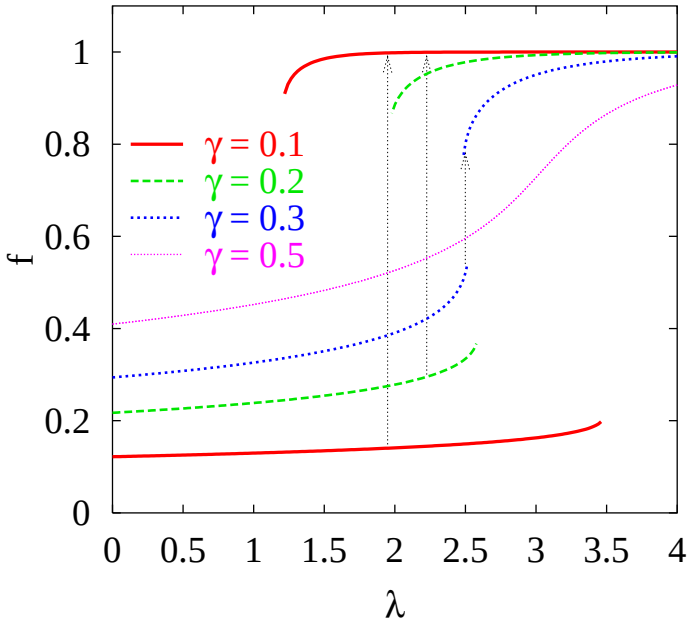

Figure 3.2: Evolution with λ of the numerical solution of the mean-field equations in the limit of infinite U for various values of γ. The vertical arrows signal the first-order transition which occur when the energies of the two solutions cross.

that all quantities are always analytical with increasing coupling strenght, hence a crossover rather than a transition should be expected for any finite value of γ[111] when polaron formation is considered, as confirmed also by DMFT studies[60, 86]. In fact we will show in the next chapter that the first-order transition found within the present approach comes from the poor description of phonon degrees of freedom; however quantitative estimates of the boundaries between regions with different physical behaviour are probably sound or at least give the correct order of magnitude, as we will see in detail in the next sections.

The above "Curie-Weiss" scenario is recovered also for finite, yet large, u, where the simplified limit $C = 1$ is relaxed and one needs to solve numerically the mean-field equations. In Fig. 3.3 we plot a paradigmatic phase diagram in the $\lambda - \gamma$ plane for a fixed value of the Hubbard repulsion, namely $u = 10$; here λ_{c1} (λ_{c2}) labels the line where the f_+ (f_-) solution disappears, while $\lambda_c(\gamma)$ is the critical value for the polaronic transition we have just discussed.

The phase diagram in Fig. 3.3 is not changed much as function of doping. This result may be understood in the following way. The phase transition line is obtained by comparing the values of the energies for the solution for f_- and f_+. As it can be inferred from Eq.(3.6), both the kinetic energy and the polaron energy differ by a quantity of order δ in the two solutions, so that the critical values of λ depend on doping through subleading corrections in δ which are quite small at $u = 10$. The physics underlying the phase diagram of Fig. 3.3 is that by increasing λ a small number δ of localized holes strongly coupled to phonons have a lower energy ($\sim -\delta\,\lambda\,D/2$, i.e., the energy of δ polaronic holes) than a bad metal that has

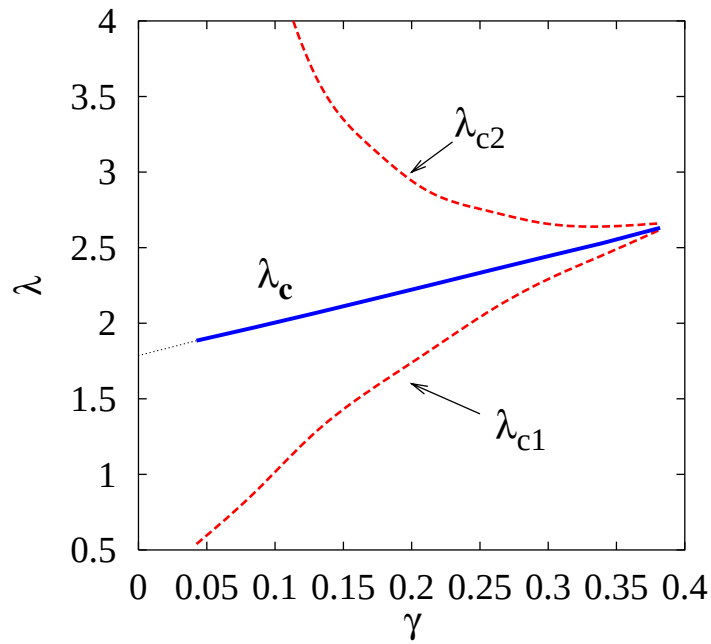

Figure 3.3: Phase diagram in the $\lambda - \gamma$ plane for the Hubbard-Holstein model as obtained in our variational LFT slave-boson approach for a fixed value $u = 10$ near half-filling.

a reduced kinetic energy, again of order δ ($\varepsilon_{eff} \sim -\delta\,|\varepsilon_0|$) due to the large effective mass ($m^* \sim 1/\delta$).

Let us conclude this section noticing that a qualitative similar behaviour of the self-consistent condition (3.15) is observed also for weaker e-e coupling ($U < U_c$) and $\delta = 0$ for interesting ranges of the parameters.

3.3 Metal-insulator transitions at half-filling

In this section we discuss the effects of e-ph coupling on the correlated metal at zero doping. As in the large$-U$ limit, some simplification occurs also when $n = 1$, and the mean-field equations (3.13),(3.15) turn out to be decoupled in a trivial equation for x^2

$$x^2 = 1 - \bar{u}, \tag{3.21}$$

and in a self-consistent condition for f:

$$f = \frac{1}{1 + \frac{2\,|\epsilon_0|}{\gamma D}\,(1 + \bar{u})\,e^{-\alpha^2 f^2}}. \tag{3.22}$$

Three different regimes are found:

i) $\bar{u} \geq 1 \;\rightarrow\; x^2 = 0$ - Mott insulating phase (MI);

ii) $\bar{u} \leq -1 \;\rightarrow\; x^2 = 2$ - bipolaronic insulating phase (BI);

iii) $-1 < \bar{u} < 1 \rightarrow x^2 \in (0,2)$ - correlated metallic phase (M).

In fact, by looking at the saddle-point values of the slave bosons, it is readily seen that when $x^2 = 0$ one has $d_0^2 = e_0^2 = 0, p_0^2 = 1/2$, i.e. only singly-occupied sites are allowed; on the other hand, for $x^2 = 2$ one gets $p_0^2 = 0$ and $d_0^2 = e_0^2 = 1/2$, that means that all the particles are bound to form local pairs (bipolarons) and sit on half of the lattice sites. In both cases quasiparticle motion is completely suppressed *because* $q = 0$, suggesting that transitions to insulating phases are due to electron interactions only, whether repulsive (MI) or phonon-mediated attractive (BI), in agreement with Ref. [94]. This is different from the polaronic transition discussed before, where the quasiparticle residue $Z = q\, e^{-\alpha^2 f^2}$ jumps to a non-zero, though exponentially small, value.

The present mean-field approach does not allow but for a poor description of the insulating phases, exactly as for the Mott phase of the pure Hubbard model, and one should include at least gaussian fluctuations around the saddle point in order to get a satisfactory picture. However, some information can be extracted by analysing the boundaries of the regions where those insulating phases establish. We stress the fact that critical values of U and λ at which transitions take place are determined by the ratio of renormalized e-e interaction and phonon-renormalized kinetic energy, hence we expect to capture the competing effects due to e-ph coupling of reduction of electron mobility and induction of attractive e-e interaction which subtracts to Hubbard repulsion. If we plug condition $\bar{u} = -1$ in Eq. (3.22) we get $f \equiv 1$ for any value of the adiabaticity parameter. This suggests that the present approach is equivalent to the Holstein approximation when the metal-bipolaronic transition is addressed. Then the condition for the bipolaronic transition can be recast as (cfr. Eq. 3.14):

$$\lambda_{BI} = \frac{U_c}{D}\left[e^{-\alpha^2} + \frac{U}{U_c}\right] \tag{3.23}$$

or, as a function of the adiabaticity parameter, as:

$$\gamma_{BI} = -\frac{\lambda}{2\ln(\lambda D/U_c - U/U_c)} \tag{3.24}$$

which corresponds, in the vanishing U limit, to the findings of Ref.[95]. On the other hand, the presence of U shifts to higher values of λ the bipolaronic transition, a somehow expected effect arising from the competition of the repulsive Hubbard term and the attractive phonon-mediated interaction. However Eqs. (3.23),(3.24) should not be considered valid as $\gamma \ll 1$, due to the unsatisfactory description of retarded effects ($f = 1$).

An analogue analysis can be carried out when considering the Mott transition line. In this case f must satisfy the self-consistent condition (3.17) with $C = 2$; by considering the limiting cases of small and large value of γ one finds $f \simeq 2\omega_0/U_c$[61] and $f \simeq 1$ respectively. Then the condition for the metal-insulator transition reads (cfr. Eq. 3.14):

$$U_{MI} = U_c + \lambda\, D\frac{2\omega_0}{U_c}, \qquad \gamma \ll 1, \tag{3.25}$$

$$U_{MI} = U_c + \lambda\, D\left(1 - \frac{U_{MI}}{2\omega_0}\right), \qquad \gamma \gg 1. \tag{3.26}$$

As expected, the coupling with phonons causes a shift of the transition towards higher values of the repulsion, due to the presence of an attractive interaction, proportional to λD, which has to be compensated. Retardation effects are captured by the coefficients multiplying λD in Eqs. (3.25), (3.26), that in both limits are controlled by the ratio $2\omega_0/U$, as already observed in Ref. [57]. Furthermore, by looking at phase diagram in the $\lambda - U$ plane, one finds that the line marking the Mott transition is given by:

$$\lambda_{MI}\, D = \frac{U_c}{2\omega_0}(U - U_c), \qquad \gamma \ll 1, \tag{3.27}$$

$$\lambda_{MI}\, D = \frac{U_c}{1 - \frac{U}{2\omega_0}}\left(\frac{U}{U_c} - 1\right), \qquad \gamma \gg 1. \tag{3.28}$$

and reproduces accurately previous diagrams obtained by DMFT[55, 56, 58].

Let us turn to properties of the metallic phase, which will allow us to characterize the way in which the two insulating phases are approached. By looking at the evolution with U and

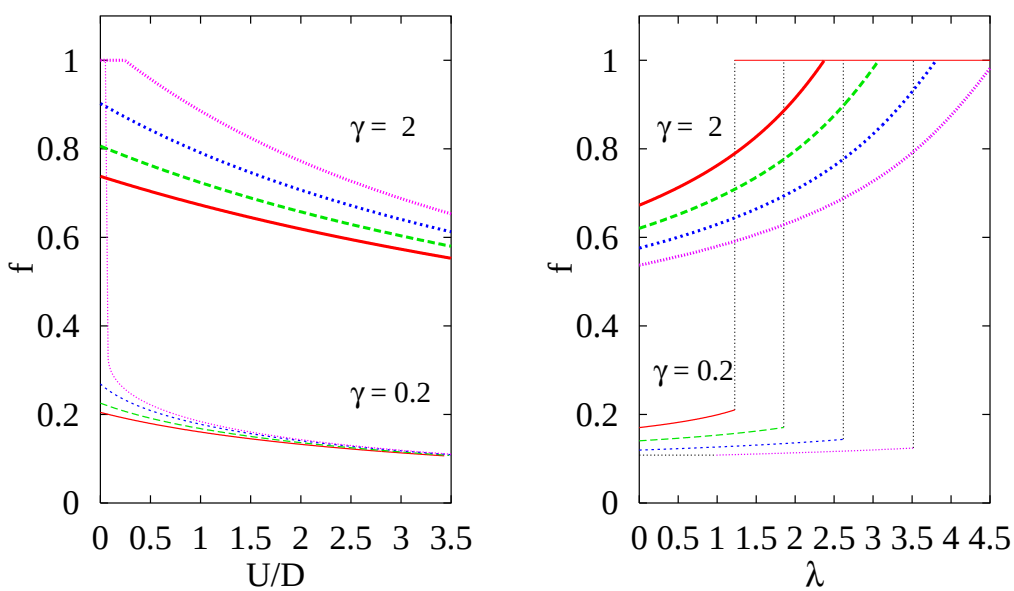

Figure 3.4: Evolution of the variational parameter f with U (left panel) and λ (right panel) by numerical solution of the mean-field equations. In both cases two values of γ are shown, representative of adiabatic ($\gamma = 0.2$) and antiadiabatic ($\gamma = 2$) regimes, with selected increasing (decreasing) λ (U) from bottom to top in the left (right) panel.

λ of the variational parameter f, which measures the effectiveness of the e-ph interaction in the system, the expected effects are recovered. From one side the increase of repulsion, which strongly suppresses charge fluctuations, makes phononic effects less relevant, as highlighted by the monotonic decrease of f with increasing U shown in Fig. 3.4. On the other hand, f is always an increasing function of the e-ph coupling constant. In both cases one can observe a smooth evolution of the mean-field solution when $\gamma > 1$, while in the adiabatic regime,

where the decrease (increase) of f is less pronounced in a wide range of U (λ), a discontinous jump to the bipolaronic solution $f = 1$ is observed, suggesting a first-order transition to the bipolaron insulator.

The interaction-driven renormalization of electronic properties is addressed in the context of slave-boson approach by looking at the behaviour of the effective mass, which is given by:

$$\frac{m^*}{m} = \frac{e^{\alpha^2 f^2}}{1 - \bar{u}^2} \tag{3.29}$$

and that has been shown to be related to the inverse of the quasiparticle residue Z. This equation clearly shows that renormalization effects on quasiparticle properties come from an effective interaction, that stems from the ratio of U_{eff} and ε_{eff}, in combination with the incremented weight due to polaron formation, namely the exponential factor $\exp[\alpha^2 f^2]$. It is worth noticing that not even in the absence of the Coulomb repulsion and in the antiadiabatic limit, where our approach should be equivalent to the LFT-based Holstein approximation, Eq. (3.29) does reduce to the known result Eq. (2.73), which is only recovered in the weak-coupling limit where the phonon-induced e-e attraction can be safely neglected. On the other hand, it fails completely when small values of γ are considered at $U = 0$, as we will detail in the following.

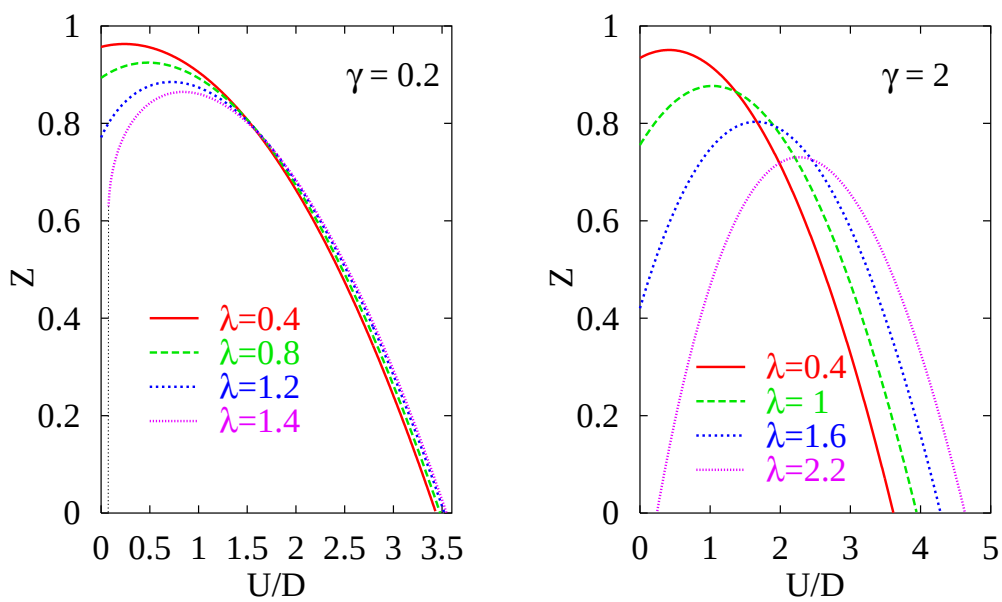

Figure 3.5: Evolution of the quasiparticle redisue $Z = (m^*/m)^{-1}$ with increasing Coulomb repulsion in the adiabatic (left) and antiadiabatic (right) regimes.

First we consider the effect of increasing U in the system with fixed λ; in Fig. 3.5 we plot the evolution of Z for two values of γ representative of adiabatic and antiadiabatic regimes,

namely $\gamma = 0.2$ (left panel) and $\gamma = 2$ (right panel). In both cases Z starts from a value smaller than one, due to the presence of a finite λ which makes quasiparticles heavier than free electrons, it increases more or less rapidly according to the strenght of the e-ph coupling, and eventually it decreases and vanishes as the Mott insulating phase is approached. As for the pure Hubbard model, the metal-insulator transition is found to be always second-order, and occurs for slightly higher values of U in the adiabatic limit, while in the opposite limit is shifted by an amount which is proportional to λD, consistently with Eqs. (3.27),(3.28). On the other hand, when moving from a pair insulator, two different behaviours are found in the considered regimes; while in the antiadiabatic regime the onset of the metallic solution is smooth with increasing Coulomb repulsion, in the adiabatic limit one finds a jump of the quasiparticle residue from zero to a sizeable value, suggesting again that in this regime the bipolaron-metal transition is first-order.

This point can be addressed directly analysing the behaviour in λ at given values of U, as we do in Fig. 3.6. We find that for large values of γ the pair insulator is approached with a smooth vanishing of the quasiparticle residue in a Hubbard-like fashion and that the critical line is shifted to larger values of the e-ph coupling, as predicted by Eq. (3.23). When considering small values of the adiabaticity parameter, however, a more complicated behaviour is observed. When the Hubbard constant U is quite small, Z decreases smoothly but it jumps discontinously to zero when the insulating phase is reached; for a slightly larger U, namely for $u = 1.5$ in Fig. 3.6, the quasiparticle residue is almost constant for quite large values of λ, before vanishing abruptly. At last, close to U_c the effect of λ is mainly to decrease the effective mass until the pair insulator is approached and the quasiparticle weight suddendly vanishes. Metallic energy crosses the insulating energy characteristic of the bipolaronic solution, hence the bipolaron transition is always first-order in the adiabatic limit; however, retardation effects are partially captured and the transition to BI is pushed to slightly larger values of λ with respect to Eq. 3.23.

A few words about the possibility of a polaronic crossover near the bipolaronic transition. We pointed out that the behaviour of the self-consistency equation for f at half-filling is analogue to the one we have discussed in the large$-U$ limit; one may expect then the opening of a coexistence region and the appearing of a polaronic transition for small values of the adiabaticity parameter. This is actually the case; however the f_+ solutions are found to be always unstable in the metallic phase, and the transition to a phase with heavy polarons is hidden by the onset of the pair insulator. On the other hand we can consider the fate of the two solutions f_-, f_+ as we approach the Mott transition from above, i.e. from $U > U_c$. As already pointed out, the present approach does not allow for a proper characterization of the Mott insulating phase, where f does not enter in the energy expression (3.6); however we can evaluate the critical $\lambda_{pol} = \lambda_c$ for the polaronic transition in the case of a vanishingly small δ. In the adiabatic regime the mean-field equations can be solved analytically and the

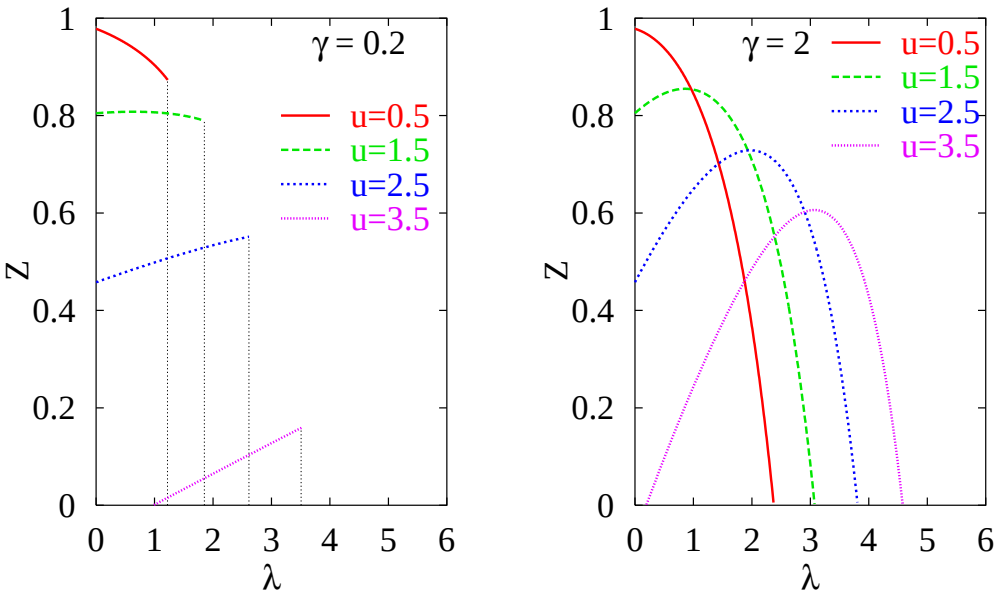

Figure 3.6: Evolution of the quasiparticle redisue $Z = (m^*/m)^{-1}$ with increasing e-ph coupling in the adiabatic (left) and antiadiabatic (right) regimes.

polaronic solution f_+ only establishes for $\delta \to 0$ at:

$$\lambda_{pol} = u\left(1 - \sqrt{1 - \frac{U_c}{U}}\right). \tag{3.30}$$

At $U \simeq U_c$ this gives $\lambda_{pol} D = U_c$, which is reduced to $U_c/2$ in the large U limit. We therefore find that in the adiabatic limit, for U close to U_c, the weak-coupling solution f_- is always the stable one even for quite large e-ph coupling up to $\lambda \simeq U$, thus showing that the Mott metal-insulator transition is robust with respect to polaron formation (of course the system is expected to switch to a bipolaronic regime when $\lambda > U$ and the attraction exceeds the repulsion). Through the stabilization of the f_- solution the strong correlations close to the Mott metal-insulator transition also protect the quasiparticles from a strong mass renormalization due to phonon effects[57]. We can also get an estimate of the Mott gap as the jump of the chemical potential $\Delta = \mu(n = 1^+) - \mu(n = 1^-)$, which, exploiting the slave-boson machinery, turns out to be:

$$\Delta = U_{eff}\,\zeta = \left(U - \alpha^2\omega_0\,(2f - f^2)\right)\sqrt{1 - \frac{1}{\bar{u}}}. \tag{3.31}$$

From this formula one finds that the Mott transition is always associated to the opening of a gap as in the pure Hubbard model and that the width of the gap is proportional to the effective interaction alone, even if the critical value for the transition is determined taking into account also polaronic renormalization of the hopping (that are however small). Finally, the inclusion of gaussian fluctuations should allow for the reconstruction of the high-energy

Hubbard bands[83]; this has been done in Ref.[61], where it has been shown that for adiabatic values of γ phonon sidebands appears only in the incoherent part of the spectral density, while the gap is slightly reduced by e-ph coupling, in good agreement with the findings of Refs. [57, 62].

To summarize, we find that the Mott metal-insulator transition is always second-order and the main effect of the e-ph coupling is to shift the transition line of an amount which depends on the value of λ and on the adiabaticity regime; to be more precise, in the $\lambda - U$ plane the slope of this line appears to be controlled by the ratio $2\omega_0/U$. However quasiparticles properties are weakly affected by phonons in the adiabatic regime, where the stable solution is characterized by small values of the variational parameter $f \propto \gamma$, as found approaching the

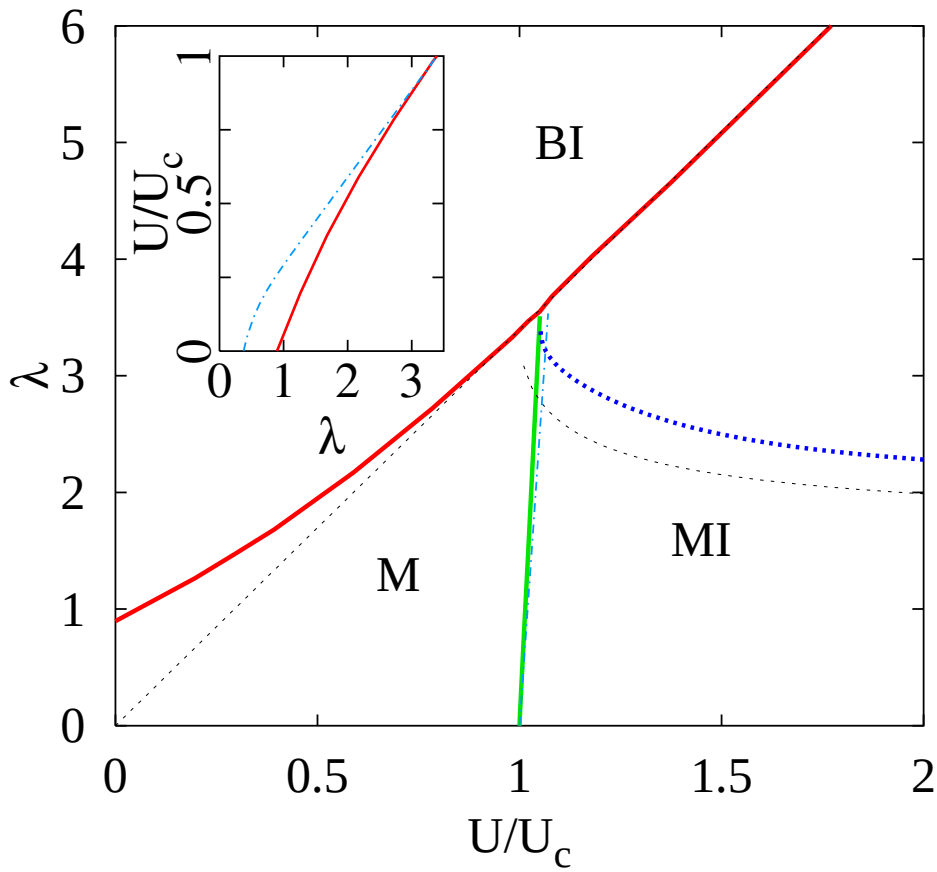

Figure 3.7: Phase diagram in the $\lambda - U$ plane of the Hubbard-Holstein model at half-filling for an adiabatic value of γ (namely $\omega_0 = 0.2|\varepsilon_0|$). Thick dotted line represents the projection of the polaronic transition line on the $\delta \to 0$ plane, while the exact adiabatic ($\gamma = 0$) results obtained in the present context for λ_{pol} and λ_{BI} are shown with thin dotted lines. For comparison also Eq. (3.23) for the Mott transition (in the inset Eq. (3.27) for the M-BI transition) is shown.

transition both from below (see Fig. 3.4) and from above (see the projection of the polaronic transition line $\lambda_{pol}(U)$ on the half-filling phase diagram Fig.3.7), and the Mott transition is therefore robust with respect to e-ph coupling and polaron formation. On the other hand the bipolaronic transition is always first-order when small values of γ are considered, while it is found to be second-order when $\gamma > 1$, as expected in the antiadiabatic regime where the Holstein model is known to map onto an attractive Hubbard model. Our analytic estimate of λ_{BI} correctly captures the qualitative behaviour of the bipolaronic transition in the presence of a repulsive Hubbard term, but it neglects retardation effects of the e-ph interaction, being equivalent to the Lang-Firsov-Holstein approximation; as a consequence screening is overestimated in the adiabatic limit and a smaller λ_{BI} is predicted with respect to the one we found by numerical solution of the mean-field equations. However, as it can be seen in the inset of Fig. 3.7, in the presence of strong repulsion Eq. (3.23) is more accurate; in fact, in order to compensate the Hubbard term and to induce an attractive interaction the strenght of e-ph interaction must be so large that strong-coupling approaches can apply.

3.4 Phonon effects on electronic properties of the correlated metal.

In this section we focus our attention on the modification induced by the e-ph coupling onto the physical properties of the correlated metal in two relevant regimes: at half filling and for small values of the doping in the large$-U$ regime.

3.4.1 Regime I : the half-filled metal

To better understand the effect of the e-ph coupling on m^*/m in the half-filling regime, when $n = 1$ and $-1 \leq \bar{u} \leq 1$, we can disentangle it from the renormalization due to the electronic correlation and expand the ratio $m^*(\lambda)/m^*(\lambda = 0)$ to lowest order in λ in the adiabatic and antiadiabatic limit, in such a way that comparison with the perturbative findings of section 2.3.1 is allowed. From Eq. (3.29) we get at half-filling:

$$\frac{m^*(\lambda)}{m^*(0)} = 1 + \frac{\lambda D}{U_c}\frac{\omega_0}{|\varepsilon_0|}\frac{m^*(0)}{m}\frac{U_c(U_c - U) - U(U + U_c)}{(U + U_c)^2} \qquad , \gamma \ll 1, \tag{3.32}$$

$$\frac{m^*(\lambda)}{m^*(0)} = 1 + \alpha^2\frac{1 + (U/U_c)^2}{1 - (U/U_c)^2} - \frac{\lambda D}{U_c}\frac{2(U/U_c)}{1 - (U/U_c)^2}, \qquad \gamma \gg 1. \tag{3.33}$$

Both formulas show that electronic correlation can change the sign of phonon-induced renormalization, consistently with the non monotonic behaviour of Z observed before. The first equation, nonetheless, does not reduce to the well-known Migdal-Eliashberg result $m^*/m = 1 + \lambda D N_0$ which is expected to hold in the adiabatic regime when taking $U = 0$, introducing

a $\gamma-$dependence that can not be interpreted as a finite band effect[1] and that would cause no renormalization in the exact adiabatic limit $\gamma = 0$; however, on the basis of the good agreement of our findings with previously reported results when approaching the Mott transition and keeping in mind that the suppression of charge fluctuations should make e-ph coupling less effective, we expect that the presence of finite Coulomb repulsion might mend this drawback. We defer further discussion on this point to the next chapter. From formula (3.32) we can compute the value of U at which the renormalization of the effective mass due to phonons is uneffective. One easily finds that at $U_0 = U_c(\sqrt{2}-1) \approx 1.47D$ corrections of $m^*(\lambda)/m^*(0)$ exactly disappear to lowest order in λ; this compensation effect is consistent with the observed almost constant dependence on λ reported in Fig. 3.6 for $u = 1.5$, suggesting also a weak dependence of the effect itself on the strength of the e-ph coupling with respect to the role played by the interplay of U and ω_0. When $U < U_0$ the effect of e-ph coupling is to increase the effective mass, as expected, while for larger values of the repulsive term the coupling with phonons causes a reduction of $m^*(\lambda)/m^*(0)$, in excellent agreement with numerical renormalization group[55, 58] and exact diagonalization[57] solutions of DMFT.

On the other hand, Eq. (3.33) does reduce to the known perturbative result $m^*/m = 1 + \alpha^2$ in the Holstein model. However we observe that in the exact antiadiabatic limit the switching on of the repulsive Hubbard interaction make the negative correction to the effective mass much more relevant than the polaron-like correction α^2, hence inducing a decrease of $m^*(\lambda)/m^*(0)$ due to phonon effects. This naïvely surprising result can be understood in terms of a reduction of the effective repulsion which prevails over the polaronic renormalization of the hopping, as one should have expected in the considered limit on the basis of the discussion of section 2.3. When considering finite but large values of the adiabaticity parameter we find that polaronic renormalizations are still relevant (enhancement of effective mass) as long as $U < U_c^2/4\omega_0$, while for larger values of the repulsion the main effect of the coupling with the phonons is to reduce the overall e-e interaction. This condition suggests that when dealing with the problem of e-ph coupling in the presence of a sizeable non-retarded interaction as the Hubbard one, the interplay between the energy scales introduced by ω_0 and U must be carefully considered, beside the more standard u,γ and λ.

In Fig. 3.8 we plot in the $U-\gamma$ plane the locus of points where the effect of e-ph coupling on $m^*(\lambda)/m^*(0)$ changes its nature. In the left region, labeled by POL, one recovers the qualitative effect observed in noncorrelated systems, namely a linear enhancement of the effective mass; in the present approach this corresponds to a major relevance of polaron-like renormalization, i.e. $\exp[\alpha^2 f^2]$. For larger values of U, on the other hand, the major effect of the coupling with phonons is to screen the Coulomb repulsion, while polaronic corrections to the kinetic energy are not able to induce sizeable enhancement of m^* at the lowest order in λ: in this region, therefore, the e-ph coupling results in a slight reduction of the effective mass, otherwise enhanced by the presence of strong correlation. As expected, screening mediated by

[1] According to the perturbative result in the presence of a finite flat band, one expects in fact a decrease of the effective mass at fixed λ with increasing γ in the adiabatic regime, namely $m^*/m \approx 1 + N_0\,\lambda D\,(1-\gamma)$.

phonons is less and less effective as the adiabatic regime is approached, enlarging the range of parameters where phonon effects on the kinetic energy are relevant; on the other hand, when $\omega_0 \lesssim D$ and the static phonon-mediated attraction is strongly reduced due to retardation effects, the presence of a sizeable U seems to protect quasiparticle properties from strong polaronic renormalizations, and we expect that for $U > 1.47D$ quasiparticle properties of the model are controlled by the physics of strongly correlated systems. We will try to explain the physical origin of this picture in the next chapter.

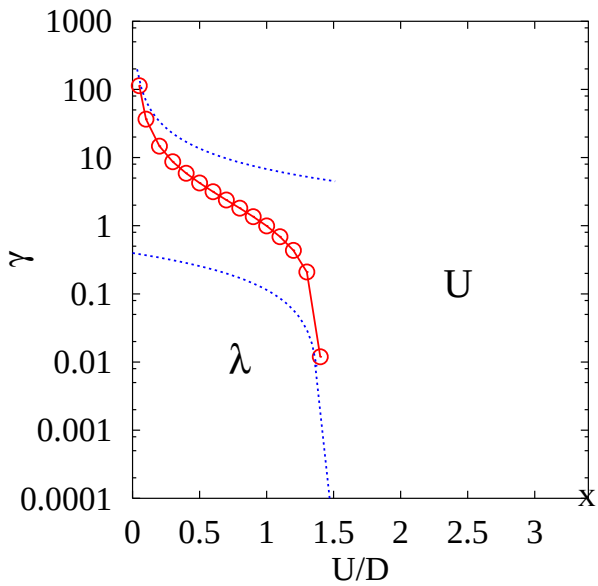

Figure 3.8: Diagram in the $U-\gamma$ plane showing the regions where phonon renormalizations are more effective than screening of the Coulomb repulsion in affecting quasiparticle properties. Dotted lines are analytical perturbative results in the adiabatic and antiadiabatic limit; circles are numerically evaluated as the points where phonon effects in $m^*(\lambda)/m^*(0)$ vanish and change sign, namely when $(1 - m^*(\lambda)/m^*(0))/\lambda D = 0$ for vanishingly small values of λ.

3.4.2 Regime II: the doped correlated metal

In the so-called vacancy regime, $\delta \ll 1$ and $\bar{u} > 1$, the effect of doping is to introduce holes and to partially restore charge fluctuations, even if they are still reduced with respect to the non-correlated system. As a consequence one can expect a stronger e-ph signature with respect to the half-filled correlated metal close to the Mott transition, namely polaronic corrections to the effective mass become more relevant if compared to renormalization effects caused by the partial screening of the Coulomb repulsion. This means that $m^*(\lambda)/m^*(0)$ should increase rather than decrease with λ in a wide range of phonon energy, and eventually become exponentially large when the polaronic transition is reached. In the present framework we

find that the effective mass to lowest order in δ reads:

$$\frac{m^*}{m} \approx \frac{e^{\alpha^2 f^2}}{2\delta} \sqrt{1 - \frac{1}{\bar{u}}}. \tag{3.34}$$

In the left panel of Fig. 3.9 we plot the typical behaviour of Z, the inverse of the effective mass, for $u = 10$ and in the adiabatic regime, $\gamma = 0.2$. As correlation effects are still relevant, being very close to the half-filling insulating phase, the e-ph coupling is not able to substantially modify the small value determined by the presence of a large U even if the expected behaviour is qualitatively observed, i.e. one finds a small reduction of Z until the polaronic transition is reached and the quasiparticle residue jumps to almost vanishing values. Another effect of the Hubbard term is to push the polaron formation to stronger couplings with respect to the weakly-correlated half-filling regime, where the bipolaronic transition occurs for values of λ that are approximatively half the value of λ_{pol} (see Fig. 3.7).

An analytical analysis similar to the one performed in the half-filling regime is less easily carried on in this case, and it proves less relevant due to the many approximations needed in order to get perturbative expansions. However, we can solve numerically the mean-field equations and analyze the weak-coupling effects of phonons on the correlated effective mass. As highlighted in the right panel of Fig. 3.9, quasiparticles properties display an unusual dependence on the phonon frequency. We consider here a finite Coulomb repulsion, $U = 5D$, not too far from the half-filling Mott point, at $\delta = 0.1$, and plot the evolution of the normalized $Z(\lambda)/Z(\lambda = 0)$ in the region $\lambda \lesssim 1$, well before the polaronic transition. It is not surprising that for $\omega_0 \gtrsim U$ the main effect of e-ph coupling is to increase Z; analogously to the half-filling regime discussed before, in this case λ mainly decreases the localizing power of Coulomb repulsion, and polaronic renormalizations are negligible. For a wide range of $\gamma \lesssim u$, on the other hand, one observes the expected reduction of the quasiparticle residue, whose slope, however, displays a nonmonotonic dependence on the phonon frequency that suggests a more complex interplay between the involved energy scales. Namely, the negative slope increases up to $\gamma \sim 0.6$, while for smaller value of the adiabaticity parameter the reduction of $Z(\lambda)/Z(0)$ becomes slower and slower. We can address this unusual frequency dependence by plotting the effective mass as a function of γ, as we do in Fig. 3.10 for three values of the e-ph coupling. One observes that up to values of $\gamma \approx 4$ increasing the e-ph coupling strenght induces an enhancement of the effective mass, while for larger values of the adiabaticity parameter screening of the Coulomb repulsion become more relevant and the effective mass is reduced; in the low-frequency region, however, a nonmonotonic behaviour is found with a maximum located at $\gamma \approx 0.7$ irrespectivly of the strenght of λ, signalling more relevant effects of e-ph coupling. This result is qualitatively consistent with Ref. [60], where the same dependence on the phonon frequency is found, even if the maximum is observed at $\gamma \simeq 0.3$. We can try to disentangle polaron-like effects from phonon-induced renormalizations of the correlation by plotting separately the exponential polaronic contribution to the effective mass and the inverse of the ratio $q(\lambda)/q(\lambda = 0)$, which in our approach captures the reduction of the kinetic energy due to the e-e interaction. As shown in the right panel of Fig. 3.10, well deep

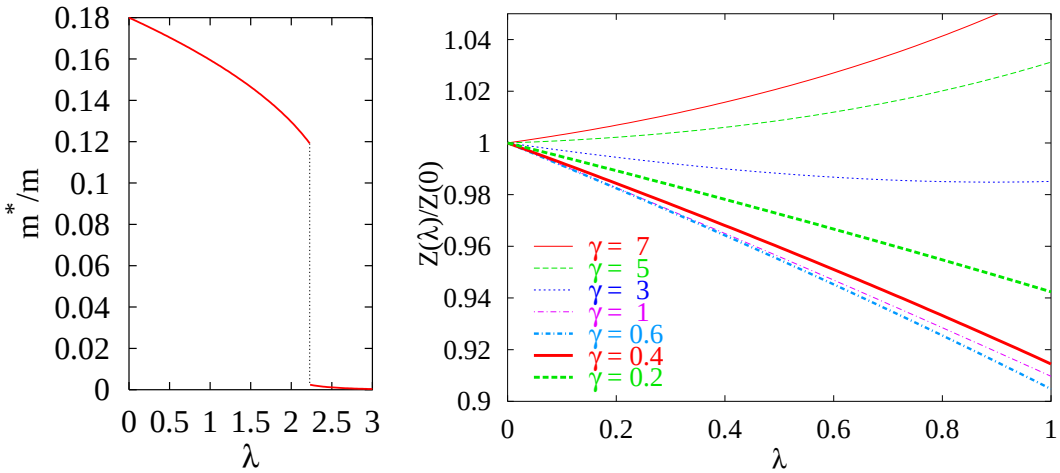

Figure 3.9: Evolution with λ of the effective mass in the doped correlated metal. Left panel: characteristic behaviour of m^*/m in the adiabatic regime ($\gamma = 0.2$), where the sudden jump signals the polaronic transition. Right panel: evolution of the inverse of effective mass normalized with the $\lambda = 0$ quasiparticle residue for different values of the adiabaticity parameter at $U = 5D$.

in the adiabatic regime screening effects are almost completely absent, and $q(\lambda)/q(0) \simeq 1$; the enhancement of $m^*(\lambda)/m^*(0)$ is due mainly to polaronic exponential renormalization. When γ is increased, screening effects begin to be effective and $q(0)/q(\lambda)$ is reduced, meaning a less repulsive e-e interaction and slightly compensating the polaronic enhancement of the effective mass. Eventually, at $\omega_0 \simeq D$, the exponential renormalization starts to decrease and the overall effect is a reduction of $m^*(\lambda)/m^*(0)$, as expected in the antiadiabatic limit.

3.4.3 Unusual isotope effects

The influence of the adiabaticity parameter on the properties of the metallic phase is reflected in unusual isotope effects on the effective mass, that can be addressed quite directly in the present approach by considering the isotope coefficient defined as $\alpha_{m^*} = -d\ln(m^*)/d\ln(M)$, where M is the ionic mass. Since $g \propto 1/\sqrt{M\omega_0}$ and $\omega_0 \propto 1/\sqrt{M}$, the e-ph coupling constant λ is independent of M and α_{m^*} can be rewritten as:

$$\alpha_{m^*} = \frac{1}{2}\frac{d\,\ln(m^*/m)}{d\,\ln(\gamma)}. \tag{3.35}$$

As discussed in Ref. [112], in the pure Holstein model at half-filling this isotope coefficient is a negative increasing function of γ in the adiabatic limit, starting from zero as predicted in Migdal-Eliashberg theory, while it displays a nontrivial behaviour for intermediate values of the adiabaticity parameter until it decreases as $1/\gamma$ approaching the antiadiabatic limit. As a function of the e-ph coupling, Paci and coworkers showed also that polaron formation is

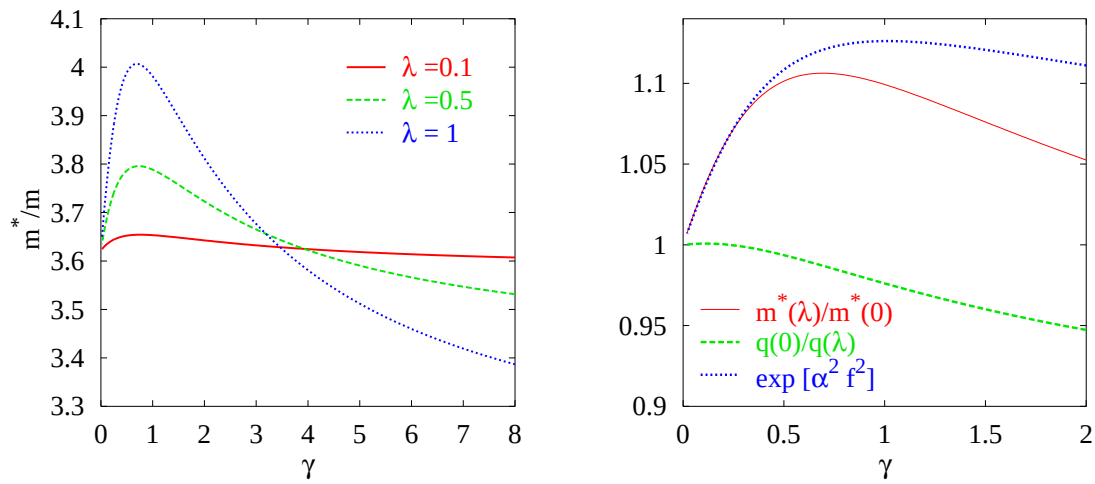

Figure 3.10: Evolution with γ of the effective mass in the doped correlated metal for three selected values of the e-ph coupling at $U = 5D$ and $\delta = 0.1$. In the right panel the two main contributions to $m^*(\lambda)/m^*(0)$, namely the correlation-induced $q(0)/q(\lambda)$ and the polaronic $\exp(\alpha^2 f^2)$ renormalization, are shown for $\lambda = 1$.

reflected in huge negative values of α_{m^*} [112]. Such a huge effect is expected also in the system we are considering, due to the $\gamma-$dependence of kinetic and interaction renormalizations. In the Hubbard-Holstein model we find that the isotope coefficient acquires the following expressions:

$$\alpha_{m^*} = 4\gamma \frac{\lambda D}{U_c} \frac{(1-f)}{1+\bar{u}} \frac{m^*}{m} \left[(1-\bar{u}-\bar{u}^2)\frac{df}{d\gamma} - \frac{f}{2\gamma}(1+\bar{u}^2) \right], \tag{3.36}$$

$$\alpha_{m^*} = \frac{\lambda}{4} \frac{f}{1-\frac{1}{\bar{u}}} \left[4\frac{\bar{u}-1}{2\bar{u}-1}\frac{df}{d\gamma} - \frac{f}{2\gamma}\frac{2\bar{u}-1}{\bar{u}} \right], \tag{3.37}$$

in regime I ($n = 1, \bar{u} < 1$) and regime II ($\delta \ll 1, \bar{u} > 1$) respectively. We can exploit the self-consistency equation Eq. (3.22) to compute the derivative $df/d\gamma$:

$$\frac{df}{d\gamma} = \frac{f(1-f)}{\gamma} \frac{1-\alpha^2 f^2 \frac{1}{1+\bar{u}}}{1-\alpha^2 f^2 (1-f)\frac{3+\bar{u}}{1+\bar{u}}} \qquad \text{Regime I,}$$

$$\frac{df}{d\gamma} = \frac{f(1-f)}{\gamma} \frac{1-\alpha^2 f^2 \frac{2\bar{u}}{2\bar{u}-1}}{1-\alpha^2 f^2 (1-f)\frac{8\bar{u}^2-4\bar{u}-2}{4\bar{u}^2-4\bar{u}+1}} \qquad \text{Regime II.}$$

At half-filling the main effect of the Coulomb repulsion is to induce in the isotope coefficient a direct proportionality to the electronic effective mass, suggesting an unexpected enhancement of phonon signatures in the metallic properties. To be more precise this means that one can observe huge isotope effects even for relatively small values of the e-ph coupling when a sizeable repulsion interaction is considered altogheter. We consider here values of U larger than $1.5D$, since we have seen in the previous sections that our approach is probably not reliable in reproducing e-ph effects in the adiabatic limit below this value of the Hubbard

interaction, introducing a wrong dependence on γ. As we will detail in the following, however, we expect to capture the right physics in the presence of sizeable e-e correlation. As shown in

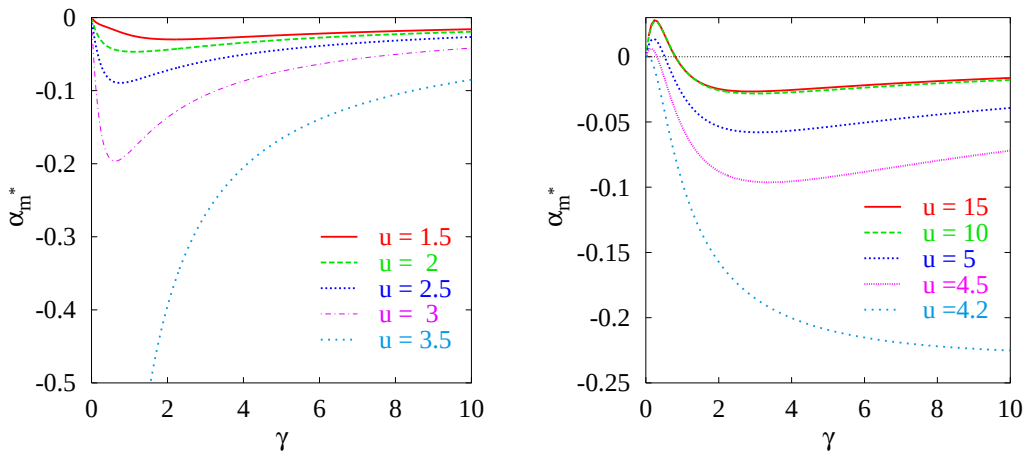

Figure 3.11: Dependence of the isotope coefficient α_{m^*} on the adiabaticity parameter for a fixed e-ph coupling ($\lambda = 0.8$) and different values of the Hubbard interaction in the half-filling metallic regime (right panel) and in the correlated vacancy regime (left panel)

the left panel of Fig. 3.11, the expected enhancement of the isotope effect on m^*/m depends crucially on the value of the Hubbard U and on the adiabaticity parameter. Consistently with our analysis of phonon effects on quasiparticle effective mass, α_{m^*} is always negative for all considered values of U, and displays a minimum at intermediate γ that gets deeper as the critical value for the Mott transition is approached, eventually leading to a divergence when the phonon-induced screening is no longer able to prevent the localization due to the strong electronic correlation.

The isotope effect has a different behaviour in the doped correlated regime. As suggested by the dependence on γ of the effective mass shown in Fig. 3.10, the isotope coefficient can be positive for rather small values of the adiabaticity parameter and change sign with increasing γ, approaching monotonically the asymptotic antiadiabatic value $-\alpha^2/2$. This behaviour is clearly shown in the right panel of Fig. 3.11, where a fixed value of the e-ph coupling ($\lambda = 0.8$) is considered for different values of U. Notice that the sign and the magnitude of α_{m^*} is very sensitive to the values of the phonon frequency and of Coulomb repulsion, and very small values of the isotope coefficient can be observed in the crossover regime between the adiabatic (with positive α_{m^*}) and antiadiabatic (with negative isotope coefficient) limit; this means that the presence of sizeable e-e correlation can result in an almost vanishing isotope coefficient without implying that a Migdal-Eliashberg picture holds. When very large values of U are considered the $\gamma-$dependence of α_{m^*} does not change much; on the other hand, when approaching the critical value for the half-filling Mott transition, the position of the zero of $\alpha_{m^*}(\gamma)$ moves toward zero. For $U = 4.2D$, that correspond to the zero-doping critical U_{MI} for the considered λ in the antiadiabatic limit, the isotope coefficient becomes

almost immediatly negative and rapidly decreases with increasing γ.

Chapter 4

Drawbacks of the variational LFT

When dealing with approximate variational methods, the identification of the range of validity of the approximations made and possibly the understanding of the reason why such approximations lead to poorly accurate results for given values of the physical parameters allow to recognize the ingredients that are missing and, if possible, to develop more accurate methods able to include them. On the other hand, control of such approximations is needed to test the quality of the guess made in the variational description of a given system, that implies that physical intuition can be checked almost directly. For this reason we devote this section to the analysis of the drawbacks of the slave-boson approach supplemented with a variational Lang-Firsov transformation.

In the previous chapter it has been often pointed out the limited accuracy of our method in the description of the adiabatic regime. This is not surprising, since the starting point of our approach, the Holstein-Lang-Firsov approximation, is known to be reliable only if large values of the adiabaticity parameter are considered, when multiphonon processes are negligible and lattice deformations rapidly adapt themselves to the electronic motion. For instance, the dependence on γ of the effective mass when no e-e correlation is included (cfr. Eq. (3.32)) would predict in the present approach no signatures at all of the e-ph coupling in the exact adiabatic limit; this result is clearly wrong and contrasts with the well-known Migdal-Eliashberg prediction of linear enhancement of m^* with increasing λ. However, by comparing our findings with the many numerically exact results existing in the literature, we can observe that the main effects of phonons on the top of the strongly-correlated system are at least qualitatively captured by our method, *even in the adiabatic regime*. This can be understood naïvely in terms of decreased mobility of the electrons due to correlation effects, that means that local lattice deformations should have the time to follow the slow varying position of electrons, hence behaving in a more "antiadiabatic" fashion. This is not always the case, as we discuss in the next section. In the following section 4.2 we will try instead to understand the approximation introduced by the variational LFT in terms of trial phonon wavefunctions.

4.1 Adiabatic failure in the weakly correlated regime

In order to evaluate to what extent our procedure fails in the adiabatic limit when weak correlations are considered, we can compare our results for $U = 0$ with ME perturbation theory. Starting from the observed linear dependence of the effective mass with increasing e-ph coupling, $m^*/m = 1 + r\lambda D$, we can analyze the evolution of the slope r as a function of the adiabaticity parameter for vanishingly small values of λ. It is known that in the exact adiabatic limit (namely for an infinite flat band in the ME framwork) $r = N_0$, i.e. the density of states at the Fermi level, that is given by $2/\pi D \simeq 0.6366$ for a semicircular density of states. In the opposite limit the lowest order perturbation theory gives $m^*/m = 1 + \alpha^2$, hence $r = 1/2\gamma D$ in our formulation. When a finite band is considered, the increase of γ is expected to induce a reduction of the coefficient r. The effective mass reads:

$$\begin{aligned} \frac{m^*}{m} &= 1 - \frac{\partial}{\partial \epsilon} Re\Sigma(\omega)\Big|_{\omega=0} = \\ &= 1 + g^2 \left(\int_{-D}^{0} d\xi \frac{N(\xi)}{(\omega_0 - \xi)^2} + \int_{0}^{D} d\xi \frac{N(\xi)}{(\omega_0 + \xi)^2} \right). \end{aligned}$$

In the simple case of a finite flat band of width $2D$ the integration is readily carried out, and one finds for the coefficient r:

$$r = \frac{N_0}{1+\gamma}. \tag{4.1}$$

When considering a semicircular density of states an analogue behaviour is actually found. In the left panel of Fig. 4.1 we show the results obtained by means of perturbation theory, both with a flat (PT-I) and semicircular DOS (PT-II), togheter with those derived in the present framework (VLF) and by means of the Dynamical Mean-Field Theory[113], comparing also with the antiadiabatic result (LF). All methods coincide in the regime of large γ, as expected. The qualitative behaviour of perturbative results (PT-I and PT-II) is the same and DMFT accurately reproduces the evolution of r for the semicircular density of states, reducing to Migdal-Eliashberg result when $\gamma \to 0$. On the other hand our approach is qualitatively correct in describing the phonon frequency dependence of r coming from the large$-\gamma$ region, even if it appears less and less accurate as the adiabatic limit is approached, *but it is completely wrong as soon as* $\omega_0 \lesssim D$.

However, as electronic correlation is introduced, we expect phonon effects to be strongly reduced due to the reduction of charge fluctuations to which phonons are coupled. We test this idea by comparing our findings for $r = (m^*(\lambda)/m^*(0) - 1)/\lambda D$ with those obtained in the DMFT framework[113], where the ratio of $m^*(\lambda)$ over the effective mass $m^*(0)$ due to Hubbard U only is taken in order to disentangle phonon effects from correlation ones. In this case the agreement is almost quantitative even for very small values of γ.

We can try to understand the origin of this behaviour by looking at the energy dependence of the self-energy discussed in sec.2.3.1. There we found that in the antiadiabatic limit, when $D \ll \omega_0$, the real part of the self-energy depends linearly on ω for all the energies in the band. On the other hand, when $D \gg \omega_0$, the phonon frequency falls inside the electronic band and

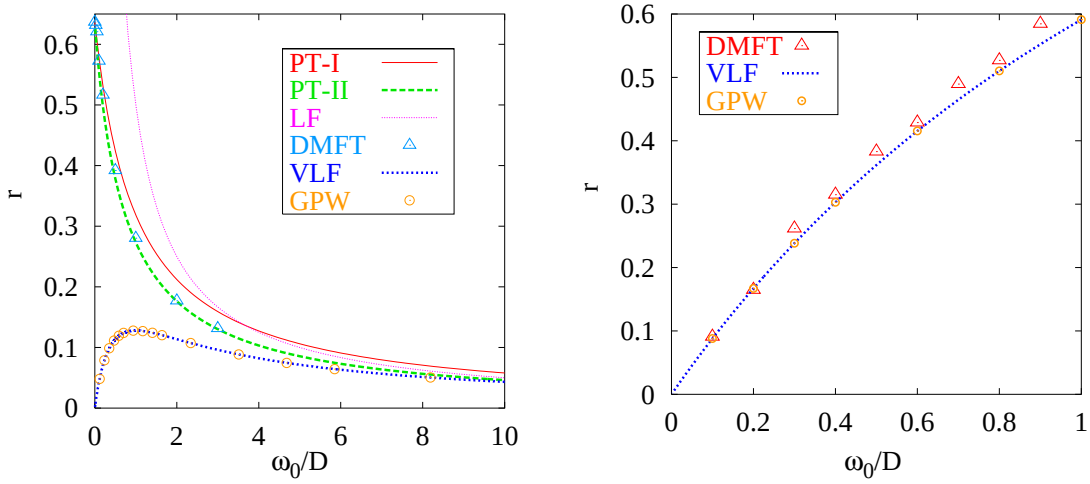

Figure 4.1: Coefficient r defined as the slope of the effective mass for small e-ph coupling constant ($r = (m^*(\lambda)/m^*(0) - 1)/\lambda D$) as a function of γ in the case of no e-e correlation (left) and for $U = 2.5D$ (right). In the pure Holstein model we compare our findings (VLF) with DMFT and perturbative analytic results; PT-I (PT-II) labels the result obtained in perturbation theory for a finite flat (semicircular) DOS, while LF is the antiadiabatic prediction. GPW results are obtained by means of a Gutzwiller phonon wavefunction to be discussed in chapter 5. In the right panel comparison between VLF and DMFT is shown.

discriminates between two energy regions, namely $|\omega| \gtrless \omega_0$; only when $|\omega| < \omega_0$ the self-energy displays a linear dependence on energy, while in the opposite limit it is proportional to $1/\omega$ with a nonzero imaginary part, signalling the emergence of incoherent contributions to the spectral function.

Let us consider then the electron Green function within our variational LFT slave-boson formulation, that reads:

$$\begin{aligned} \mathcal{G}(\mathbf{k},\omega) &= \frac{q\, e^{-\alpha^2 f^2}}{\omega - q\, e^{-\alpha^2 f^2}\, \xi_{\mathbf{k}}} \\ &= \frac{q}{\omega - q\, \xi_{\mathbf{k}} - \Sigma_{ph}(\omega)}, \end{aligned} \tag{4.2}$$

where the phonon effect is included in the self-energy

$$\Sigma_{ph}(\omega) = -\omega \left(e^{\alpha^2 f^2} - 1 \right). \tag{4.3}$$

Therefore in the context of a mean-field approximation, phonon effects on the electron Green function are described by a self-energy that depends linearly on the energy ω. This explains why our approximation is expected to give reliable results even in the weakly-correlated regime as long as $\omega_0 \gtrsim D$; on the other hand it clearly fails to describe the adiabatic limit of the Holstein model (when $q = 1$) since it can not capture the incoherent phononic contributions arising for electronic energies inside the band. However, the Green function given

by Eq. (4.2) describes quasiparticle properties inside a renormalized band of half bandwidth qD. In the presence of strong e-e interaction $q \ll 1$, and even in the adiabatic regime it may happens that relation $\omega_0 \gg qD$ holds, which is nothing but an antiadiabatic condition for the renormalized band. This finding seems to suggest the e-e correlation pushes the system toward a more antiadiabatic regime, slowing down the electron dynamics so that the phonons can catch up.

We notice that the renormalized adiabaticity parameter ω_0/qD we have just introduced should be considered as a control parameter for the validity of our approach, and it does not necessarily mean that the system displays antiadiabatic physics when large values of U are considered. As we have discussed previously, the effective Hubbard interaction close to the Mott transition is weakly reduced by the e-ph coupling, while it is known that screening effect is highly effective when phonons are fast enough to follow electronic motion. Actually the renormalization of U is controlled by the ratio $2\omega_0/U$ rather than ω_0/qD, suggesting a more adiabatic behaviour of screening processes. This point has been addressed in Ref. [57], where the adiabatic limit of the Hubbard-Holstein model close to the Mott transition has been inspected by means of DMFT. Sangiovanni and coworkers found that the low-energy properties of the system can be reproduced by an effective Hubbard model with a reduced interaction $U_{eff} = U - \eta\lambda D$, where $\eta = 2\omega_0/U/(1 + 2\omega_0/U)$. On the basis of analogy with Kondo processes they explained this finding as follows: quasiparticle motion arise from virtual processes in which doubly-occupied (empty) sites are created, processes that are rare but very fast (with a time scale $\propto 1/U$). When the phonon frequency is small with respect to U, one has $1/\omega_0 \gg 1/U$ and phonon degrees of freedom are frozen during the virtual excitation processes. Therefore, despite the overall electron motion is quite slow *due to the small number of virtual processes*, phonons can not follow hopping processes and the e-ph interaction has no major effect than a slight reduction of the total static repulsion.

On the light of this picture, therefore, the physical meaning of the validity condition derived before is the following. When considering the weakly-correlated system, incoherent contributions to electronic spectral function due to e-ph coupling are relevant as long as $\omega_0 \lesssim D$, and our approach is not able to capture them: this is reflected in the simplified form of the phonon self-energy Eq. (4.3). The presence of a sizeable U, however, induces a separation between a low- (coeherent) and a high- (incoherent) energy sector; this is a well-known property of the pure Hubbard model, where this separation is clearly evident in the density of states already for $U = 2D$ (second panel from the top in Fig. (2.1). In this case the phonon incoherent contributions to the electron spectral function are pushed outside the renormalized band of half width qD and mainly affect the Hubbard bands, while major renormalization on the effective mass comes from the presence of a repulsion term which, in the adiabatic limit, is little reduced by the e-ph coupling. This should explain from one hand the somehow unexpected good description of the correlated regime in the adiabatic limit provided by our variational mean-field approach, and on the other the physical origin of the robustness of Mott transition, and in general of the correlated physics (when $n = 1$), with

respect to polaron fomation. We notice that these considerations should not apply in the doped correlated regime, as no clear separation of energy scales occurs. However when very large values of the Coulomb repulsion are taken into account electrons still move very slowly, even if real hopping processes are gradually restored with increasing doping; this means that phonons can actually catch up and more rapidly adapt to the slow-in-time varying position of electrons, giving rise to polaronic renormalizations of the effective mass, clearly displayed in Fig. 3.10.

4.2 Polaron formation in the adiabatic regime

As already pointed out in the derivation of the effective electronic Hamiltonian for the Hubbard-Holstein model, the present approach takes poorly into account phonons, that are substantially described as displaced harmonic oscillators. Their displacement is controlled by the variational parameter f and is determined by minimizing the balance between the potential energy gain due to local deformations of the lattice and the depletion of electronic kinetic energy resulting from the increased weight of the charge carriers followed by the multiphonon cloud that arises from the lattice deformation. In this way one hopes to partially capture retardation effects, particularly strong in the adiabatic regime, that would cause a less pronounced distortion of the lattice. This is reflected in the decreasing behaviour of f with lowering γ.

However it is known that such retardation effects strongly affect the shape of the phonon wavefunctions when in the adiabatic regime[88] and this may explain the scarse accuracy of our method in this limit; if one can expect to capture the modification of electron properties induced by the coupling with the phonons for some range of the parameters, as discussed previously, there is little hope to describe accurately phonon quantities, not even their true displacement. This means that the polaron formation can be actually addressed only by looking at the strong renormalizations of the charge-carriers effective mass, while the phonon displacement probability distribution function (PDF), that has been often introduced as a key quantity in the characterization of local polarization[92, 95], is not reliable when evaluated in the present approach. To better understand the origin of this drawback, let us reformulate our approach in a slightly different way.

Instead of deriving an effective Hubbard-like Hamiltonian with renormalized parameters and apply the slave-boson machinery on the top of this model, we can try to exploit the capability of the slave bosons to describe the local charge states. This should be sensible, as phonons couple with local charge density in the Holstein model and lattice displacements are connected to local electron occupations (cfr Eq. 2.50). We can therefore operate a variational transformation on the Hubbard-Holstein model with its electronic part expressed in terms of the slave operators as in Eq. (2.35), since it has been proved that the two formulations are completely equivalent as long as the constraints given by Eqs. (2.31)-(2.32) are satisfied[80, 82]. Within the same spirit of the transformation (3.2) we perform a generalized LFT U^S

with:

$$S = \alpha \sum_i \left[f_i^{(0)} e_i^\dagger e_i + \sum_\sigma f_{i\sigma}^{(1)} p_{i\sigma}^\dagger p_{i\sigma} + f_i^{(2)} d_i^\dagger d_i \right] (a_i - a_i^\dagger), \tag{4.4}$$

where we have introduced four variational parameters for each site i, namely $f_i^{(0)}, f_{i\sigma}^{(1)}, f_i^{(2)}$, and average over the phonon vacuum state in order to get rid of phonon degrees of freedom (Holstein approximation). The variational parameters represent then the degree of phonon displacement for a given charge state at site i. The way in which the e-ph coupling affects hopping processes is made clearer in this formulation, as the bosonic operators $z_{i\sigma}$ which describe charge mobility read now:

$$\tilde{z}_{i\sigma}^\dagger = \frac{p_{i\sigma}^\dagger e_i e^{-\frac{\alpha^2}{2}(f_i^{(0)} - f_{i\sigma}^{(1)})^2} + d_i^\dagger p_{i\bar{\sigma}} e^{-\frac{\alpha^2}{2}(f_{i\bar{\sigma}}^{(1)} - f_i^{(2)})^2}}{\sqrt{1 - d_i^\dagger d_i - p_{i\sigma}^\dagger p_{i\sigma}} \sqrt{1 - e_i^\dagger e_i - p_{i\bar{\sigma}}^\dagger p_{i\bar{\sigma}}}}. \tag{4.5}$$

It is then clear that polaronic renormalization arises in the present framework from the overlap between the displaced harmonic oscillators associated to the two charge states involved in the hopping process[1]. When phonons are coupled to charge density fluctuations, one finds at the mean-field level and in the half-filling paramagnetic phase that $f_\sigma^{(1)} = 0$ and $f^{(0)} = -f^{(2)} \equiv f$ and, as detailed in the appendix, one recovers the results discussed in the previous chapter.

We are now in the position to discuss the unaccuracy of the variational Lang-Firsov-Holstein approximation in describing phonon displacements and polaron formation when adiabatic regimes are considered. As shown in Fig. 4.2 for the single-polaron problem, when small values of γ are considered the phonon wavefunction can acquire a non-Gaussian shape for intermediate values of the e-ph coupling; in particular, even if the peak position shifts toward the strong-coupling value $X_0 = \sqrt{2}\alpha$, it can develop a shoulder for smaller X that illustrates the retardation effect of the motion of the electron and that of the molecular deformation. In our case, where phonons are coupled to charge density fluctuations, we expect that the singly-occupied state will not be followed by any deformation, while the empty and doubly-occupied states will cause lattice displacement in opposite directions, consistently with our finding of vanishing $f_\sigma^{(1)}$ and that $f^{(0)} = -f^{(2)}$. By looking at Fig. 4.2 it is clear that the overlap between the displaced wavefunction and the oscillator centered in zero can be enhanced by the presence of the shoulder, even if the actual distortion, signalled by the position of the peak, is rather strong. Our approximate variational wavefunction can exploit only the amount of the displacement, since its shape remains that of a gaussian function while it rigidly adjusts to minimize the energy that emerges from the balance of potential energy gain and kinetic energy loss. We can therefore expect an underestimation of the

[1] This is readily understood by considering the overlap between a harmonic oscillator $|0\rangle$ centered in zero and an oscillator displaced of an amount $\sqrt{2}\delta$, that can be expressed as $|\delta\rangle = e^{i\hat{P}\sqrt{2}\delta}|0\rangle = e^{\delta\,(a - a^\dagger)}|0\rangle$; one then finds that $\langle\delta|0\rangle = e^{-\delta^2/2}$.

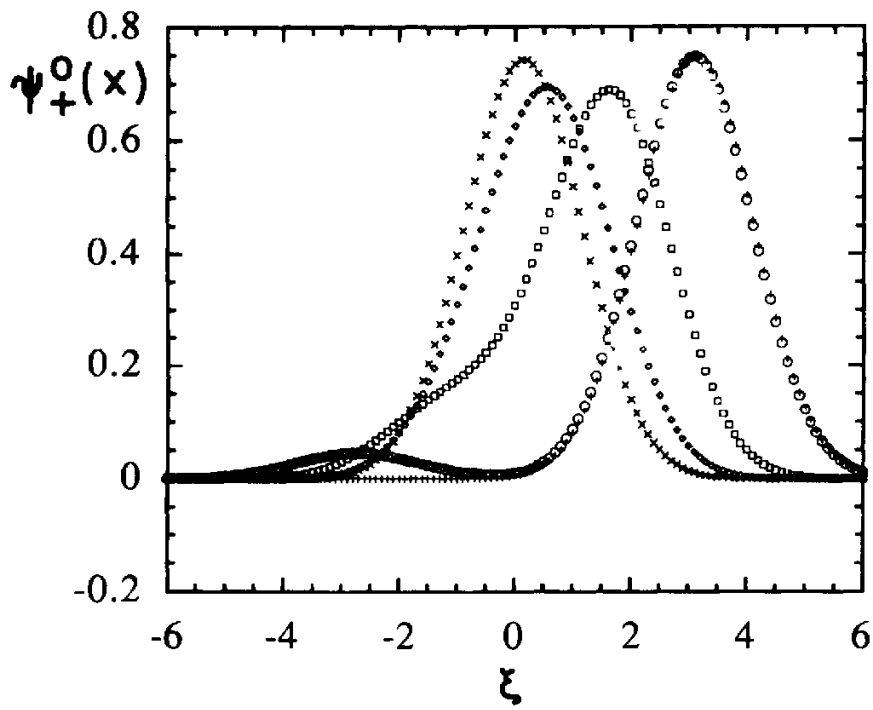

Figure 4.2: Ground-state oscillator wavefunction of the two-site single-polaron problem as a function of the phonon displacement $\xi = X/\sqrt{2}$ for various values of the deformation coupling α in the adiabatic regime (from Ref. [88]).

phonon displacement, that can be crucial in the intermediate coupling regime where polaron formation is expected to occur.

The rigidity of the trial wavefunction with respect to phonons can be responsible for the first-order BI transition observed in the half-filling regime for small values of the adiabaticity parameter and especially for the lack of polaron formation signatures just before the bipolaronic insulating phase is reached. Nonetheless, such a polaron formation is reflected in the development of a bimodal PDF observed by many authors in the Holstein model [92]-[96] and the order of the bipolaronic transition has been found to be second-order at least in the weakly-correlated limit of the Hubbard-Holstein model[55]. Of course one has to remember that a strong-coupling approach to the e-ph problem alone is probably not suitable even when sizeable e-e interaction is mediated by the phonons, and probably mending of this drawback is not able to provide an accurate description of the system. On the other hand the first-order polaronic transition found in the doped correlated regime is a clear outcome of the poor description of phonon wavefunction, since in this case the correlated physics described by the slave-boson approach proves to be the correct starting point in order to include phonon effects. The next chapter is therefore devoted to a suitable generalization of the trial phonon wavefunction in the presence of strong correlation.

Chapter 5

Extended Gutzwiller approach

5.1 Introducing the method

We have seen in chapter 2 that the Gutzwiller approach and the slave-boson technique at the mean-field level are exactly equivalent when dealing with electronic correlation alone. The advantage of the second approach with respect to the first one is that dynamical quantities such as the Green functions become accessible, and generalization to the finite temperature case is straightforward in the functional integral representation; furthermore, slave bosons provide the proper framework in which corrections to mean-field results can be included by considering fluctuations of the slave operators around their saddle-point values. However, the Gutzwiller approach allows for a direct analysis of the trial wavefunction in a variational spirit, and the equivalence with the more sophisticated slave-boson technique suggests in fact that such a trial wavefunction, where the quantity to be optimezed is substantially the occupation probability distribution in the presence of a local non-retarded interaction, correctly describes the low-energy physics of a strongly-correlated system.

On the basis of this equivalence and of the discussion made in the previous chapter, our search for the best variational wavefunction able to describe phonons in the presence of strong correlation will build on the Gutzwiller wavefunction, already defined in section 2.2.1:

$$|\Psi_{GPW}\rangle = \prod_i \mathcal{P}_i |\Psi_0\rangle, \tag{5.1}$$

where $\mathcal{P}_i$ is a many-particle correlator acting on a general noninteracting (single-particle product) state $|\Psi_0\rangle$. Within this representation the Gutzwiller approach can be actually generalized to different many-body problems, since one has a certain arbitrariness in choosing the form of the uncorrelated wavefunction and that of the correlator $\mathcal{P}_i$. In the spirit of the original proposal of Gutzwiller, this last quantity generally projects the uncorrelated state over the exact eigenstates of the atomic limit of the model. This means that local correlations are usually treated quite accurately, whereas the main approximations arise in the description of hopping processes. Of course, when introducing a retarded interaction, this approach can turn less accurate, since the atomic limit is not necessarily a good starting point due to the

dynamical effects that are indeed relevant to determine the local properties of the system.

5.1.1 The electron-phonon Gutzwiller wavefunction

In the following we will be concerned with the paramagnetic phase of the Hubbard-Holstein model. The most suitable uncorrelated wavefunction to start from is then the Slater determinant describing a Fermi sea as:

$$|\Psi_0\rangle = \prod_{|k|<k_F} c^\dagger_{k\uparrow} c^\dagger_{k\downarrow} |0\rangle. \tag{5.2}$$

In order to make the comparison with the atomic limit easier, we consider a slightly different Hamiltonian for the model, namely:

$$H = -t \sum_{<i,j>,\sigma} c^\dagger_{i\sigma} c_{j\sigma} + \frac{U}{2} \sum_i (n_i - 1)^2 + \omega_0 \sum_i a^\dagger_i a_i - \alpha\omega_0 \sum_i (n_i - 1)(a^\dagger_i + a_i), \tag{5.3}$$

where the electron-phonon and the correlation terms have been rescaled in order to include the chemical potential shift $\mu = U/2 - 2\alpha^2\omega_0$ of the highly symmetric half-filling case. By considering the atomic limit of this Hamiltonian, one immediately finds the following eigenstates and eigenvalues for the ground state:

$$\begin{aligned}
&\varphi_0(X)\,|0\rangle && \text{with energy} \quad E_{at}(0) = \frac{1}{2}\Big(\omega_0 + U - 2\alpha^2\omega_0\Big) \\
&\varphi_1(X)\,|1\rangle && \text{with energy} \quad E_{at}(1) = \frac{\omega_0}{2} \\
&\varphi_2(X)\,|2\rangle && \text{with energy} \quad E_{at}(2) = \frac{1}{2}\Big(\omega_0 + U - 2\alpha^2\omega_0\Big)
\end{aligned} \tag{5.4}$$

where $\varphi_l(X)$, i.e. the eigenfunctions of the local phonons, are displaced harmonic oscillators $\phi(X - X_0(l))$ with the displacement depending on the number of electrons sitting on the atom according to $X_0(l) = \sqrt{2}\alpha(l-1)$. The atomic solution suggests the introduction of different phonon wavefunctions for different charge states, and we can generalize the projection operator defined within the formulation developed by Bünemann *et al.*[74] (cfr. section 2.2.1) as follows:

$$\mathcal{P}_i(X_i) = \sum_{l=0,1,2} \sqrt{\frac{P_l}{P_l^{(0)}}}\, \varphi_l(X_i)\; |l_i\rangle\langle l_i|. \tag{5.5}$$

As for the pure Hubbard model discussed previously, here $|l_i\rangle\langle l_i|$ represent the projection operator at site i onto states with l electrons, while $P_l^{(0)}$'s (P_l's) are the occupation probabilities of the $l-$electron configuration in the uncorrelated $|\Psi_0\rangle$ (correlated $|\Psi_{GPW}\rangle$) wavefunctions. In the paramagnetic sector with an average electron density n, the coefficients $P_0(l)$ are given by:

$$P_0^{(0)} = (1 - n/2)^2, \qquad P_1^{(0)} = (n/2)(1 - n/2), \qquad P_2^{(0)} = (n/2)^2,$$

whereas the occupation probabilities of the correlated state are variational parameters to be determined by minimization of the energy. Phonons are described here by the normalized

wavefunctions $\varphi_l(X_i)$ *that have to be determined variationally.* This means that we have at disposal a virtually infinite number of variational degrees of freedom, a great improvement with respect to the variational LFT where only one parameter f was introduced to mimic phonon effects.

Along the lines of section 2.2.1, we can impose the following normalization conditions without loss of variational freedom[74, 75]:

$$\int dX_i \langle\Psi_0| \, |\mathcal{P}_i|^2 \, |\Psi_0\rangle = 1, \tag{5.6}$$

$$\int dX_i \langle\Psi_0| \, n_i \, |\mathcal{P}_i|^2 \, |\Psi_0\rangle = n. \tag{5.7}$$

The first condition can be interpreted as a normalization condition on the variational wavefunction, whereas the second one implies that the on-site single-particle density matrix is untouched by the Gutzwiller projection. Being the phonon wavefunctions normalized, these two equations lead to the constraints:

$$P_0 + P_1 + P_2 = 1, \tag{5.8}$$

$$P_1 + 2P_2 = n, \tag{5.9}$$

completely analogous to those found for the pure Hubbard model (cfr. section 2.2.1).

Evaluation of the expectation value of the Hamiltonian (5.3) over the variational state $|\Psi_{GPW}\rangle$ is then carried on following Refs. ([74, 75]). We choose a Bethe lattice with infinite coordination number and semicircular density of states $2D$ wide; in infinite dimensions, in fact, the computation of the ground-state energy can be carried out exactly, and it coincides with the Gutzwiller approximation for finite-dimension lattices. The variational energy per-site reads:

$$\frac{E}{L} = \sum_{l=0,1,2} P_l \, \langle h_0(X)\rangle_l + \sqrt{2}\alpha\omega_0 \big[P_0\langle X\rangle_0 - P_2\langle X\rangle_2\big] - \frac{2\,|S|^2}{1-\delta^2}|\varepsilon| + \frac{U}{2}\left(P_2 + P_0\right) + E_c, \tag{5.10}$$

where

$$h_0(X) = \frac{\omega_0}{2}\left(-\frac{\partial^2}{\partial X^2} + X^2\right), \tag{5.11}$$

is the hamiltonian describing the undisplaced harmonic oscillator, and we have introduced

$$\langle ...\rangle_l \equiv \int_{-\infty}^{\infty} \mathrm{d}X \; \varphi_l^*(X)...\varphi_l\,(X) \tag{5.12}$$

to indicate the average over the phonon wavefunction $\varphi_l(X)$. As usual, $|\varepsilon|$ is the kinetic energy for uncorrelated electrons, while S measures the overlap of phonon wavefunctions on neighbouring sites, and it controls the renormalization effects of both electron correlation and e-ph interaction:

$$S = \sum_{l=0,1} \sqrt{P_l P_{l+1}} \int \mathrm{d}X \; \varphi_{l+1}^*(X)\varphi_l\,(X). \tag{5.13}$$

In Eq. (5.10) we have included also a term which enforces the constraints (5.8),(5.9) and the normalization of the phonon wavefunctions, that reads:

$$E_c = \lambda^{(1)}\,(P_0 + P_1 + P_2 - 1) + \lambda^{(2)}\,(n - P_1 - 2P_2) + \sum_{l=0,1,2} \epsilon_l\,(1 - \langle\varphi_l|\varphi_l\rangle). \tag{5.14}$$

Here the parameters $\lambda^{(1)}, \lambda^{(2)}$ are analogue to the Lagrange multipliers introduced in section 2.2.2; in fact, we will see in the following that the present approach is equivalent to a proper slave-boson description of the Hubbard-Holstein model, where a variational ansatz is assumed for the phonon problem while P_0, P_1, P_2 actually correspond to e_0^2, $2p_0^2$, d_0^2 respectively.

5.1.2 The variational equations.

The variational parameters are determined through minimization of the ground-state energy Eq. (5.10). We can neglect for the time being the equations determining the value of the Lagrange multipliers $\lambda^{(1)}, \lambda^{(2)}$ and use the constraints (5.8),(5.9) to get:

$$P_0 = d + \frac{\delta}{2}, \tag{5.15}$$

$$P_1 = 1 - 2\,d, \tag{5.16}$$

$$P_2 = d - \frac{\delta}{2}, \tag{5.17}$$

where we have introduced $d = (P_0 + P_2)/2$ as a measure of the doubly-occupation probability ($0 \le d \le 1/2$) and the standard doping parameter defined as $\delta = 1 - n$. Minimization with respect to d then leads to the following mean-field equation:

$$U + (\langle h_0(X)\rangle_0 + \langle h_0(X)\rangle_2 - 2\langle h_0(X)\rangle_1) + \sqrt{2}\alpha\omega_0(\langle X\rangle_0 - \langle X\rangle_2) - \frac{2|\varepsilon|}{1-\delta^2}\frac{\partial|S|^2}{\partial d} = 0, \tag{5.18}$$

whereas that with respect to the phonon wavefunctions yields the following non- linear second-order differential equations:

$$\frac{\epsilon_0}{P_0}\varphi_0 = h_0(X)\varphi_0 + \sqrt{2}\alpha\omega_0\,X\,\varphi_0 - \frac{2|\varepsilon|}{1-\delta^2}S\sqrt{\frac{P_1}{P_0}}\varphi_1, \tag{5.19}$$

$$\frac{\epsilon_1}{P_1}\varphi_1 = h_0(X)\varphi_1 - \frac{2|\varepsilon|}{1-\delta^2}\left(S^*\sqrt{\frac{P_0}{P_1}}\varphi_0 + S\sqrt{\frac{P_2}{P_1}}\varphi_2\right), \tag{5.20}$$

$$\frac{\epsilon_2}{P_2}\varphi_2 = h_0(X)\varphi_2 - \sqrt{2}\alpha\omega_0\,X\,\varphi_2 - \frac{2|\varepsilon|}{1-\delta^2}S^*\sqrt{\frac{P_1}{P_2}}\varphi_1, \tag{5.21}$$

which represent the core of the present approach. In the most general case, therefore, one has to consider four coupled mean-field equations. The phonon wavefunctions are determined through a set of Schrödinger-like coupled equations, where the complicated non-linear coupling term is expected to capture the modifications induced by the retarded e-ph coupling on phonon properties. In fact, in the absence of electron motion the three equations (5.19)-(5.21) are decoupled and describe exactly the harmonic oscillators found in the atomic limit, i.e. $\varphi_l(X) = \phi(X - \sqrt{2}\alpha\,(l-1))$. When introducing a finite hopping, we can still distinguish

between two regimes. When $\omega_0 \gg |\varepsilon|$, the coupling term can be considered as a perturbative small correction, hence the gaussian shape of the phonon wavefunctions is almost untouched and a charge-depending shift of the phonon displacement is sufficient to capture the ground-state properties of the system. This is consistent with the fact that phonons are fast enough in this limit to follow electron motion. On the other hand, the opposite regime $\omega \ll |\varepsilon|$ is where the non-linear coupling term is more effective, and strong deviations from the harmonic oscillator shape are expected, in excellent agreement with Ref. [88]. The strenght of this coupling is also controlled by the Gutzwiller weights P_l, which suggest a non-trivial dependence of φ_l on both e-e and e-ph interactions.

An analytical solution in the general case is still difficult to obtain. We will consider in the following two important limits. First we will analyze the infinite$-U$ limit, where the double occupancy is strictly forbidden because energetically unaccesible: by introducing holes (vacancy doping), one can study the effect of e-ph coupling on the doped strongly-correlated regime of the model by considering only two equations, namely Eqs. (5.19),(5.20), since the electronic problem is trivially solved and the determination of φ_2 is irrelevant due to the absence of double occupation. In the subsequent section we will turn to the half-filling regime; our symmetrized Hamiltonian will allow us to get rid of one of the three coupled equations for the phonons, but the electron occupation probability will have to be self-consistently determined. Before doing so, we just sketch the connection with the variational slave-boson approach based on the LFT.

5.1.3 Connection with the variational LFT and slave-boson approach

As we already pointed out, in the variational slave-boson framework that we have analyzed previously the phonons are described by displaced harmonic oscillators whose displacements are controlled by the variational parameter f. Starting from this consideration we have introduced in the previous chapter a generalized LFT to be performed over the slave-boson representation of the Hubbard-Holstein model, in such a way that different phonon displacements are connected to the local charge states described by the slave operators. This is quite similar in spirit to the approach we are presenting in this chapter, and the possible connection between the two methods deserves some words.

The generalization of the Gutzwiller wavefunction provided by the projection operator Eq. (5.5) relies mainly on the assumption that the phonon wavefunctions are determined by the local charge state. The true phonon wavefunction is then expressed as a proper combination of such projected phonon wavefunctions, that are determined by the coupled equations Eqs. (5.19)-(5.21) without imposing any constraint on them but that to be associated to the number of electrons occupying a given site i. Solving these coupled equations remains a difficult task in the general case. However we can assume a variational ansatz and look for the best phonon wavefunctions in a given class of trial wavefunctions. According to the

qualitative analysis of the Schrödinger-like equations for the phonons we can assume:

$$\varphi_l(X) = e^{i\sqrt{2}\alpha\, f_l\, \hat{P}}\,|0\rangle = e^{\alpha\, f_l\,(a-a^\dagger)}|0\rangle, \tag{5.22}$$

where $|0\rangle = \phi(X)$ is the undisplaced harmonic oscillator and $\hat{P} = -i(a-a^\dagger)/\sqrt{2}$ is the momentum operator of the phonon field. By means of the standard formulae:

$$\begin{aligned}
\langle 0|e^{i\eta\hat{P}}\, h_0\, e^{i\beta\hat{P}}|0\rangle &= \frac{\omega_0}{2}\, e^{-(\eta+\beta)^2/4}\,(1-\eta\beta),\\
\langle 0|e^{i\eta\hat{P}}\, X e^{-i\eta\hat{P}}|0\rangle &= \eta,\\
\langle 0|e^{i\eta\hat{P}}|0\rangle &= e^{-\eta^2/4},
\end{aligned}$$

one finds that the variational energy to be minimized is given by:

$$\frac{E}{L} = \frac{\omega_0}{2} - \frac{2|\varepsilon|}{1-\delta^2}|S|^2 + \frac{U}{2}\left(P_2+P_0\right) + +\alpha^2\omega_0\left[(f_0^2+2f_0)\,P_0 + f_1^2\,P_1 + (f_2^2-2f_2)\,P_2\right] + \tilde{E}_c, \tag{5.23}$$

where the reduction of the kinetic energy reads:

$$|S| = \sqrt{P_0P_1}\, e^{-\frac{\alpha^2}{2}(f_0-f_1)^2} + \sqrt{P_2P_1}\; e^{-\frac{\alpha^2}{2}(f_1-f_2)^2}. \tag{5.24}$$

At last, being the chosen trial wavefunctions (5.22) already normalized, the contribution of the constraints to the variational energy is simply $\tilde{E}_c = \lambda^{(1)}\,(P_0+P_1+P_2-1)+\lambda^{(2)}\,(n-P_1-2P_2)$.

It is readily seen that energy (5.23) is exactly the same as that evaluated at the saddle point of the slave-boson representation of the effective model discussed in the appendix A, once P_0, P_1, P_2 are replaced by e_0^2, $2p_0^2$, d_0^2 (cfr. Eq. A.6). The two approaches are then equivalent when one imposes that phonon wavefunction shape is not affected by the e-ph coupling, whose effect consists only in a renormalization of the displacement induced by the electrons. This finding confirms that the present approach, which enlarges the variational freedom in choosing the best phonon wavefunctions, is the most suitable in order to include ground-state phonon properties in a strongly-correlated description of the Hubbard-Holstein model.

5.2 Limit of infinite Hubbard repulsion

When an infinitely strong repulsion between electrons is considered, one has to consider only the hole-doped regime of the system and condition $d = 0$ can be plugged in the mean-field equations. As a major simplification one gets the trivial solution of the electronic problem:

$$P_0 = \delta, \tag{5.25}$$

$$P_1 = 1-\delta. \tag{5.26}$$

As a consequence, since Eq. (5.21) becomes irrelevant, the coupled equations are greatly simplified. In the limit of small doping we can expand the uncorrelated kinetic energy as

$|\varepsilon| \simeq |\varepsilon_0|(1 - a\delta^2)$ and recast Eqs. (5.19),(5.20) as:

$$\frac{\epsilon_0}{\delta}\varphi_0 = h_0(X)\varphi_0 + \sqrt{2}\alpha\omega_0\, X\, \varphi_0 - 2|\varepsilon_0|\frac{1 - a\delta^2}{1 + \delta} \int \mathrm{d}X'\, K_0(X, X')\varphi_0(X'), \quad (5.27)$$

$$\frac{\epsilon_1}{1 - \delta}\varphi_1 = h_0(X)\varphi_1 - 2|\varepsilon_0|\frac{1 - a\delta^2}{1 - \delta^2}\,\delta \int \mathrm{d}X'\, K_1(X, X')\varphi_1(X'), \quad (5.28)$$

where we exploited the mean-field solutions for the occupation probability weights and introduced the "kernel" operator $K_{0(1)}(X, X') = \varphi^*_{1(0)}(X')\varphi_{1(0)}(X)$. The last equation appears to be decoupled at leading order in the limit of vanishing doping, hence $\varphi_1(X)$ is simply the harmonic oscillator centered in the origin; therefore we can expand $\varphi_0(X)$ onto the eigenfunctions $\phi_n(X)$ with eigenstates $\mathcal{E}_n = \omega_0(1/2 + n)$ as:

$$\varphi_0(X) = \sum_{n=0}^{N_{ph}} c_n\, \phi_n(X). \quad (5.29)$$

Since we are looking for the ground-state solution, we can impose $\varphi_1(X) = \phi_0(X)$ and exploit Eq. (5.27) to determine the coefficients $\{c_n\}$. This implies the diagonalization of a tridiagonal matrix, as the coupling term reduces to a shift of the lower level for the eigenvalue problem represented by Eq. (5.27) and the displacement operator couples oscillator states whose quantum number n differs only for a factor 1.

We can generalize this approach to the finite doping case and expand both the variational wavefunctions over the eigenfunctions of h_0 as $\varphi_0(X) = \sum_{n=0}^{N_{ph}} c_n\, \phi_n(X)$, and $\varphi_1(X) = \sum_{m=0}^{N_{ph}} d_m\, \phi_m(X)$, obtaining the following coupled equations:

$$\left[\left(\frac{\epsilon_0}{P_0} - \mathcal{E}_n\right)\delta_{nn'} - \sqrt{2}\alpha\omega_0\, X_{n'n} + \frac{2|\epsilon|}{1 - \delta^2}P_1 d_n d^*_{n'}\right] c_{n'} = 0, \quad (5.30)$$

$$\left[\left(\frac{\epsilon_1}{P_1} - \mathcal{E}_m\right)\delta_{mm'} + \frac{2|\epsilon|}{1 - \delta^2}P_0 c_m c^*_{m'}\right] d_{m'} = 0, \quad (5.31)$$

for the sets of coefficients $\{c_n\}, \{d_m\}$ which can be solved by iteration keeping an arbitrary number N_{ph} of harmonic oscillator levels. In practice a hundred of levels are enough to get very accurate results for the ground state. We plot in the right panel of Fig. 5.1 the computed value of ϵ_0 by keeping different numbers of harmonic oscillator levels at a rather strong e-ph coupling, where we expect that a larger value of N_{ph} is needed to account for the shift induced by the electrons; it is clear that with 30 levels we already obtain the converged solution. These converged solutions are typically obtained after few iterations; the most time-consuming cases are the intermediate e-ph coupling regime and the quarter-filling case, where both φ_0 and φ_1 have equal weight (cfr. left panel in Fig. 5.1), thus implying a sizeable coupling between Eqs. (5.30),(5.31).

We show in Fig. 5.2 the typical evolution of the phonon wavefunctions with increasing e-ph coupling in the adiabatic regime. For small values of λ, φ_0 is slightly modified by the presence of the e-ph coupling, and the major effect amounts to a shift of the position of its peak and a small broadening of its width. However, at intermediate couplings, its shape

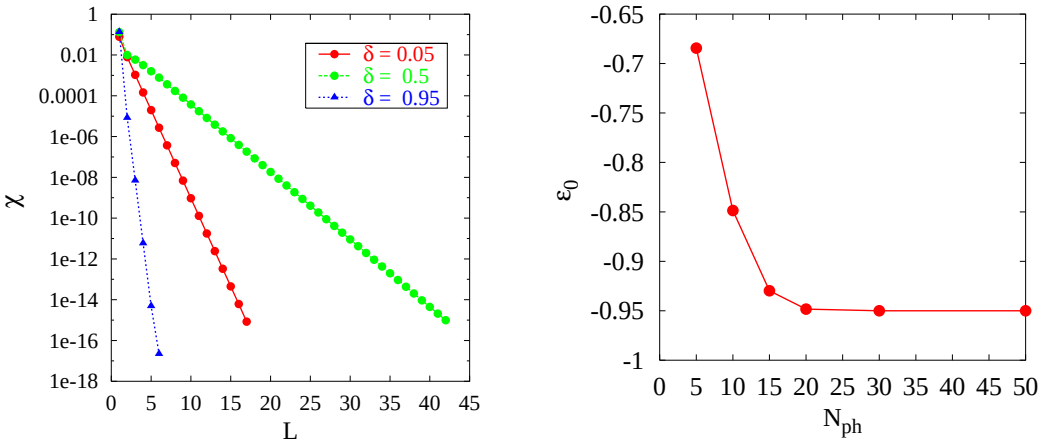

Figure 5.1: Left: measure of the algorithm velocity. L is the number of iterations, while $\chi^2(L) = (1/N_{ph}) \sum_{n=0}^{N_{ph}} \left[c_n(L) - c_n(L-1)\right]^2$ measures the difference between the set of coefficients $\{c_n\}$ determined at step L and that obtained in the previous step $L-1$ of the algorithm. A solution is satisfactory converged when $\chi < 10^{-8}$, that means that no sizeable deviations in computed quantities are found by imposing more severe accuracy. Here $\lambda = 2$, hence we are in the intermediate e-ph coupling regime, and the effect of doping is shown. Right: ground-state energy for φ_0 at $\lambda = 4, \gamma = 0.2$ and $\delta = 0.05$ as obtained with different values of N_{ph}.

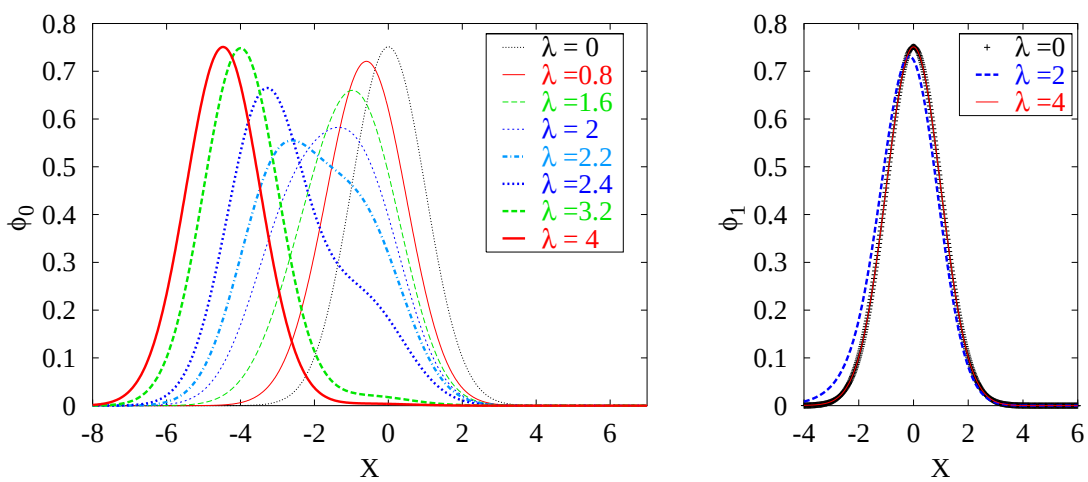

Figure 5.2: Evolution of the phonon wavefunctions with increasing λ at $\gamma = 0.2$ and $\delta = 0.1$. As expected, φ_0 strongly deviates from the gaussian shape characteristic of the free harmonic oscillator at intermediate couplings, while it corresponds to a displaced oscillator when large values of λ are considered, whereas φ_1 is almost untouched for any e-ph coupling.

strongly deviates from the gaussian function that describes the displaced harmonic oscillator, which is eventually recovered only for large λ. Furthermore one observes that, even if the

position of the peak signals a strong displacement of the phonon, a shoulder develops in order to maximize the overlap with φ_1, which on the other hand remains almost centered in $X = 0$, being slightly shifted only at intermediate couplings. Therefore one finds that a sizeable distortion can be accompanied by a less severe reduction of the overlap between phonon wavefunctions. This is exactly the effect that, along the discussion of the previous chapter, we hoped to capture. We will devote the next sections to analyze its implications.

5.2.1 Polaron crossover

In this section we discuss the polaron formation in the generalized Gutzwiller framework we have just introduced. In order to characterize the polaron crossover and to make connections with previous studies, we start our analysis from the behavior of the effective mass, which, according to Eq.(5.13), is given by

$$m^*(\lambda) = m^*(0)|\langle\phi_1|\phi_0\rangle|^{-2}, \tag{5.32}$$

where the overlap $\langle\phi_1|\phi_0\rangle$ between the two wavefunctions associated to empty and singly occupied sites contains the effect of phonons, while $m^*(0) = (1+\delta)/2\delta$ includes all the correlation effects.

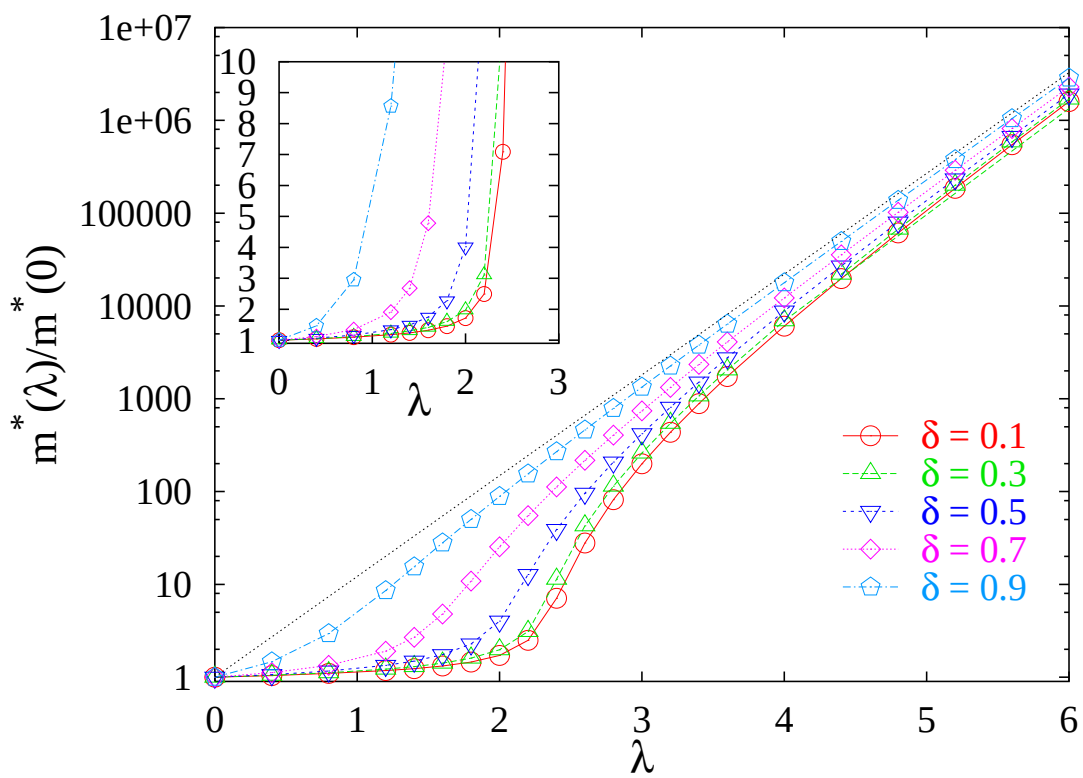

Figure 5.3: Effective mass as function of λ and for different values of δ at $\gamma = 0.2$. The solid line is the pure Lang-Firsov result $\exp(\alpha^2)$.

Thanks to the almost analytical nature of the method, all parameters regimes are easily accessible, as shown by the example of Fig. 5.3, where the effective mass (5.32) is plotted as function of λ for $\gamma = 0.2$, a value for which standard Lang-Firsov methods are not accurate. The inset of Fig. 5.3 emphasizes the formation of polarons, testified by the rapid growth of the effective mass. It is also evident that *the formation of polarons is a crossover for all densities*. By approaching half-filling the crossover moves to larger λ due to the increased correlation effects, and it becomes sharper. Notice that, even in the most metallic situation, the results are still far away from the standard Lang-Firsov predictions. For instance, at $\delta = 0.9$ and $\lambda = 0.8$, the Lang-Firsov result overestimates the effective mass by more than a factor two (cfr. the log scale on the vertical axis). Furthermore, due to the presence of an infinite local repulsion between electrons, bipolaronic instabilities are ruled out at large λ and the ground state is always a strongly-correlated polaronic metal even if with exponentially large effective mass.

As we pointed out before, the Gutzwiller phonon wavefunction (GPW) allows for a direct evaluation of the lattice probability distribution function (PDF), defined as $P(X) = \langle GS|X\rangle\langle X|GS\rangle$ with $|GS\rangle$ representing the ground state (approximated by $|\Psi_{GPW}\rangle$ in our approach) and $|X\rangle\langle X|$ the projection operator on the subspace where the displacement operator has the given value X. In the present framework it reads:

$$P(X) = \sum_l P_l \, |\varphi_l(X)|^2. \tag{5.33}$$

This definition is analogue to the one given for the antiadiabatic limit in Eq. (40) of Ref. [95], with the difference that here the phonon wavefunctions are not harmonic oscillators and must be determined by means of Eqs. (5.19)-(5.21). When an infinite Hubbard repulsion is considered, the PDF is obtained as the sum of two contributions only, coming from the empty and singly-occupied sites, and one has:

$$P(X) = \delta|\varphi_0(X)|^2 + (1-\delta)|\varphi_1(X)|^2. \tag{5.34}$$

This is consistent with the findings of Ref. [60], where it was pointed out that the presence of strong correlation unfavours double occupancies and the system can acquire polaronic ground state only exploiting the empty sites.

In Fig. 5.4 we show the evolution of the PDF with increasing e-ph coupling strenght in the adiabatic regime ($\gamma = 0.2$) for two different values of the doping, namely $\delta = 0.1$ and $\delta = 0.5$, where empty and singly-occupied sites display the same occupation probability. At weak coupling $P(X)$ has only one peak, and the main effect of the coupling with electrons is to broaden its width. Increasing λ, one observes a shoulder developing for negative X at $\delta = 0.1$, that is related to the displacement of φ_0, which becomes a well defined peak that marks the formation of the polaron at $\lambda = 2.8$, where the polaronic correction to the effective mass is already huge. At larger λ the PDF displays simply two peaks corresponding to two displaced oscillators whose centers are distant $\sqrt{2}\alpha$ with weight given by δ and $1-\delta$

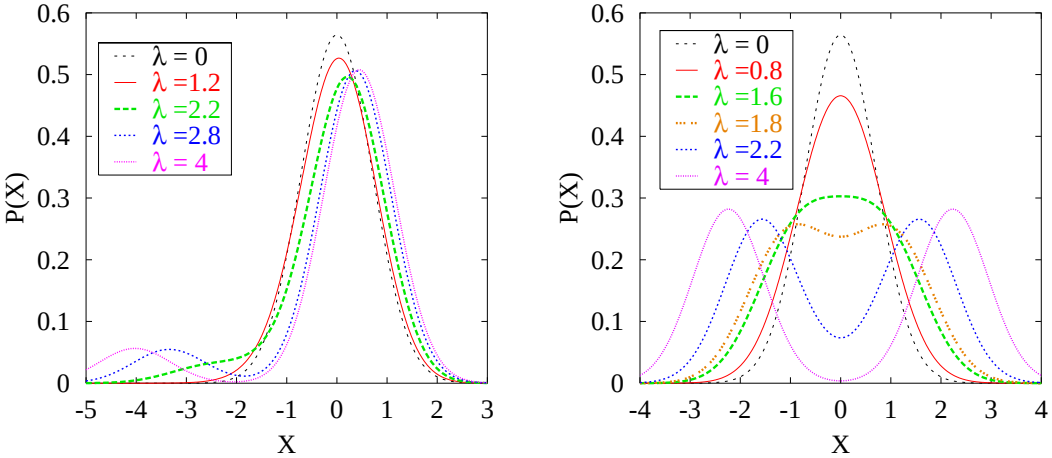

Figure 5.4: Lattice probability distribution functions for different values of the e-ph coupling in the adiabatic regime $\gamma = 0.2$ and for two different values of the doping, $\delta = 0.1$ (left) and $\delta = 0.5$ (right). Both PDF are shifted with respect to the uniform displacement $\delta\sqrt{2}\alpha$ induced by the particular choice of the e-ph coupling, with phonon displacement $\hat{X}$ coupled to $n - 1$.

respectively. A similar behaviour is observed at quarter filling, where however the two peaks are equally weighted and the bimodal shape develops for smaller values of λ. At larger values of the doping polaron formation occurs for even smaller couplings, and the same qualitative behaviour of $\delta = 0.1$ is found, upon a reversal of the peaks weight,with the major contribution to PDF coming from φ_0 and φ_1 determining the development of the shoulder at positive X. At last we notice that, even in the strong-coupling regime, the minimum between the two peaks is never exactly zero except for infinite α, since the PDF stems from the combination of two gaussian functions which vanish asimptotically when their arguments tend to infinite. This explains the finite, even if exponentially large, value of the effective mass, since in the present framework this last quantity is completely determined by the overlap between the two phonon wavefunctions associated to empty and singly-occupied sites (cfr. Eq. 5.32).

5.2.2 Comparison with DMFT results

To assess the quantitative reliability of the Gutzwiller phonon wavefunction method, in Fig. 5.5 the evolution of $m^*(\lambda)/m^*(0)$ as a function of γ for $\lambda = 1.5$ and $\delta = 0.3$ is compared with variational Lang-Firsov and slave-boson (VLF)[114] and with DMFT[115], which provides the exact reference in the infinite-dimensions limit. The qualitative behavior is similar in all methods. $m^*(\lambda)/m^*(0)$ is an increasing function of γ in the adiabatic regime. Then a maximum is reached, followed by a decrease for large γ (cfr. Fig. 3.10 and Ref. [60]). As expected, all methods quantitatively agree in the large-γ region. The Gutzwiller approach always represents a sizeable improvement on the VLF for all values of γ. As the phonon

frequency is decreased, the GPW stays extremely close to the DMFT results for a wide range, and they bifurcate only for small γ, where GPW is still significantly closer to DMFT than VLF.

Remarkably, the method provides a qualitatively correct description of the nature of the polaron formation even in the adiabatic regime, where the quantitative estimate of the effective mass is less accurate. To appreciate this in Fig. 5.6 we show the overlap $\langle\phi_1|\phi_0\rangle$, which in the present framework determines the renormalization of the effective mass due to phonons through Eq. (5.32) for two values of γ in the adiabatic region where the quantitative agreement with DMFT is poorer (namely we choose $\gamma = 0.6$ and $\gamma = 0.2$). We compare again with both DMFT and VLF. For $\gamma = 0.6$ all methods give a rather smooth crossover, similar to what happens for large values of γ, although the Gutzwiller phonon wavefunctions significantly improve on the variational slave-boson result for intermediate values of λ, making the crossover smoother.

On the contrary, at smaller $\gamma = 0.2$, namely inside the adiabatic regime, the GPW closely follows the continuous behavior of DMFT, while VLF yields the already discussed first-order transition where the overlap discontinuously jumps as a function of λ. Our GPW wavefunction therefore correctly reproduces the physics of the polaron crossover for all values of the phonon frequency, whereas variational methods based on LFT are less reliable in the adiabatic regime.

We notice that the discrepancy between GPW and DMFT seems to be more pronounced

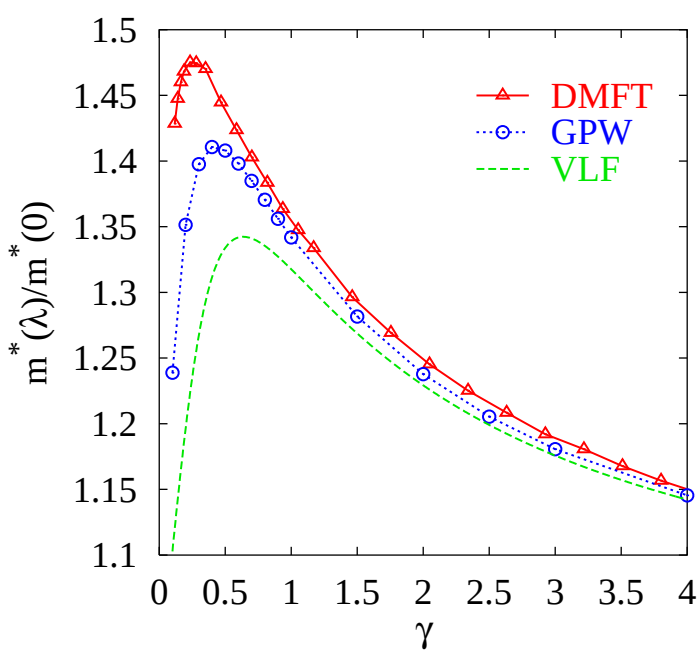

Figure 5.5: Effective mass as function of γ at $\lambda = 1.5$ and $\delta = 0.3$ as obtained with GPW (open circles) and VLF (solid line).

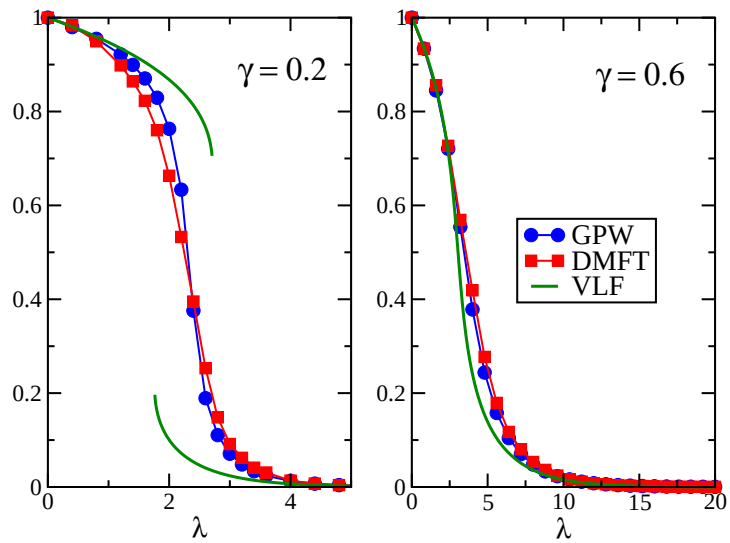

Figure 5.6: $\langle\varphi_0|\varphi_1\rangle$ as function of λ at $\delta = 0.1$ for $\gamma = 0.2$ and $\gamma = 0.6$ in GPW, DMFT and VLF, where it is given by $e^{-\alpha^2 f^2/2}$.

in the effective mass rather than in the overlap $\langle\varphi_0|\varphi_1\rangle$. Actually, even if these two quantities are closely related in the present approach, we observe that the overlap is indeed a ground-state property, and it may be that it is not enough to determine the effective mass of the quasiparticles. This would be the case if there were a residual interaction between such quasiparticles. On the other hand, Fig. 5.6 suggests that ground-state properties are correctly described by the Gutwiller phonon wavefunction.

5.2.3 Properties of the ground-state phonon wavefunctions

A deeper understanding of the improvement brought by GPW can be achieved by studying the phonon wavefunctions and their difference with respect to a pure harmonic oscillator, adopted, e.g., in the VLF scheme. We have seen that the coupling between electrons and phonons induce strong modifications on the ground-state phonon wavefunctions (cfr. Fig. 5.2). Here we would like to quantify the modifications induced by the e-ph coupling in the phonon properties with respect to the atomic limit in different physical regimes, and to make explicit the connection with the variational scheme introduced in chapter 3. As usual, λ and γ define the influence of the e-ph coupling and of the adiabaticity regime in determining the properties of the ground state, whereas in the present limit the doping is a measure of the effectiveness of electronic correlation.

In figs. 5.7 and 5.8 we show the evolution of the phonon wavefunctions projected onto empty and singly-occupied states with increasing adiabaticity ratio and doping, respectively, for selected values of the e-ph coupling. In the first case we choose $\lambda = 1.5$ at $\delta = 0.3$,

i.e., a value of the e-ph coupling large enough to see strong modifications of the phonon wavefunctions but still well before the polaron crossover. We see that the strong-coupling result, where $\varphi_l(X) = \phi(X - X_0(l))$, is recovered only in the antiadiabatic regime, as expected; decreasing γ one observes a less pronounced shift of φ_0 with respect to the atomic limit (marked by vertical arrows) on one hand, and an e-ph induced shift of φ_1 on the other, while both wavefunctions broaden in order to maximize their overlap.

A more complex behaviour emerges as a function of doping in the adiabatic regime. For small λ, both φ_0 and φ_1 are shifted with respect to the atomic limit, indicated by the vertical arrows; in particular, φ_0 approaches the atomic shape with increasing doping, while φ_1 displays a nonmonotonic dependence on δ, where the deviations from the atomic limit are larger around $\delta = 0.7$. On the other hand, in the opposite limit of large $\lambda = 5.6$ both phonon wavefunctions are actually undistinguishable from displaced harmonic oscillators, as expected. For an intermediate value of the e-ph coupling, the most outstanding deviations from the atomic limit appears in φ_0 at small values of the doping, where a shoulder develops in a position that roughly corresponds to the position of φ_1; the disappearence of this feature at the given λ with increasing doping is related to the decrease of correlation effects, which implies that away from half-filling $\lambda = 2.4$ is enough to induce polaron formation. We stress the fact that this feature is not exactly the same observed, for instance, in Fig. 4.2; in

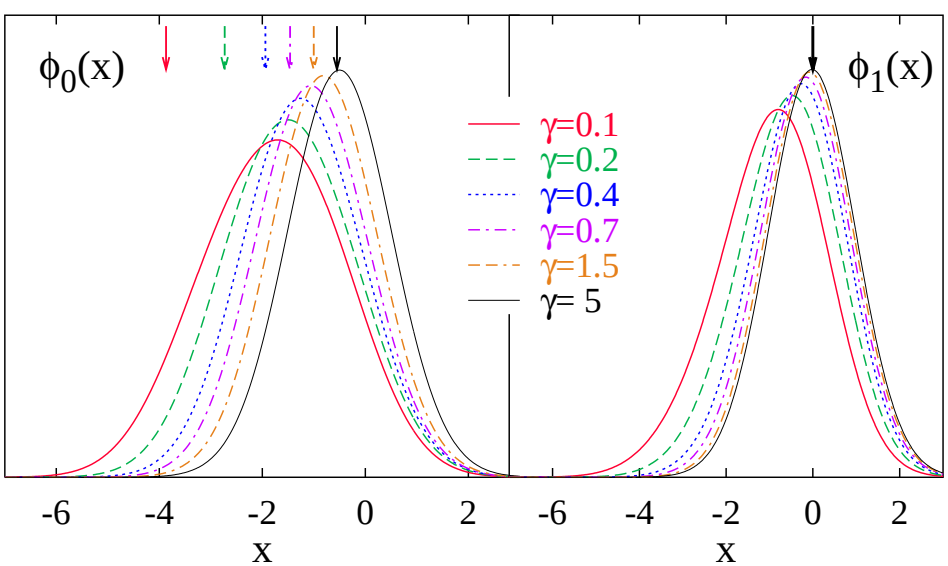

Figure 5.7: Evolution of phonon wavefunctions as function of γ for $\lambda = 1.5$ and $\delta = 0.3$. The arrows indicate the displacement in the atomic limit.

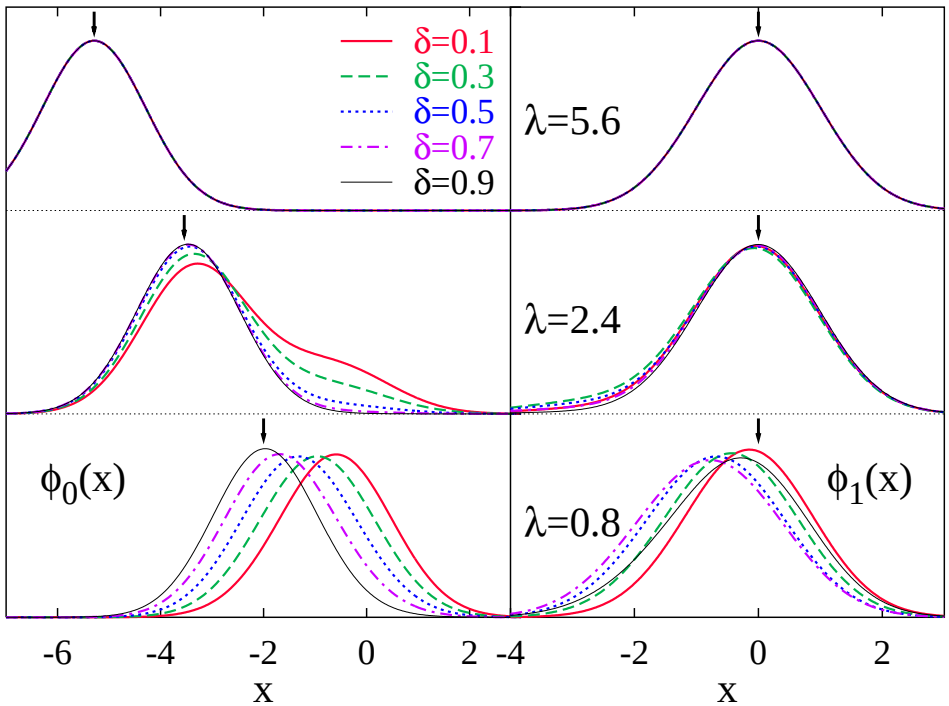

Figure 5.8: Evolution of phonon wavefunctions as function of doping for different values of e-ph coupling at $\gamma = 0.2$ (right). The arrows indicate the displacement in the atomic limit.

that case, in fact, the whole phonon wavefunction was shown, whereas the shoulder that we observe is developing in the phonon wavefunction projected onto the $n = 0$ state. From this point of view, a direct comparison should be carried on between the Gutzwiller PDF (cfr. Fig. 5.4) and the unprojected phonon wavefunction of Fig. 4.2.

We can try to quantify the two major effects of e-ph coupling on the phonon wavefunctions, i.e., the shift and the broadening of $\varphi_l(X)$, by introducing $\langle X\rangle_l$ and $\langle (X - \langle X\rangle)^2\rangle_l$, that measure the displacement and the fluctuations (hence the width) of the local wavefunctions when a given number l of electrons is sitting on a lattice site. This allows for a direct comparison with the atomic limit and the LFT-based approaches, where the phonon wavefunctions are gaussian functions centered in $\langle X\rangle_l = \sqrt{2}\alpha(l-1)$ (to which a factor f_l should be added when a variational LFT is applied onto the slave-boson representation of the model) and with $\langle (X - \langle X\rangle)^2\rangle_l$ equal to 1/2. In Fig. 5.9 we plot our results in the adiabatic regime ($\gamma = 0.2$) for increasing λ at $\delta = 0.1$. In the strong-coupling limit we find that the variational LFT is quite accurate in describing the ground-state properties of the phonon, as expected. For small values of λ, on the other hand, the displacement of the phonons is strongly reduced with respect to the atomic limit, but the variational scheme described in chapter 3 is still quite accurate; as we have discussed previously, the variational parameter f actually measures the relative displacement between phonon wavefunctions associated to

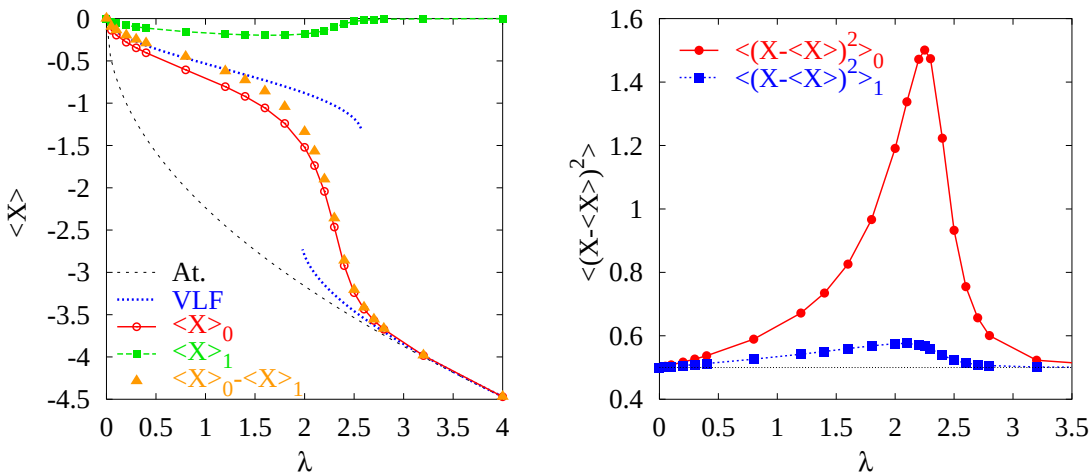

Figure 5.9: Evolution of the displacement and fluctuations of the phonon wavefunctions φ_0 and φ_1 as function of λ at $\delta = 0.1$ and $\gamma = 0.2$.

empty and singly-occupied states (cfr. appendix A), and the comparison between $\sqrt{2}\alpha f$ and $\langle X\rangle_0 - \langle X\rangle_1$ shows that the two methods agree quite well up to $\lambda \sim 1.5$. The origin of the biforcation at intermediate couplings becomes clear by looking at the right panel of Fig. 5.9, where the averaged fluctuations from the expected value of the shift are plotted; here we see that the width of the phonon wavefunctions rapidly increases with respect to that of a harmonic oscillator, and displays a maximum for intermediate couplings, exactly where the difference between the variational methods are more pronounced. In fact, VLF allows to get an estimate of the effective displacement induced by the e-ph coupling, but it keeps the width of the phonon wavefunctions fixed to the noninteracting value 1/2. Due to the increased width found in GPW, the overlap between φ_0 and φ_1 can be larger than that between two harmonic oscillators rigidly displaced of the same amount; since the reduction of the kinetic energy due to e-ph coupling is given by this overlap in the present approach, while the gain in potential energy is roughly determined by $\langle X\rangle$, this suggest that the Gutzwiller trial wavefunction is more effective in capturing their balance.

We can perform the same analysis varying γ and keeping the other relevant parameters fixed. To get meaningful physical informations, it proves useful to shift the averaged displacement $\langle X\rangle_l$ of an amount $(1-n)\sqrt{2}\alpha$, that corresponds to the trivial uniform displacement induced by the phonons coupling with $n-1$, choice that we made in order to compare with the atomic limit. In such a way we can evaluate the effect of charge fluctuations around the averaged charge density n. As a consequence of this rescaling, $\varphi_1(X)$ will be shifted towards positive values of X, in the opposite direction with respect to $\varphi_0(X)$. Two major effects are observed (Fig. 5.10). When moving from the antiadiabatic limit, the shift induced by the e-ph coupling increases, as one could have expected by considering that such a shift is roughly proportional, at least in the strong-coupling limit, to $1/\gamma$. If λ is large enough, this behaviour

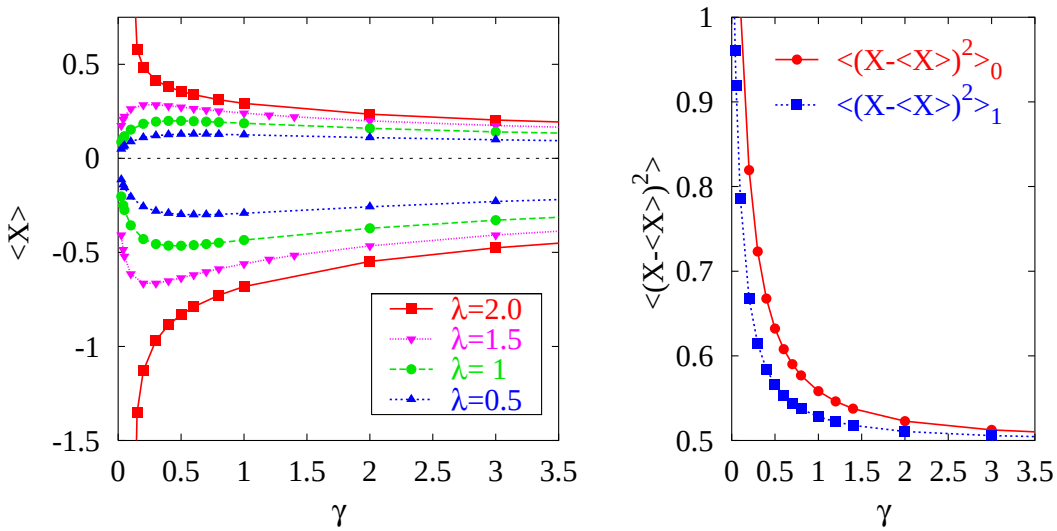

Figure 5.10: Evolution of the rescaled displacement of φ_0 and φ_1 as function of γ at $\delta = 0.3$ for different values of λ. In the right panel the broadening of the phonon wavefunctions is shown for $\lambda = 1.5$

leads to a divergence when $\gamma \to 0$, that should signal the polaron formation[1]. However, for weak and intermediate couplings, the dependence on the adiabaticity parameter changes drastically while approaching the adiabatic limit, and the phonon wavefunctions tend to coincide for $\gamma \to 0$. At the same time, their width is monotonically increased with decreasing γ. This means that when the adiabatic limit is considered φ_0 and φ_1 are coincident, reflecting the fact that phonons are not able to follow instantaneously the varying positions of electrons and they do not adapt, at the ground-state level, to the local charge density; on the other hand, the broadening of the phonon wavefunctions suggest that a larger number of phonons is involved in the ground state due to the e-ph coupling. In conclusion, for large values of the adiabaticity parameter e-ph coupling induces a sizeable distortion of the lattice, which can be described in terms of displaced harmonic oscillators that are essentially localized in space; on the other hand, for vanishingly small γ, lattice sites undergo very small distortions, but the corresponding phonon wavefunctions extend over a wider region of space.

[1]This observation comes clear by considering the dimensionful displacement operator X_{class}, which is related to the present X by the multiplicative factor $1/\sqrt{M\omega_0} = \sqrt{\omega_0/K}$, where M, K are the mass and the spring constant of the ions. By rescaling $\langle X \rangle$ in the left panel of Fig. 5.10 with $\sqrt{\gamma}$ and letting γ go to zero, one finds that $\langle X_{class} \rangle \to \sqrt{\lambda}$, that implies a sizeable distortion of the lattice associated to the formation of polarons.

5.3 The half-filling regime

In this section we focus our attention on the ground-state properties of the system at half filling, i.e., when $n = 1$. Exploiting the constraints (5.8),(5.9) one finds that the occupation probabilities of the correlated Gutzwiller phonon wavefunction are expressed in terms of d, which measure the doubly-occupation probability, as:

$$P_0 = P_2 = d, \tag{5.35}$$

$$P_1 = 1 - 2d. \tag{5.36}$$

The parameter d must be determined by solving Eq. (5.18), that requires the solution of the three coupled equations for the projected phonon wavefunctions. A closer look at Eqs. (5.19)-(5.21), however, allows us to exploit the simmetry of the half-filling regime which implies:

$$\varphi_1(-X) = \varphi_1(X), \tag{5.37}$$

$$\varphi_2(-X) = \varphi_0(X). \tag{5.38}$$

Plugging the first condition in Eqs. (5.19),(5.21), in fact, implies that the only odd contribution to φ_0 and φ_2 comes from the displacement term, that is equal but opposite in sign for the two phonon wavefunctions. On the other hand, the second condition guarantees that φ_1 is actually an even function and our assumption proves to be self-consistent[2]. As a consequence, we can deal with just two phonon equations in the search for the variational ground state, namely Eqs. (5.19),(5.20), since we can exploit condition (5.38) to obtain φ_2. In order to implement a suitable numerical algorithm, we expand the phonon wavefunctions on the eigenstates $|n\rangle$ of h_0, as we did in the infinite$-U$ limit, namely:

$$\varphi_0(X) = \sum_{n=0}^{N_{ph}} c_n\, \phi_n(X), \qquad \varphi_1(X) = \sum_{m=0}^{N_{ph}} d_m\, \phi_m(X).$$

Due to the parity of φ_1, only even harmonic oscillator eigenstates enter in its expansion, hence $d_{2m+1} = 0$. Then one gets the coupled equations for the coefficients $\{c_n\}, \{d_m\}$:

$$\left[\left(\frac{\epsilon_0}{d} - \mathcal{E}_n\right)\delta_{nn'} - \sqrt{2}\alpha\omega_0 X_{n'n} + 4|\varepsilon_0|(1-2d)d_n d^*_{n'}\right] c_{n'} = 0, \tag{5.39}$$

$$\left[\left(\frac{\epsilon_1}{1-2d} - \mathcal{E}_m\right)\delta_{mm'} + 8|\varepsilon_0| d c_m c^*_{m'}\right] d_{m'} = 0, \tag{5.40}$$

which must be solved togheter with

$$1 - 4d = \frac{1}{8|\varepsilon_0||\sum_n c_n d_n|^2}\left(U + 2\sqrt{2}\alpha\omega_0\langle x\rangle_0 + 2\left(\langle h_0\rangle_0 - \langle h_0\rangle_1\right)\right), \tag{5.41}$$

where $|\varepsilon_0| \simeq 0.4244D$ is the kinetic energy of uncorrelated electrons on the half-filled Bethe lattice.

[2]Of course, these considerations hold as long as ground-state solutions are analyzed.

Eventually one has to evaluate $2N_{ph}+1$ variational parameters. The numerical solution can be obtained following the algorithm introduced in the limit of infinite U, i.e., one evaluates by iteration the convergent phonon wavefunctions at given d and then enforces condition (5.41) until convergence is reached for all the parameters. Alternatively, one can start from a given d and keep fixed, for example, φ_0 in order to determine φ_1; this generate a new value for the parameter d, that can be used to evaluate φ_0 and the final value for d to be used in the following iteration. In this second procedure the convergence of the $2N_{ph}+1$ parameters is checked at once, and the algorithm proved to be faster, whereas the first procedure provides more rapidly convergent solutions for the phonon wavefunctions if the initial choice for d is close to its correct value. Tipically for $50-70$ harmonic oscillator levels we get very accurate results for the ground state, as in the simpler limit discussed previously. However, due to the more involved electron problem, convergence is reached slower expecially when adiabatic values of γ are considered (as noted before, this implies a larger coupling term between the phonon equations).

It can be useful to define at the end of this section the physical quantities that will allow us to characterize the paramagnetic ground-state properties of the system. Since it is known that at half filling two insulating phases are stable for some values of the parameters, we define here their energies. As it is clear from Eq. (5.10), when the kinetic energy of electrons is zero, the local problem coincides with the atomic one, hence one gets for the Pair (bipolaronic) and Mott insulator energy $E_{BI}=P_0E_{at}(0)+P_2E_{at}(0)$ and $E_{MI}=P_1E_{at}(1)$ respectively, i.e.

$$E_{BI} = d\Big(\omega_0+U-2\alpha^2\omega_0\Big)=\frac{1}{2}\Big(\omega_0+U-2\alpha^2\omega_0\Big), \tag{5.42}$$

$$E_{MI} = (1-2d)\frac{\omega_0}{2}=\frac{\omega_0}{2}, \tag{5.43}$$

where we have exploited Eqs. (5.35),(5.36) and the fact that $d=1/2$ and $d=0$ in the BI and MI respectively. Besides the ground-state energies, the present approach allows for a direct evaluation of the quasiparticle renormalization factor, that from Eq. (5.13) reads:

$$Z=8d(1-2d)|\langle\phi_1|\phi_0\rangle|^2, \tag{5.44}$$

and of the lattice probability distribution function Eq. (5.33):

$$P(X)=d\big[\,|\varphi_0(X)|^2+|\varphi_2(X)|^2\big]+(1-2d)|\varphi_1(X)|^2 \tag{5.45}$$

through which electronic and phononic properties of the model can be investigated.

5.3.1 Holstein model: comparison with DMFT

We devote this section to the discussion of the results of our approach when applied to the Holstein model, i.e. taking $U=0$. We know that this is the worst situation for the GPW method to be applied, due to the the strong entanglement between electronic and phononic degrees of freedom which makes retardation effects the most relevant. However, since the Holstein model maps in the antiadiabatic limit onto an attractive Hubbard model whose

physics is correctly described by slave-boson and Gutzwiller approaches, it may be useful to test GPW in this system.

One of the problems we experienced with VLF was the missing of the effective mass enhancement at weak-coupling predicted by the Migdal-Eliashberg theory. We found that the present approach and the VLF are completely equivalent when small values of λ are considered, as shown in Fig. 4.1, therefore the Gutzwiller phonon wavefunction is not able to mend this drawback. The equivalence of GPW and VLF at weak e-ph couplings can be easily understood, since small values of λ are not able to change drastically the shape of the projected phonon wavefunctions, and the harmonic ansatz for φ_l proves therefore quite accurate in the extended Gutzwiller approach. As a consequence, all considerations we made in the analysis of the drawbacks of VLF at weak coupling apply also to GPW.

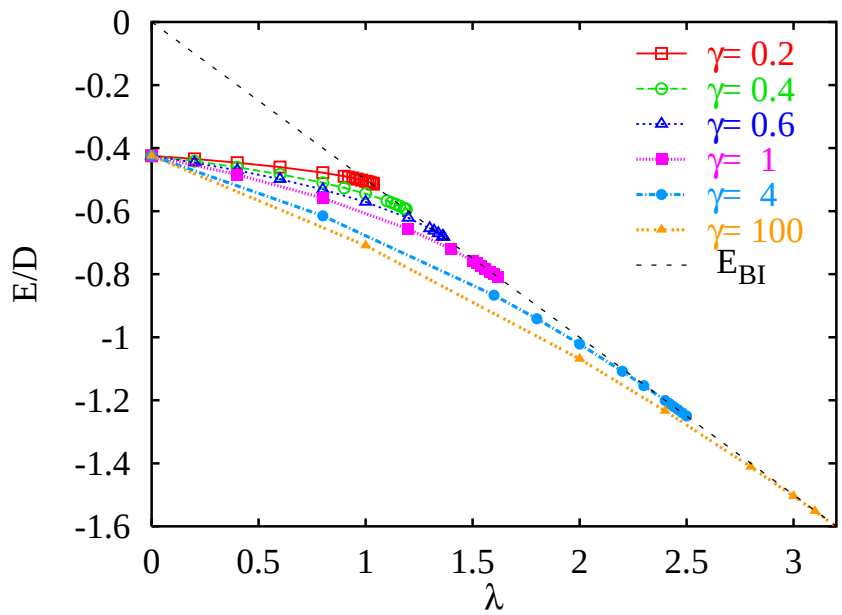

Figure 5.11: Paramagnetic metal energies for different values of γ in the Holstein model.

We then turn to the problem of bipolaron instability, relying on the fact that the enlarged variational freedom of the Gutzwiller phonon wavefunction has already proved to be reliable or at least to clearly improve on VLF at intermediate and strong couplings. As expected we find that at a critical value of the e-ph coupling a Pair (bipolaronic) insulator establishes; in the antiadiabatic limit one has $\lambda_c = U_c/D \simeq 3.39$, the critical value for the Mott metal-insulator transition of the Hubbard model, whereas λ_c gets smaller and smaller as adiabatic values of γ are approached. The energies of the paramagnetic metal at different γ are shown in Fig. 5.11 and compared to the bipolaronic insulator energy. In order to make the comparison clearer, the constant contribution $\omega_0/2$, corresponding to the energy of noninteracting phonons, has been removed, and all lines start from ε_0, the kinetic energy of free electrons. We found that the transition is second order for large values of γ, since the metallic energies smoothly

evolve until they coincide with the bipolaronic energy. On the other hand, as soon as $\gamma < 0.6$, the two energies cross, hence signalling a first-order transition that is reflected also in the discontinuity observed in the evolution with λ of d, the averaged number of doubly-occupied sites, and of Z, the inverse of the effective mass. These findings were obtained also by means of slave-boson mean field implemented with variational LFT[61, 114], but we stress the fact that GPW, providing a more accurate description of the intermediate-coupling regime, pushes to smaller values the range of γ in which the second-order character of the transition is correctly reproduced.

To make this point more explicit, in Fig. 5.12 we compare d and Z as obtained in the GPW and VLF (bold lines) frameworks. Moving from the antiadiabatic results $d = (1 + \lambda D/U_c)/4$ and $Z = 1 - (\lambda D/U_c)^2$, one can see that the two methods provide the same results as long as $\gamma > 1$; at $\gamma = 1$ a quantitative improvement can be seen in both quantities for intermediate λ, while for $0.6 < \gamma < 1$ VLF fails in capturing the smooth evolution of d and Z towards the insulator values 0.5 and 0, respectively. However, when the exact adiabatic limit is

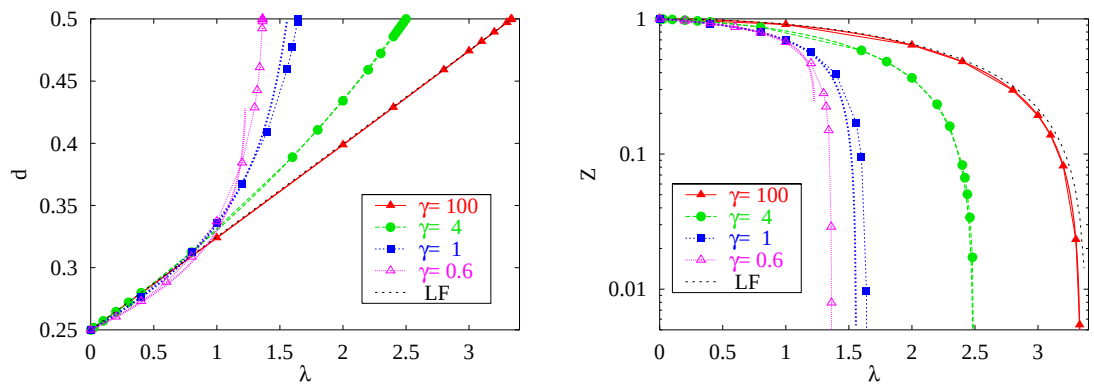

Figure 5.12: Averaged number of doubly-occupied sites d and quasiparticle renormalization factor Z as obtained in GPW at $U = 0$ and for different γ, compared with the antiadiabatic result (LF) and with VLF (bold lines).

approached, a discontinuity at the transition is recovered for both d and Z also in GPW; according to previous studies of the half-filled Holstein model, the first order of the transition is probably a spurious outcome of the Gutzwiller phonon wavefunction[92, 93, 95].

To understand the extent of the reliability of GPW, we compare in Fig. 5.13 our results for Z with those obtained by means of DMFT[116], which provides the exact reference in the infinite-dimension limit, for two values of the adiabaticity parameter, $\gamma = 1$ and $\gamma = 0.1$. In both cases, the quasiparticle residue evaluated in the GPW method deviates from the DMFT result as λ is increased. However a qualitative difference emerges between the adiabatic case shown in the right panel and the $\gamma = 1$ case (left panel)[3]. In fact at $\gamma = 0.1$ GPW

[3]We notice that $\omega_0 = D$ is where GPW fails to capture even qualitatively the weak-coupling corrections to the effective mass (cfr section 4.1).

predicts extremely weak corrections to Z with increasing λ, and the establishing of bipolaronic insulator is not signalled by a divergence of the effective mass in the present framework. This is clearly in contrast with DMFT, where Z vanishes much faster than the exponential and the transition takes place at $\lambda \simeq 0.76$ with a diverging m^*/m. On the other hand, for $\gamma = 1$ the qualitative behaviour of the quasiparticle residue is correctly captured by our approach, even if GPW overestimate of Z pushes the metal-bipolaron transition to a slightly larger value of $\lambda \simeq 1.45$; we notice also that the error found in GPW is smaller than that observed in other approximate schemes such as the standard Migdal-Eliashberg approximation and the self-consistent noncrossing approximation[94, 100].

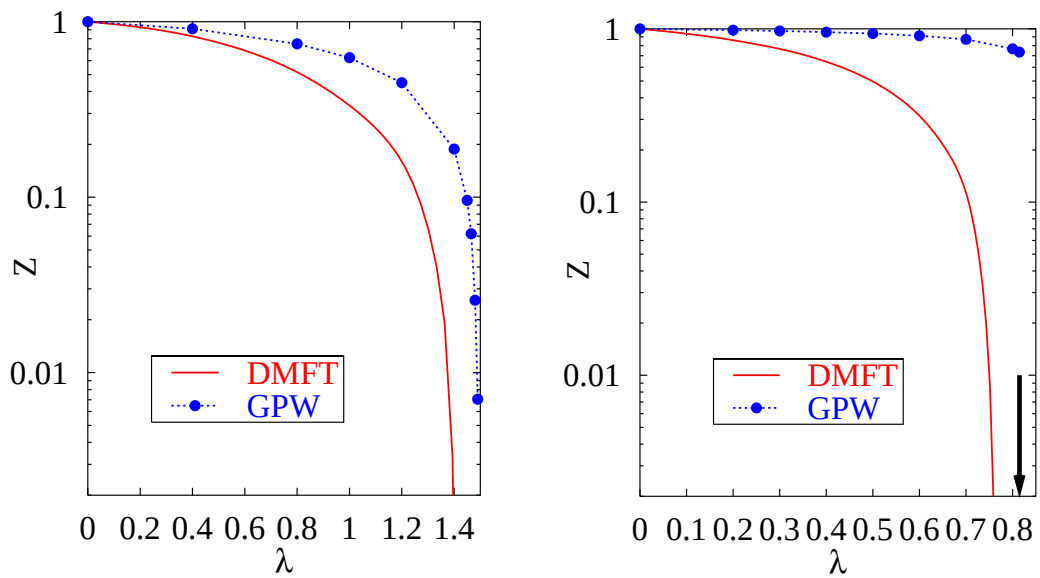

Figure 5.13: Quasiparticle renormalization factor Z as obtained by GPW and DMFT for two values of the adiabaticity parameter, namely $\gamma = 1$ (left) and $\gamma = 0.1$ (right). The vertical arrow in the right panel marks the first-order metal-bipolaron transition (from the energy crossing). To make the comparison meaningful, the energy scales in the GPW calculations are scaled such that the critical values of bipolaron transition coincide with DMFT in the antiadiabatic limit.

In order to check whether the Gutzwiller phonon wavefuncion is able to describe ground-state properties of the system, we compare also the lattice probability distribution function as evaluated in GPW and in DMFT[116]. With respect to the infinite$-U$ limit, the situation under examination presents a richer and more involved physics, and we expect it to be captured in the PDF. In the former case, in fact, electron and phonon degrees of freedom are actually decoupled, due to the infinite repulsion between electrons. This was reflected in the fact that electron parameters P_0 and P_1 entered as independent variables in the variational equations for the phonon wavefunctions. At half filling this is clearly not the case, as electron and phonon problems have to be solved togheter in a self-consistent way.

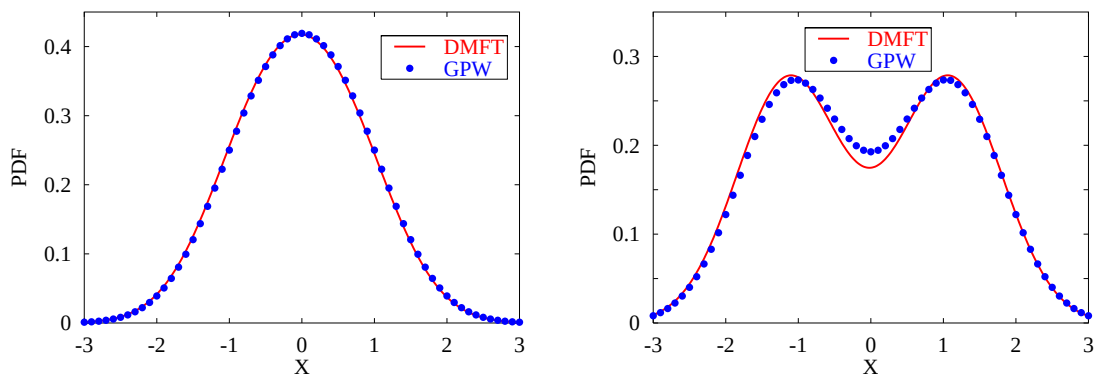

Figure 5.14: PDF evaluated in DMFT and in GPW for $\lambda = 0.8$ (left) and $\lambda = 1.4$ (right) at $\gamma = 1$.

We start by considering the $\gamma = 1$ results. In Fig. 5.14 we plot the PDF evaluated in the present framework compared with that computed in DMFT for an intermediate $\lambda = 0.8$ and a strong $\lambda = 1.4$ close to the bipolaron transition. In the first case, shown in the left panel, the agreement is indeed remarkable, even if at the same value of e-ph coupling GPW estimate of Z is already sizeably wrong. On the other hand, at $\lambda = 1.4$ the two curves are not coincident, but the Gutzwiller phonon wavefunction reproduces qualitatively the bimodal shape of the PDF and the positions of the two peaks. This findings are consistent with those discussed in the infinite$-U$ limit; in that case the deviation at small γ from DMFT results were larger in the effective mass rather than in the overlap between phonon wavefunctions, i.e. in the evaluation of a ground-state property.

A different situation is found at $\gamma = 0.1$, as shown in Fig. 5.15. In this case the two approaches lead to qualitatively different results. In particular, the Gutzwiller phonon wavefunction is not able to reproduce the bimodal shape which signals the polaron formation. However one can wonder if this result stems from a worse treatment of the phonon rather than electron degrees of freedom. In fact, the shape of the lattice probability distribution function stems from two contributions in the GPW method, namely the projected phonon wavefunctions, that roughly determine the position of the peaks, and the electron weights P_l. It might happen that such weights are uncorrectly evaluated by GPW while projected phonon wavefunctions qualitatively capture the shift induced at the ground-state level by the e-ph coupling. This would imply that the Gutzwiller approach is not able to account properly for the e-e interaction mediated by the phonons, that is ultimately responsible for the evaluation of d and consequently of P_l, whereas the modification induced by the e-ph interaction on ground-state phonon properties are at least qualitatively captured. Of course this interpretation is a bit tricky, since the P_l's enter in the coupled equations that determine the phonon wavefunctions φ_l, and no rigorous conclusions can be drawn. However a quick glance at Eqs. (5.39),(5.40) suggests to test this idea with $\gamma \gtrsim |\varepsilon_0|$, in order to consider the

coupling term mediated by the electrons as an almost perturbative correction. Then we can

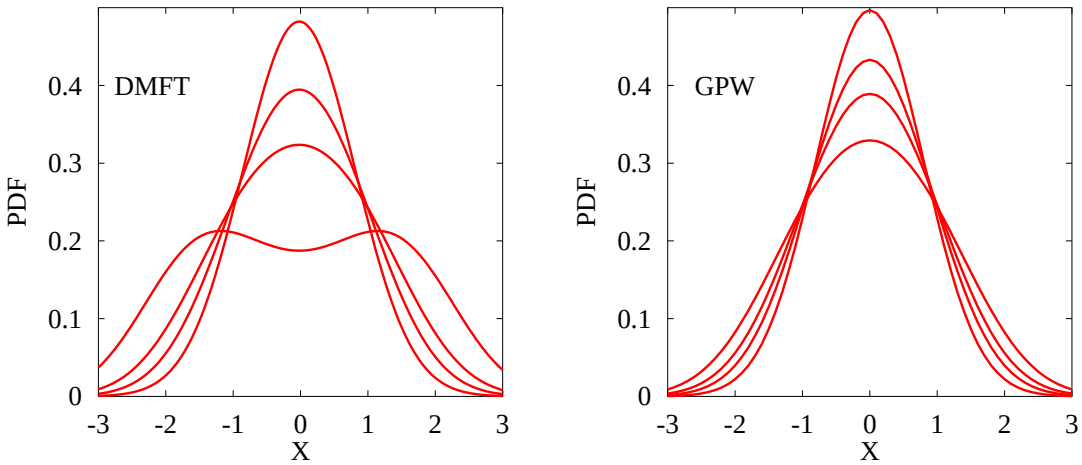

Figure 5.15: PDF evaluated in DMFT and in GPW at $\gamma = 0.1$ for increasing λ from bottom to top.

assume that Eq. (5.44) still holds and extrapolate d from the quasiparticle factor Z obtained in DMFT as $d = (1+\sqrt{1 - Z/|\langle\phi_1|\phi_0\rangle|^2})/4$, where the overlap is that evaluated in GPW. This last assumption is reasonable if our hypotesis of accurate phonon wavefunctions come true; on the other hand, this procedure comes from the observation that in DMFT the relevant quantity that measures the effectiveness of e-ph coupling in determining physical properties of the model is the quasiparticle residue Z rather than d. Plugging the extrapolated d in Eq. (5.45) without changing φ_0 and φ_1 we obtain a rescaled PDF, shown in Fig. 5.16 for $\lambda = 1$ at $\gamma = 0.4$ For these values of the parameters a bimodal shape is already found in the GPW framework, however the peak positions are closer and the depletion at $X = 0$ is less pronounced with respect to the DMFT phonon probability distribution function. With the rude procedure just described a remarkable improvement is observed, and the PDF thus obtained almost coincide with that derived in the DMFT framework.

To summarize, a sizeable improvement is observed with respect to the variational LFT scheme. Quasiparticle effective masses are qualitatively captured down to values of ω_0 that are comparable with the uncorrelated kinetic energy $|\varepsilon_0|$, and a second-order transition to a Pair (bipolaron) insulating phase is found in this range of γ. Most notably, ground-state properties of the phonon can be addressed in a very intuitive way, at the same time providing very accurate results as long as $\omega_0 \gtrsim D$. In particular, a bimodal shape, that signals the formation of polarons, develops in the phonon probability distribution function just before the bipolaronic insulator is reached, in agreement with previous studies[94, 95]. We conclude that the adiabatic failure of the Gutzwiller phonon wavefunction applied to the Holstein model is associated to an unaccurate treatment of the retarded e-e interaction mediated by the e-ph coupling, that might lead to a residual interaction between the quasiparticles defined

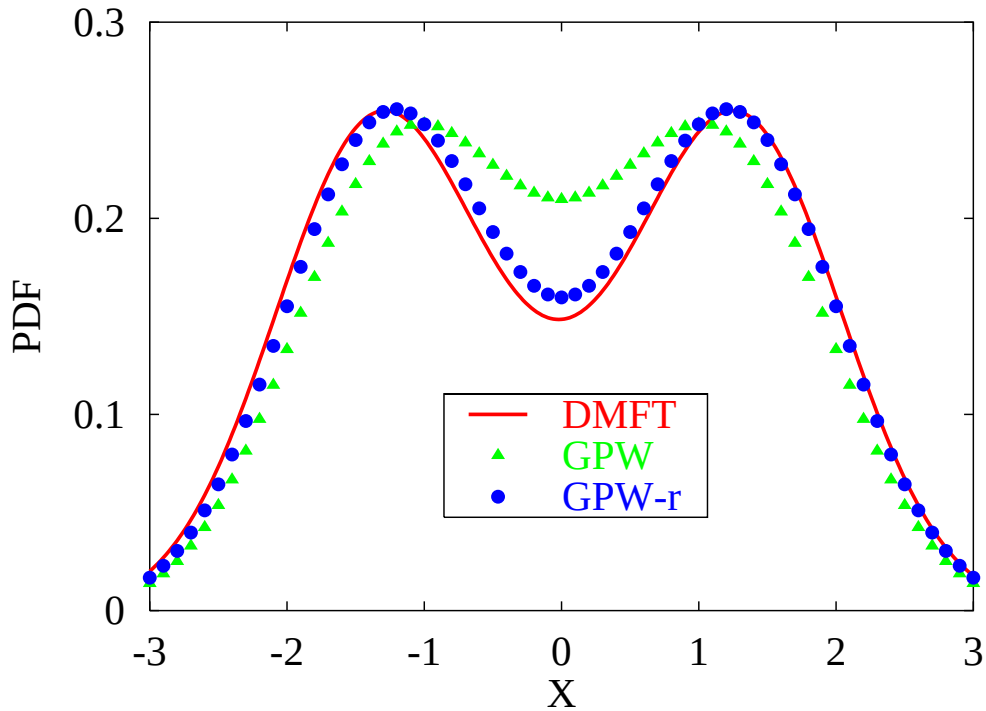

Figure 5.16: PDF evaluated in DMFT and in GPW for $\lambda = 1$ at $\gamma = 0.4$, shown togheter with the PDF obtained as a combination of GPW phonon wavefunctions and electron weights P_l extrapolated from DMFT quasiparticle residue (GPW-r).

by the GPW which becomes large as $\gamma \to 0$. Even if this point deserves deeper analysis, it is reasonable that the presence of sizeable e-e correlation deplects the effects of the retarded contribution to e-e interaction, along the discussion made in section 4.1. According to Fig. 3.8, we can also assume that for $U \gtrsim 1.5$ the ground-state physics of the model is that of a correlated system with reduced repulsion due to the screening induced by phonons.

5.3.2 Metal-insulator transitions at half filling

As in the infinite$-U$ limit previously discussed, the improvement of the Gutzwiller phonon wavefunction with respect to the analogue slave-boson approach to the effective Lang-Firsov-transformed model is more pronounced at intermediate e-ph coupling, where retardation effects are responsible for sizeable deformations of the phonon wavefunctions. In fact, the LFT is expected to provide the correct physical picture when λ is large, whereas at weak coupling we have shown that GPW and VLF are completely equivalent (cfr. Fig. 4.1), since the harmonic ansatz for the projected phonon wavefunctions proves to be essentially correct. On the other hand GPW provides a reliable tool, through the analysis of PDF, to address the problem of polaron formation, that has been shown to be not necessarily associated to the metal-insulator transition induced by the increasing of λ, which is instead due to pair

formation[94]. Therefore in this section we try to complete the picture that has been traced out in section 3.3, with particular attention to the metal-bipolaron insulator transition in different adiabaticity regimes.

To this purpose, in Fig. 5.17 we show the evolution with λ of the averaged number of doubly-occupied sites d and of the renormalization of the electronic kinetic energy Z for a value of Hubbard repulsion close to the metal-Mott insulator transition in the absence of e-ph interaction, namely we choose $U = 0.8U_c$. In the antiadiabatic limit the transition to the Pair insulator is shifted to larger e-ph coupling, according to $\lambda_{BI}D = U + U_c$, that simply reflects the competition between the Hubbard U with the attractive non-retarded e-e interaction mediated by phonons. As a consequence, d linearly increases from the value determined by correlation in the absence of phonons $d(\lambda = 0) = 0.25(1 - U/U_c)$ until it saturates at the metal-insulator transition, where $d = 0.5$ and all electrons are bound to form local pairs. On the other hand, Z increases as long as the effect of λ is to reduce the local repulsion, it has a maximum when the attractive and repulsive interactions exactly compensate ($Z = 1$ and $d = 1/4$ as for the noninteracting system) and it eventually decreases and vanishes as in the attractive Hubbard model. Moving from the antiadiabatic limit two major effects

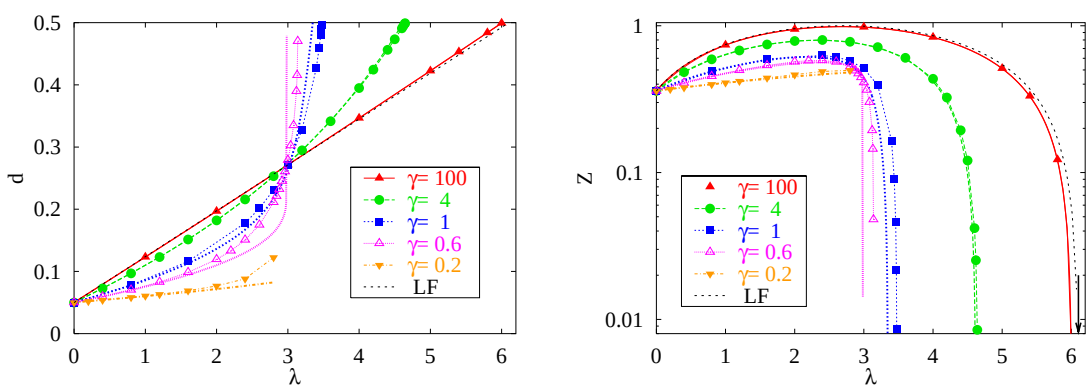

Figure 5.17: Averaged number of doubly-occupied sites d and quasiparticle renormalization factor Z as obtained in GPW at $U = 0.8U_c$ and for different γ, compared with the antiadiabatic result (LF) and with VLF (bold lines). Vertical arrow in the right panel marks the antiadiabatic prediction for the establishment of BI.

are observed. First, the critical value λ_{BI} at which the bipolaronic insulator establishes is shifted to smaller values, as qualitatively predicted by Eq. (3.23). Second, even if the value of λ at which the repulsive and phonon-induced attractive e-e interactions compensate is not changed much, phonon screening of U is less and less effective with decreasing γ as long as the repulsion is dominant, as highlighted by the almost constant behaviour of both d and Z when, for example, $\gamma = 0.2$. On the other hand, the transition to bipolaron is sharper, and it is found to be first order already at $\gamma = 0.6$ at the given value of U. We notice that GPW and VLF results agree very well at $\gamma > 1$ in the whole range of λ, whereas they bifurcate at

intermediate couplings for smaller values of the adiabaticity parameter; in particular, λ_{BI} as evaluated in GPW is slightly larger than that computed in the variational LFT framework.

We address now the problem of polaron formation in the presence of sizeable $U/U_c = 0.8$ by looking at the lattice probability distribution function, shown in Fig. 5.18 for different values of λ at $\gamma = 0.6$ and $\gamma = 4$. In the last case one sees the same evolution discussed in the absence of Coulomb repulsion, namely a broadening of the curve that keeps a unimodal shape until the distortion of the lattice site induced by the e-ph coupling is such that a bimodal distribution develops. Notice that for larger values of γ, the displacement of the phonons, being proportional to $\sqrt{\lambda/2\gamma}$, is not able to separate the two peaks characteristic of the bimodal PDF before the bipolaronic insulator phase, signalled by the vanishing of $P_1 = 1 - 2d$ (i.e. the singly-occupation probability, which enters in the PDF as the weight of the central peak), is reached. Of course one can consider the case of larger values of U, which would require a stronger e-ph coupling to exceed the repulsion and to induce the formation of local bipolarons, thus allowing for a polaron crossover before the M-BI transition.

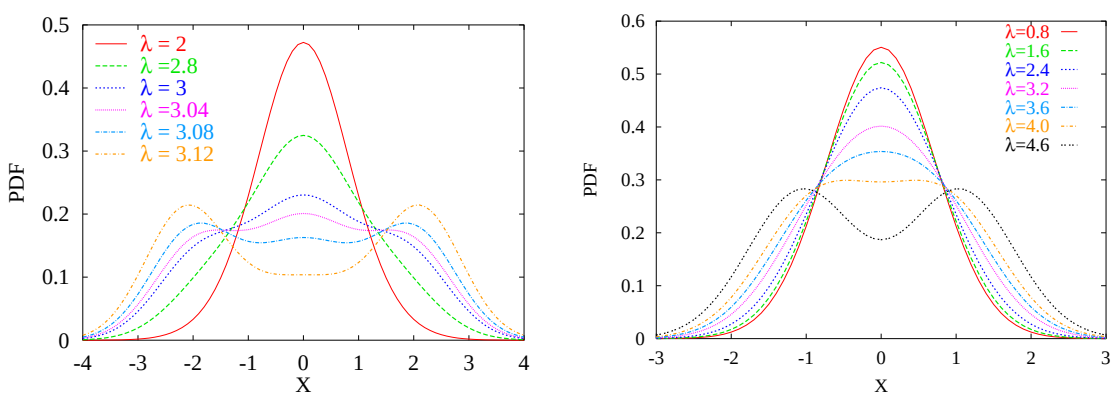

Figure 5.18: Evolution with λ of PDF at $U/Uc = 0.8$ and for two values of γ representative of adiabatic (left, $\gamma = 0.6$) and nonadiabatic (right, $\gamma = 4$) regimes.

A qualitative different situation is observed at smaller γ. As long as the repulsion is not compensated by the attractive term due to λ, i.e. $\lambda \lesssim 2.94$ when $U/U_c = 0.8$ and $\gamma = 0.6$, the singly-occupied state has a larger probability than empty and doubly-occupied ones, and the PDF as given by Eq. (5.45) displays a peak centered in the origin that is only broadened by the e-ph coupling. For larger λ two shoulders appear in addition to the central peak, which rapidly evolve in two symmetric peaks coexisting with that centered in $X = 0$ in a very narrow range of λ, until the bipolaronic insulator is reached.

To characterize the polaron crossover we can analyze the behaviour of the second derivative of $P(X)$, following Ref. [95]. At half-filling, due to the symmetry properties of the phonon wavefunctions, it is straightforward to demonstrate that $dP(X)/dX|_{X=0} = 0$ for any value of the parameter, meaning that $X = 0$ is always an extremal of the PDF. Of course, the change from negative to positive values of the second derivative evaluated in the origin

indicates that $X = 0$ changes from being a maximum (absence of finite distortions of the lattice) to a minimum (polaron formation). Therefore the condition for polaron formation $d^2P(X)/dX^2|_{X=0} \geq 0$ reads in our approach:

$$4d\left[\varphi_0(0)\,\frac{d^2\varphi_0}{dX^2}\Big|_{X=0} + \left(\frac{d\varphi_0}{dX}\right)^2_{X=0}\right] + 2(1-2d)\,\varphi_1(X=0)\,\frac{d^2\varphi_1}{dX^2}\Big|_0 \geq 0. \tag{5.46}$$

In the antiadiabatic limit, where phonon wavefunctions are displaced harmonic oscillators, this condition can be recast as[95]:

$$e^{-2\alpha^2}(4\alpha^2-1) \geq \frac{2d}{1-2d}. \tag{5.47}$$

If we plug in this formula the bipolaronic condition $d = 1/2$, we conclude that polaron formation occurs at the M-BI transition only if condition $\alpha^2 > 1/4$ is fullfilled togheter with Eq. (3.23). This is not the case in the Holstein model, where the pair insulator establishes in the antiadiabatic limit for much smaller λ than those required to obtain a bimodal PDF (cfr. Fig. 2.4). However Eq. (3.23) indicates that a sizeable Coulomb repulsion shifts λ_{BI} towards larger values, while condition $\alpha^2 > 1/4$ is not changed by the presence of U. As a consequence the e-e correlation can stabilize polaron formation before the attraction mediated by phonons is able to localize the quasiparticles, as we showed in the right panel of Fig. 5.18. This is not surprising, since polarons represent a single-particle problem from the point of view of electrons, and e-e interactions do not affect directly polaron formation, whereas they are responsible for the bipolaronic transition.

Relaxing the antiadiabatic condition, the left-hand side of Eq. (5.46) has to be evaluated numerically. This can be done straightforwardly in the present framework exploiting the expansion of φ_l on harmonic oscillator eigenstates, allowing us to enrich the phase diagram for the half-filled Hubbard-Holstein model (Fig. 5.19) by adding lines representing polaron formation. We notice that condition (5.46) may not be significative when PDF assumes different shapes rather than unimodal or bimodal ones, e.g. the three-peak structure plotted in Fig. 5.18, however we expect to capture the correct order of magnitude of the critical parameters for the polaron crossover.

To summarize, we compare in Fig. 5.19 the phase diagram obtained in the present framework for different adiabaticity regimes. In the antiadiabatic limit the metal-Mott insulator and the metal-Pair insulator transition are symmetric around the line $d = 0.25$, which signals the exact balance between instantaneous Hubbard bare repulsion and phonon-mediated attraction (dotted lines in Fig. 5.19), and are both second order. With decreasing γ the M-MI transition line increases its slope and slightly changes its curvature, bending at intermediate e-ph couplings towards larger values of U. We compare our findings with the relation extracted from a fitting procedure to the quasiparticle residue in DMFT analysis of the model[57, 60]:

$$\lambda_{MI}D = \frac{1+2\omega_0/U}{2\omega_0/U}\big(U-U_c\big), \tag{5.48}$$

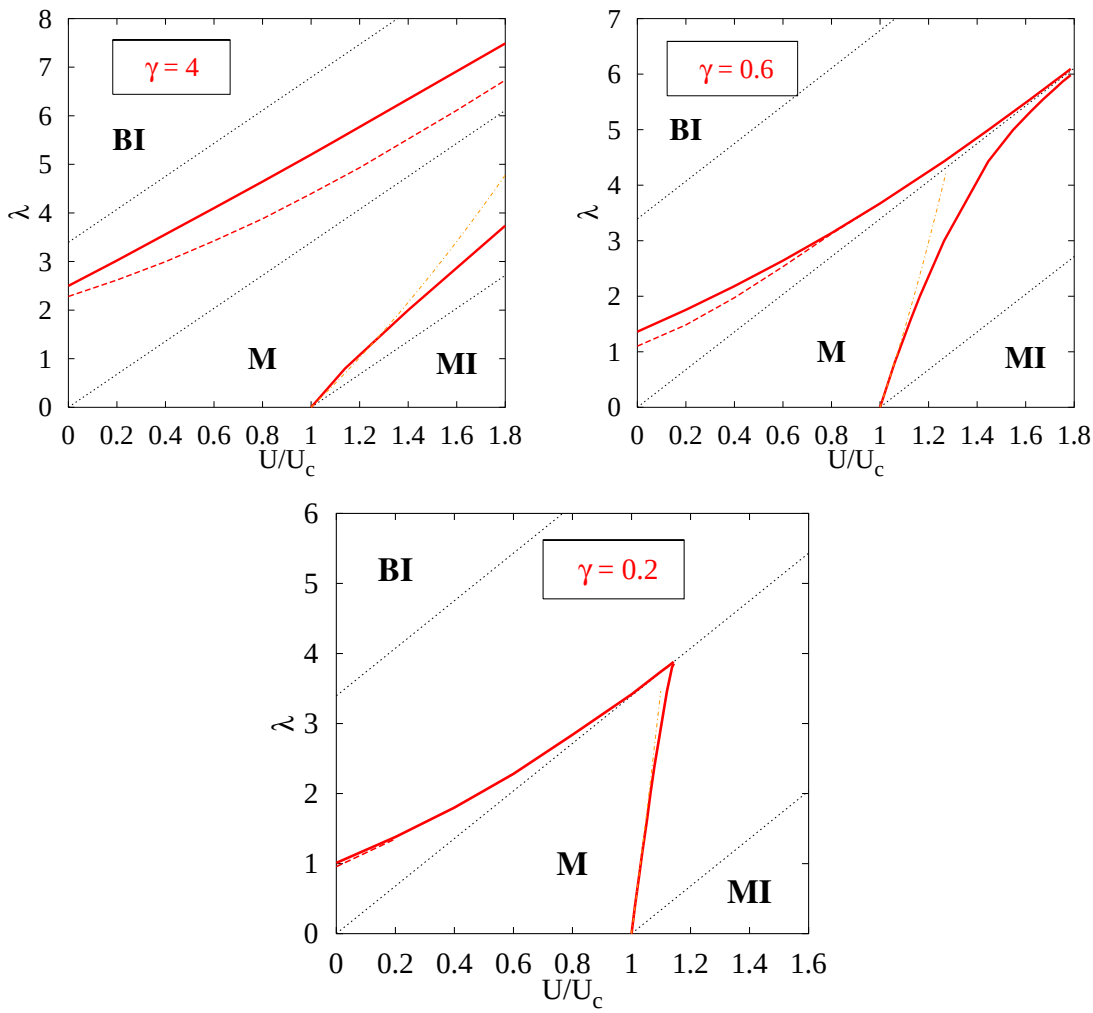

Figure 5.19: Phase diagram for the half-filled Hubbard-Holstein model as obtained in the GPW framework for different values of γ. Bold lines represent the M-BI and the M-MI transitions. Thin dotted lines are the antiadiabatic prediction for transitions and vanishing of the e-e interaction ($d = 0.25$). Thick dotted lines are the polaron crossover from bimodality of PDF. The M-MIT transition line is compared with analytical predictions.

which reduces to Eqs. (3.27),(3.28) in the adiabatic and antiadiabatic limit respectively. On the other hand, the bipolaronic insulator establishes at smaller λ as γ is reduced. At $\gamma = 4$ the transition is found to be always second-order, that means that no crossing between energies is observed as the metal energy smoothly merges with the bipolaron one (analogously to the $U = 0$ regime discussed in the previous section). In agreement with condition $\alpha^2 > 1/4$, we find that a polaron crossover occurs before the BI phase is reached already at $U = 0$; the effect of U is to slightly enlarge the region in which mobile polarons are more stable than localized pairs. This is not the case at $\gamma = 0.6$, where the presence of U tends to shrink the region where polarons are formed; as already noticed, we stress the fact that our estimate of

polaron crossover from the change in sign of $d^2P(X)/dX^2|_{X=0}$ may not be significative in the presence of exotic PDF as the one shown in Fig. 5.18. On the other hand we found that metal and bipolaron energies cross in a range of U between $\sim 0.5U_c$ and $\sim 1.1U_c$, signalling a first-order transition. This suggests again a highly nontrivial competition between electronic and phononic energy scales; the problem of the order of M-BI transition in the Hubbard-Holstein model has been already addressed in Ref. [55], where a change from second to first order has been observed as $U \gtrsim 0.5U_c$ at a lower phonon frequency, $\gamma = 0.1$. Unfortunately our approach is not suitable to analyze accurately the very small γ regime, as already pointed out in our analysis of the Holstein model; as a consequence the bipolaron transition for $\gamma = 0.2$ is found to be first-order for any value of the repulsion, and almost no polaron formation is observed, except in a very narrow region at small U.

5.3.3 Properties of the ground-state phonon wavefunctions

We conclude this section by performing an analysis of the ground-state phonon wavefunctions analogously to that in the infinite$-U$ limit. As in that case we will consider $\langle X\rangle_l$ and

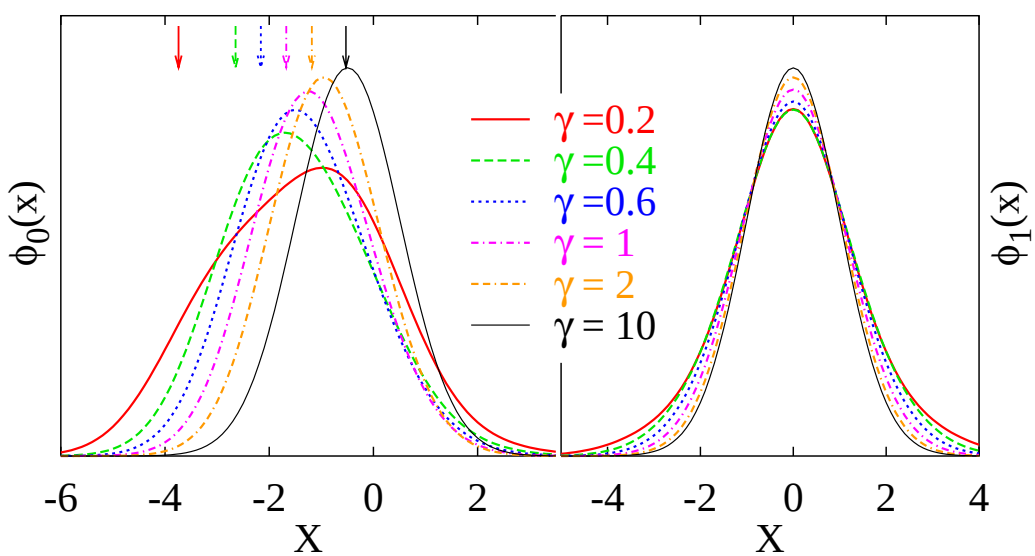

Figure 5.20: Evolution of phonon wavefunctions as function of γ for $\lambda = 2.8$ and $U/U_c = 0.8$. The arrows indicate the displacement in the atomic limit.

$\langle (X - \langle X\rangle)^2\rangle_l$ as a measure of the effective displacement of the lattice site and of the extent of the phonon fluctuations induced by e-ph coupling. Just to give the flavour of what we expect to find we show in Fig. 5.20 the evolution of φ_0 and φ_1 as γ is decreased for an

intermediate e-ph coupling $\lambda = 2.8$ and in the presence of a sizeable electronic correlation $U = 0.8U_c$. Due to the symmetry properties of the half-filling regime, the only effect of the e-ph coupling on φ_1 is to broaden its width, being $\langle X \rangle_1 = 0$, corresponding to the atomic limit value. On the other hand, the displacement of φ_0 is strongly reduced with respect to the atomic limit (indicated by the vertical arrows) as the adiabatic regime is approached, while at the same time fluctuations of the phonon increase (the same occurs for φ_2, whose peak is shifted, according to Eq. (5.38), in the opposite direction with respect to the origin). In particular we observe a non monotonic dependence of the peak position on γ, as the maximum of φ_0 is closer to the origin at $\gamma = 0.2$ rather than at $\gamma = 0.4$, whereas its width seems to increase monotonically as the adiabatic limit is approached.

To begin with, we consider the effect of increasing λ when $U = 0$ and close to the metal-MI transition, namely $U = 0.8U_c$, comparing with the atomic limit, where $\langle X \rangle_l = \sqrt{2}\alpha(l-1)$, and with VLF. Since the most outstanding deviations from LFT results occur in the adiabatic limit, in Fig. 5.21 we consider $\gamma = 0.6$, a value of the adiabaticity parameter at which our method is quite reliable even in the absence of Coulomb repulsion. As already pointed out,

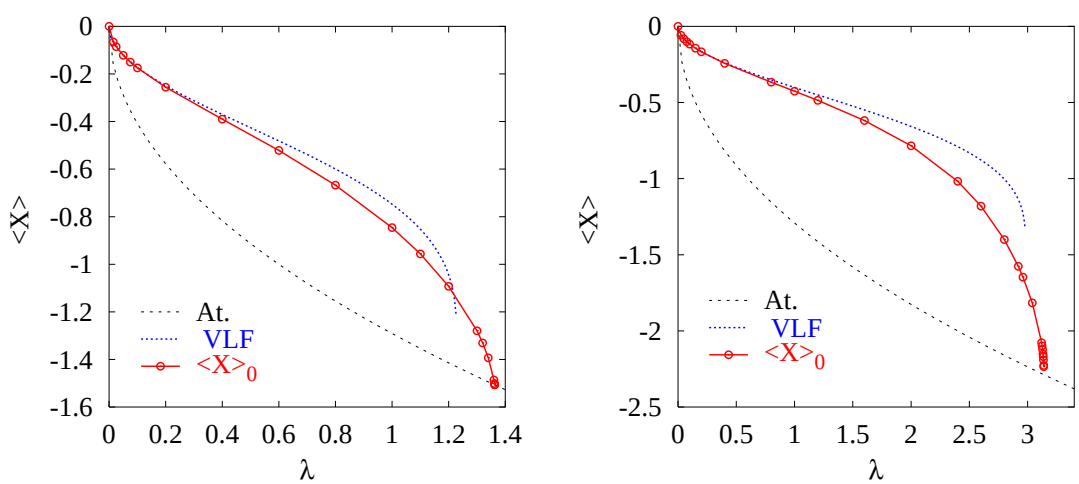

Figure 5.21: Evolution of the displacement of the phonon wavefunction φ_0 as function of λ at $\gamma = 0.6$ and $U = 0$ (left), $U/U_c = 0.8$ (right), compared with the atomic limit and VLF.

both GPW and VLF capture the smaller displacement of the lattice sites in the adiabatic regime with respect to the atomic limit. However, even if they coincide as long as small values of e-ph coupling constant are considered, VLF clearly underestimates the lattice distortion in the intermediate-coupling regime, hence it fails in describing the way in which the bipolaronic insulator is approached. We notice that, when $U = 0$, the metal-BI transition is accompanied by a local distortion equal to that predicted in the atomic limit; at $U/U_c = 0.8$, on the other hand, $\langle X \rangle_0$ at the transition is still slightly different from the atomic value, confirming the first order character of the metal-BI transition in the presence of sizeable Coulomb repulsion and for small values of γ. We compare also the broadening of φ_0 and φ_1 in Fig. 5.22. Again

we find that the major deviations from the atomic limit value 1/2 occur in the intermediate e-ph coupling regime for what concerns φ_0, and that the broadening is enhanced but shifted to larger λ by the presence of U. On the other hand, the width of φ_1 is monotonically increased as the bipolaronic phase is approached and the associated weight P_1 goes to zero.

To better understand the effect of U on the ground-state phonon wavefunctions, we show in Fig. 5.23 the evolution of the mean displacement and the width of φ_l, togheter with their overlap $\langle\varphi_0|\varphi_1\rangle$, as the Hubbard repulsion is increased at $\gamma = 0.6$ and $\lambda = 1$. As expected, the presence of U counteracts the effect of e-ph coupling, reducing the induced distortion of the lattice of a factor greater than 1/2 for the given values of the parameters when the Mott insulator establishes. At the same time, retardation effects due to phonon dynamics are less relevant as the metal-MI transition is approached; this is highlighted by the behaviour of $\langle(X - \langle X\rangle)^2\rangle_l$ in the central panel of Fig. 5.23, where it is shown that the width of the phonon wavefunctions tends to 1/2, the value characteristic of the harmonic oscillator, as $U \to U_c(\lambda = 1) \approx 1.07U_c$. In particular, this is exactly true as φ_1 is concerned. In fact it reduces to a harmonic oscillator centered in the origin, consistently with the description of the Mott insulating phase predicted by the Gutzwiller phonon wavefunction, where the insulator is depicted as a collection of atomic sites with only one electron on each of them. On the other hand, φ_0 still deviates from the gaussian shape at the transition but its contribution to the physical properties of the system becomes negligible as the number of empty and doubly-occupied sites vanishes due to the presence of U. At last we notice that the agreement with VLF is very good when considering the overlap between phonon wavefunctions associated to different charge states; in both GPW and VLF, this quantity is essential to determine the phonon-induced renormalization of electronic kinetic energy. As already pointed out, such an agreement implies, due to the harmonic assumption made in LFT-based approaches, that the

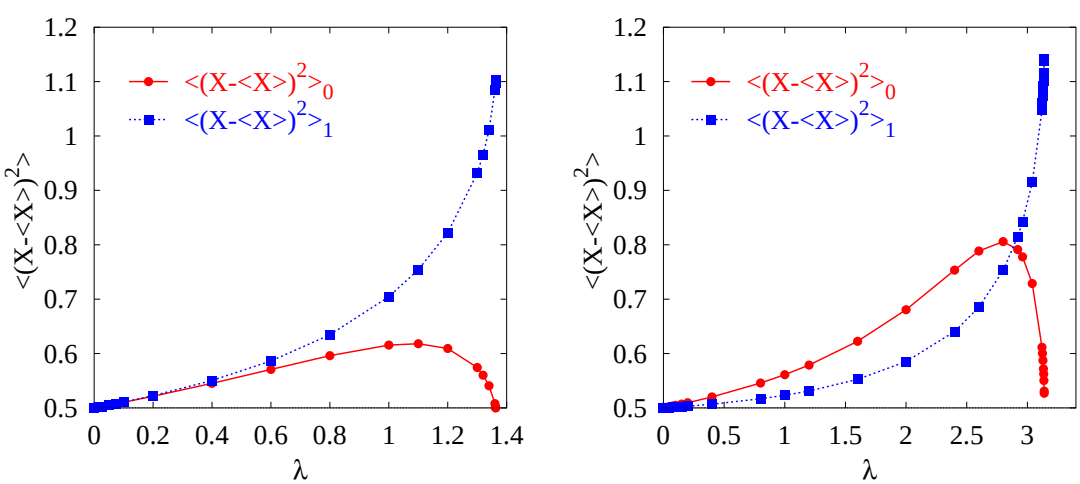

Figure 5.22: Fluctuations of the phonon wavefunctions with increasing λ at $\gamma = 0.6$ and $U = 0$ (left), $U/U_c = 0.8$ (right).

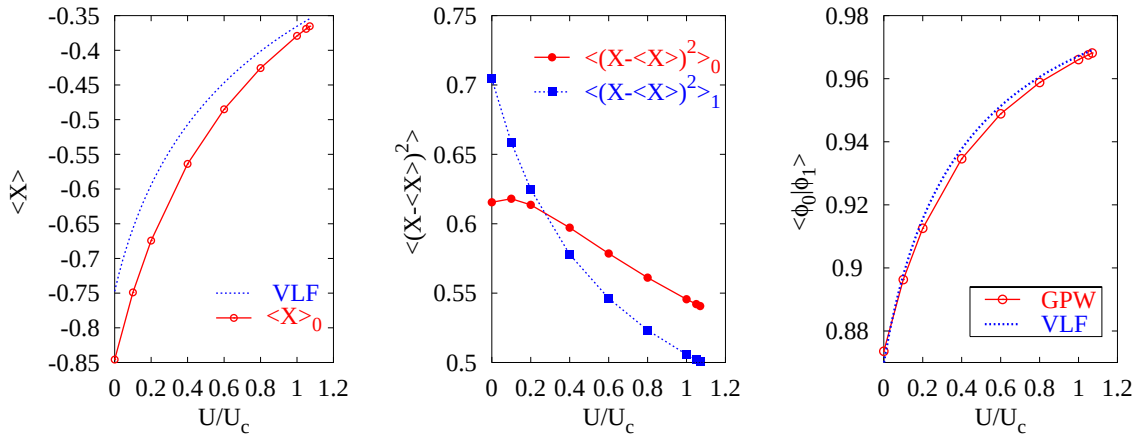

Figure 5.23: Evolution of mean displacement, fluctuations and overlap between φ_0, φ_1 as function of U at $\lambda = 1$ and $\gamma = 0.6$. $\langle X\rangle_0$ and $\langle\varphi_0|\varphi_1\rangle$ are compared with VLF results.

actual distortion of the lattice sites is underestimated (cfr. left panel of Fig. 5.23) since the broadening of φ_l induced by phonon dynamics is not taken into account; this means that a sistematic error is introduced in VLF when evaluating the potential energy gain due to e-ph coupling. Anyway, on the basis of the present analysis, a sizeable U is able to reduce the size of this error, thus explaining the quantitative accuracy of Eqs. (3.27),(3.28).

At last we focus our attention on the $\gamma-$dependence of the ground-state properties of phonon wavefunctions. As already observed in the infinite$-U$ limit, the mean displacement

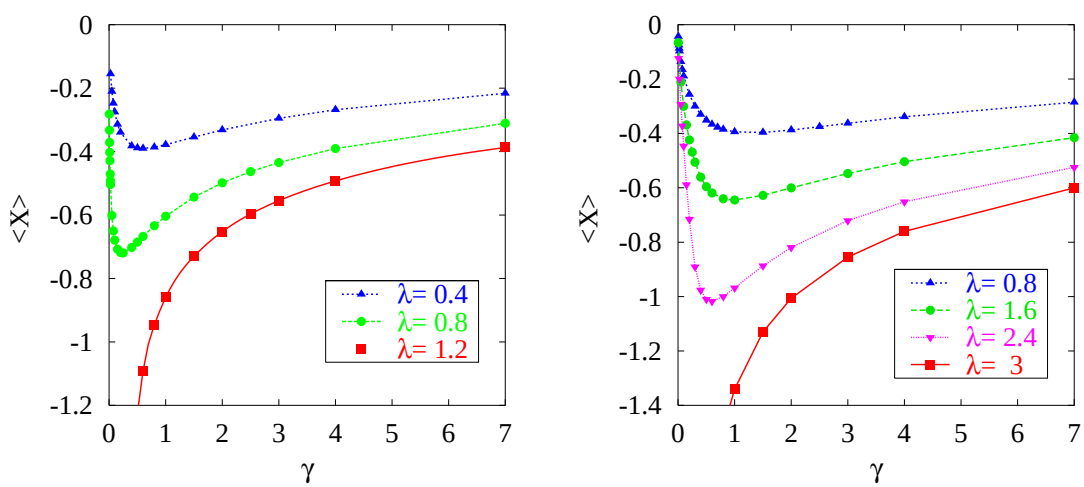

Figure 5.24: Evolution of the mean displacement of phonon wavefunction φ_0 as function of γ at $U = 0$ (left) and $U/U_c = 0.8$ (right) and for different values of e-ph coupling constant.

of φ_0 (and in this case that of φ_2, symmetric to φ_0 with respect to the origin) increases and diverges roughly as $\sqrt{1/\gamma}$ when moving from the antiadiabatic regime at strong e-ph

coupling[4], whereas in the intermediate- and weak-coupling regimes it displays a maximum and then decreases, suggesting the tendency of φ_l to coincide as $\gamma \to 0$. This behaviour is observed both with and without electronic correlation, as shown in Fig. 5.24, even if the vanishing of $\langle X \rangle$ is observed at $U/U_c = 0.8$ rather than in the Holstein model where the mean displacement seems to tend to some finite value as γ approaches 0. A more outstanding difference emerges when fluctuations of phonon around the mean displacement are considered. In fact, in the pure Holstein model (left panel in Fig. 5.25) one recovers a monotonical broadening of phonon wavefunctions as the exact adiabatic limit is approached. This finding is equivalent to that discussed at the end of section 5.2.3; as in that case it means that phonons are weakly dependent on the local charge density, since they are not able to follow instantaneously electrons as they move in the lattice, and that at the same time the phonon wavefunctions extend over a wider region of space. We notice that, even if the present approach has proven to be scarcely accurate in the weakly-correlated adiabatic regime of the system, this finding qualitatively agrees with the common wisdom according to which the size of polarons, i.e. of the electron surrounded by the multiphonon cloud induced by e-ph coupling, increases in the adiabatic limit, involving more and more phonons. On the other hand, when a sizeable Hubbard repulsion is considered, the width of all phonon wavefunctions displays a maximum and then tends to coincide for vanishing γ, remaining comparable with that of a gaussian harmonic oscillator; for example, at $\lambda = 1.6$, we found that the extrapolated value of $\langle (X - \langle X \rangle)^2 \rangle_l$ for $\gamma \to 0$ is $\simeq 0.56$ (marked by the orizzontal arrow in the right panel of Fig. 5.25) when evaluated for φ_0 and φ_1. With an analogue extrapolating procedure, one also finds that $\langle X \rangle_0 \to 0$ as the exact adiabatic limit is attained. Therefore in the presence of strong electronic correlation e-ph coupling appears strongly renormalized and is little effective

[4]In order to obtain a non trivial adiabatic limit of $\langle X \rangle$, cfr. footnote at page 85.

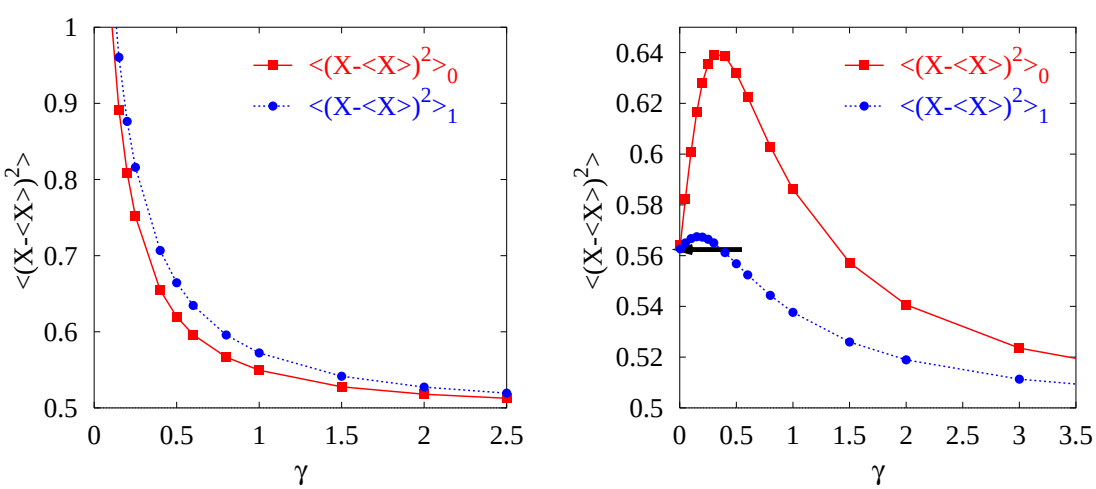

Figure 5.25: Fluctuations of the phonon wavefunctions as function of γ at $U = 0$ and $\lambda = 0.8$ (left), $U/U_c = 0.8$ and $\lambda = 1.6$ (right).

in inducing lattice deformations but for large values of λ; furthermore the size of polarons remains small even in the adiabatic limit, and a small number of phonons is involved at the ground-state level.

We conclude this section by noticing that the average displacement of the phonon wavefunctions can be related straightforwardly to the static local electron-displacement correlation function $C_0 = \langle n_i(a_i + a_i^\dagger)\rangle$ that is often introduced as a measure of the polaronic character of electrons. In fact in GPW framework C_0 is simply given by:

$$C_0 = \sqrt{8}\, P_2 \, \langle X \rangle_2, \tag{5.49}$$

where $\langle X \rangle_2 = -\langle X \rangle_0$ due to the symmetry properties of the half-filling regime. According to our previous discussion, this formula immediatly allows us to recover the strong coupling result 2α for the bipolaronic insulator, denoting large electron-lattice local correlations, whereas it gives $C_0 = 0$ in the Mott insulator. By looking at figs. 5.21 and 5.22, and keeping in mind that $P_2 = d$ is an increasing function of λ (cfr. figs. 5.12 and 5.17), one deduces that in the adiabatic regimes small polaronic character establishes only at intermediate and strong e-ph coupling, and that the presence of U counteracts the onset of strong electron-lattice correlations until the BI is approached. Usually the small value of C_0 at weak couplings is interpreted as a measure of the finite extension of the polaron over several shells of lattice neighbours[86]. As pointed out previously, this is consistent with the broadening of the phonon wavefunctions when small values of electronic correlation are considered. However the vanishing of C_0 as the Mott insulator is approached probably corresponds to a minor relevance of electron-displacement correlations, since the absence of a sizeable broadening of φ_l does not suggest the onset of large polaronic character.

Conclusions

In this work we presented two variational approaches to the electron-phonon interaction in strongly correlated systems. The problem of the interplay between sizeable e-e and e-ph interactions has proven to be relevant in many compounds including the HTSC cuprates. In fact, the importance of strong electronic correlation in these compounds is nowadays widely accepted, and a number of experiments suggests a non-negligible coupling between electrons and lattice dynamics which can lead to unexpected behaviour of physical observables. As a relevant model for the analysis of this problem we chose the Hubbard-Holstein model, which displays a very rich phase diagram and whose physical properties depend on many parameters and energy scales, including phonon frequency, bandwidth and electronic correlation, thus representing a complicated many-body problem. Generally speaking, one could wonder how the electron properties are modified by the presence of the e-ph coupling, or equivalently analyze the modifications induced by the correlated electrons on the phonons. The first approach that we discussed focuses mainly on the first aspect of the problem, whereas the second one completed the picture including a faithful description of phonon properties. We tested both in the paramagnetic sector of the Hubbard-Holstein model at $T = 0$, focusing on ground-state properties of both electrons and phonons.

Variational Lang-Firsov transformation supplemented by slave-boson mean field. The first method we discussed is based on a proper variational formulation of the well-known Lang-Firsov-Holstein approximation and allows mainly for a description of the modifications induced by the phonons onto the correlated system, providing an effective model for renormalized electrons. This model has been analysed in the slave-boson mean-field framework that implies a neglect of spatial correlations and, consequently, an approximate description of hopping processes. However the effect of e-ph coupling in the strongly-correlated regime of the model is captured in a satisfactory way by the variational parameter f, which is determined through a balance of the energy gain coming from the potential energy of the deformed lattice and the energy loss due to the reduced mobility of the electrons coupled with phonons. At half filling the presence of sizeable U, that suppresses charge fluctuations, leads to a substantial depression of polaronic effects; close to the Mott metal-insulator transition the main effect of e-ph coupling is a slight reduction of the Coulomb repulsion, which is controlled by the ratio ω_0/U, in excellent quantitative agreement with previuos DMFT results, that

are supplemented by some analytical results. Such a weak effect on low-energy properties of the electrons is due to the fact that phonons cannot react to the rare and fast virtual hopping processes. Doping the system in the strongly-correlated regime partially restores charge fluctuations, but electrons move so slowly that phonons can catch up and polaronic effects turn out to be relevant expecially in the adiabatic regime, where screening of the bare repulsion is less effective. Also in this case the evolution from weak to strong e-ph coupling is controlled by the adiabaticity parameter γ. Such a dependence on the phonon frequency leads to unusual isotope effects on the effective mass; at half filling we found that the presence of U can strongly enhance the isotope coefficient when approaching the transition, even if the effective mass does not show polaronic signatures. On the other hand in the doped regime a strongly nonmonotonic dependence of the effective mass on γ is observed, and we found that the isotope coefficient can be even zero in the presence of a sizeable e-ph coupling.

Unfortunately this approach provides a very poor insight in phonon physics, since lattice degrees of freedom enter in the renormalized electronic properties only through the single variational parameter f, which in the context of LFT can be interpreted as a measure of the effective displacement of the ground-state phonons, that is reduced as the adiabatic limit is approached. This unaccurate description of phonons does not allow for a proper characterization of polaron formation and it is ultimately the origin of the polaronic transition (rather than a crossover) found in the strongly-correlated doped regime at small values of γ. On the other hand the absence of polaron signatures at the metal-bipolaronic insulator phase at half filling suggests that such transition is mainly driven by electronic correlations, namely the bipolaron phase establishes as soon as the attractive e-e interaction mediated by phonons is able to bind electrons in order to form local pairs, the bipolarons.

Gutzwiller phonon wavefunction. Exploiting the equivalence between slave-boson mean field and the Gutzwiller approach we then introduced a generalization of the trial wavefunction where phonons are described by first-quantization wavefunctions associated to different local charge states. Since the Hubbard repulsion induces an unbalance of the occupation probabilities for the electrons, which is correctly captured by the Gutzwiller approach (where the variational quantity to be optimized is exactly the correlated probability distribution of electrons), we believe that the implicit assumption according to which phonons are determined by the local electron density is reasonable in the presence of strong correlation; on the other hand, when $U = 0$ it may lead to wrong results as weak e-ph couplings and/or very small values of the adiabaticity parameter are considered. This assumption can be enforced also in the slave-boson framework by performing the variational LFT on the boson representation of the model, thus introducing a variational parameter f_i for each auxiliary operator, describing the effective displacement of the lattice site in the presence of 0, 1 or 2 electrons. Nonetheless only two independent phononic parameters are required to determine the mean-field solution, which represent the relative displacements between different charge states; the polaronic-like exponential renormalization of the hopping term is then interpreted

as the overlap between phonon wavefunctions associated to different local electronic occupations. We notice that in the symmetric half-filling regime or in the limiting case of infinite Hubbard repulsion, only two occupation probabilities are needed to determine the ground state, namely the empty(=double occupancy at half filling) and single occupancy probabilities, hence just one independent f parameter is needed; this finding puts on solid grounds the analysis we carried out in chap. 3, and at the same time suggests a proper generalization of that approach to general case of $n \neq 1$.

We proved that the GPW method provides the same result of variational LFT applied on the slave-boson representation of the model as long as a harmonic ansatz is assumed for the phonon wavefunctions, which are then described as displaced harmonic oscillators. Even though such assumption proves to be correct for large values of the adiabaticity parameter (and to some extent in the weak-coupling limit), the larger variational freedom of the GPW method allowed us to capture the deviations from harmonic phonon wavefunctions due to retardation effects of the e-ph coupling, that proved particularly relevant in the adiabatic limit. Generally the coupling with electrons has two major effects for small γ: it induces a smaller displacement of the lattice site with respect to the atomic limit and at the same time enhances the fluctuations around the mean displacement in such a way that the overlap between phonon wavefunctions associated to different charge state is maximized. This implies that, expecially at intermediate e-ph couplings, each phonon wavefunction tends to acquire partial character of the others. As a consequence the mobility of electrons is not reduced as much as one could have expected. The first effect can be approximatively accounted for by the variational LFT, whereas the second is completely missed within the harmonic ansatz for phonon wavefunctions.

This improvement in the description of phonon ground-state properties allowed us to demonstrate that polaron formation is a crossover rather than a transition for any value of the doping in the strongly- correlated regime and for any value of U at half filling. In the first regime, the effect of correlation is to make the crossover sharper and to push it to larger values of λ. On the other hand we found that in the half-filling regime polaron formation does not occur at large γ, hidden by the onset of bipolaronic insulator, whereas at intermediate and small values of the adiabaticity parameter a bimodal shape of the phonon probability distribution function, which signals polarization of the lattice, can develop in the metallic phase just before the transition. The effect of U is to slightly enlarge the region between polaron crossover and bipolaron transition at intermediate values of γ, when the Mott transition is pushed to very large U, whereas it is reduced at small γ, in such a way that the correlated regime close to the Mott transition is always robust with respect to polaron formation. This point has been directly addressed by analysing both effects of e-ph coupling on phonon wavefunctions, namely their displacement and their broadening. In particular we found that the electron-induced displacement of the lattice sites is always reduced when a sizeable U is considered, and at the same time the extent of phonon fluctuations is always comparable to that in the absence of e-ph coupling, even deep in the adiabatic regime. This

explains why almost no phonon effects are observed in the effective mass close to the Mott transition, albeit for a small reduction due to partial screening of the repulsion. On the other hand we found that in the weakly-correlated regime and in the infinite$-U$ limit at $n \neq 1$, small γ implies very small distortion of the lattice but phonons fluctuating in a wide region of space.

Concluding remarks and future developments. This last finding suggests that in the adiabatic limit our approaches, that are expected to capture local properties of the system, are not quite reliable. In fact, our analysis of the weak-coupling perturbative corrections to the effective mass in the $U = 0$ case showed that both methods discussed in the present work fail in describing quasiparticle properties as $\gamma \to 0$. We interpreted this failure in terms of an unaccurate description of phonon contribution to electron self-energy as long as e-e interaction is neglected; then it is reasonable to think that a residual interaction between electrons and phonons becomes relevant as γ is reduced and large non-local electron-lattice correlations come into play. According to GPW formulation, such a drawback is most relevant in the weakly-correlated half-filling regime, when phonon and electron degrees of freedom are tightly entangled, while it is expected to affect our mean-field description of quasiparticle but not of ground-state properties in the infinite$-U$ limit, where our variational equations for electron probability distribution and phonon wavefunctions are actually decoupled. Due to the equivalence between GPW and VLF at weak-coupling, one can try to exploit the slave-boson machinery in order to improve the mean-field picture, and hopefully to capture or at least to understand the nature of the residual e-ph interaction.

At last it can be tempting to apply our methods to the symmetry-broken phases of the Hubbard-Holstein model, due to their relevance in the comprehension of real physical systems such as the superconducting cuprates. Some preliminary study has been carried out for the antiferromagnetic phase at half filling (cfr. Appendix B), where we found that in the limit of large U the e-ph interaction is less efficient than in the paramagnetic phase, being $f \sim \omega_0/U$. This finding is in contrast with available results for the interplay of e-ph coupling and antiferromagnetic correlations, which show that the phonon-induced mass renormalization is larger in the antiferromagnetic rather than in the paramagnetic phase[37, 63, 117]. The origin of our wrong prediction lies in the inadequacy of static mean field to describe nonlocal correlations (in this case between spins), that are at least partially captured in dynamical mean-field theory through quantum fluctuations[118]. On the other hand, the possibility to include superconductivity in a Gutzwiller-correlated BCS wavefunction has been investigated By Bünemann *et al.* on the attractive Hubbard model[119], leading to some promising improvement with respect to standard BCS theory. On the light of physical insight provided by our Gutzwiller phonon wavefunction, we believe that inclusion of electron-phonon coupling in such Gutzwiller-correlated BCS framework is worthwhile and may deserve future investigations.

To conclude with, we investigated in a mean-field framework the paramagnetic phase

of the Hubbard-Holstein model in a wide region of parameter space. We found that both variational LFT and GPW are not reliable in the adiabatic limit of the weakly-correlated system; this failure is in our opinion associated to the poor description of nonlocal electron-lattice correlations provided by our static mean-field framework. Nonetheless our approaches proved to capture correctly the effect of e-ph coupling in the presence of sizeable electronic correlation, as main physical properties of the system are local in nature. In particular a harmonic ansatz is sufficient at very weak and at strong coupling, where the effect of e-ph coupling in the presence of sizeable U is substantially a rigid displacement of the lattice sites, whereas an accurate treatment of phonon degrees of freedom is required at intermediate e-ph couplings and in the adiabatic regime. The set of coupled Schrödinger-like equations for phonon wavefunctions provided by GPW method accomplishes this task, giving access to many phonon properties (not provided by variational LFT) that are necessary to characterize properly polaron formation.

Appendix A

Variational unitary transformations on boson representation

We start from the Kotliar-Ruckenstein slave-boson representation of the Hubbard-Holstein model with phonons coupled to charge density fluctuations, whose Hamiltonian reads:

$$\begin{aligned} H_{SB} &= -t \sum_{<i,j>,\sigma} z^{\dagger}_{i\sigma} z_{j\sigma} c^{\dagger}_{i\sigma} c_{j\sigma} + U \sum_i d^{\dagger}_i d_i + \omega_0 \sum_i a^{\dagger}_i a_i \\ &\quad + g \sum_i (n_i - \langle n_i \rangle)(a^{\dagger}_i + a_i) - H_c \end{aligned} \tag{A.1}$$

where $H_c = \sum_i \lambda^{(1)}_i (1 - d^{\dagger}_i d_i - e^{\dagger}_i e_i - \sum_\sigma p^{\dagger}_{i\sigma} p_{i\sigma}) + \sum_{i\sigma} \lambda^{(2)}_{i\sigma} (d^{\dagger}_i d_i + p^{\dagger}_{i\sigma} p_{i\sigma} - c^{\dagger}_{i\sigma} c_{i\sigma})$ is introuduced to enforce the constraints $c^{\dagger}_{i\sigma} c_{i\sigma} = p^{\dagger}_{i\sigma} p_{i\sigma} + d^{\dagger}_i d_i \ \ \forall i, \sigma; 1 \ = \sum_\sigma p^{\dagger}_{i\sigma} p_{i\sigma} + d^{\dagger}_i d_i + e^{\dagger}_i e_i \ \ \forall i$ that guarantee the equivalence with the original Hamiltonian Eq. (3.1). The Hubbard term appears to couple only with the d_i boson and the effect of correlation on the kinetic term is captured by the $z_{i\sigma}$ operators which are defined, following Ref. [80, 82], as

$$z^{\dagger}_{i\sigma} = \frac{\left(p^{\dagger}_{i\sigma} e_i + d^{\dagger}_i p_{i\bar{\sigma}} \right)}{\sqrt{1 - d^{\dagger}_i d_i - p^{\dagger}_{i\sigma} p_{i\sigma}} \sqrt{1 - e^{\dagger}_i e_i - p^{\dagger}_{i\bar{\sigma}} p_{i\bar{\sigma}}}}. \tag{A.2}$$

As far as the constraints are exactly satisfied at each site and any time, the Hamiltonian (A.1) is strictly equivalent to the original Hubbard-Holstein model: in fact it is simply the projection representation of Eq.(3.1) on the empty, doubly and singly σ occupied states. One can observe that Holstein e-ph coupling occurs between local displacements and local charge density, and that different phononic configurations are in general expected for different values of electronic occupation. This fact suggests us to perform a unitary transformation $U = e^S$ within the same spirit of the variational Lang-Firsov approach [114, 61], but operating on slave bosons directly instead of fermions, namely:

$$S = \alpha \sum_i \left[f^{(0)}_i e^{\dagger}_i e_i + \sum_\sigma f^{(1)}_{i\sigma} p^{\dagger}_{i\sigma} p_{i\sigma} + f^{(2)}_i d^{\dagger}_i d_i \right] (a_i - a^{\dagger}_i) \tag{A.3}$$

where $f_i^{(0)}, f_{i\sigma}^{(1)}, f_i^{(2)}$ are variational parameters to be determined. In order to get rid of phononic degrees of freedom, we adopt the standard Holstein approximation and average $e^{-S}H_{SB}e^{S}$ over the vacuum state of the transformed phonons. The following effective model is obtained:

$$H_{eff} = -t \sum_{<i,j>,\sigma} \tilde{z}_{i\sigma}^{\dagger} \tilde{z}_{j\sigma} c_{i\sigma}^{\dagger} c_{j\sigma} + U \sum_i d_i^{\dagger} d_i - H_c + H_I \tag{A.4}$$

where H_c remains the same, and

$$\begin{aligned} H_I &= \alpha^2 \omega_0 \sum_i \Big[\Big((f_i^{(0)})^2 + 2\langle n_i \rangle f_i^{(0)} \Big) e_i^{\dagger} e_i + \Big((f_i^{(2)})^2 + 2\langle n_i \rangle f_i^{(2)} - 4 f_i^{(2)} \Big) d_i^{\dagger} d_i + \\ & \sum_{\sigma} \Big((f_{i\sigma}^{(1)})^2 + 2\langle n_i \rangle f_{i\sigma}^{(1)} - 2 f_{i\sigma}^{(1)} \Big) p_{i\sigma}^{\dagger} p_{i\sigma} \Big] \end{aligned}$$

takes into account the effect of e-ph coupling on electronic properties. The kinetic term changes accordingly, and Eq. (A.2) becomes

$$\tilde{z}_{i\sigma}^{\dagger} = \frac{p_{i\sigma}^{\dagger} e_i e^{-\frac{\alpha^2}{2}(f_i^{(0)} - f_{i\sigma}^{(1)})^2} + d_i^{\dagger} p_{i\bar{\sigma}} e^{-\frac{\alpha^2}{2}(f_{i\bar{\sigma}}^{(1)} - f_i^{(2)})^2}}{\sqrt{1 - d_i^{\dagger} d_i - p_{i\sigma}^{\dagger} p_{i\sigma}} \sqrt{1 - e_i^{\dagger} e_i - p_{i\bar{\sigma}}^{\dagger} p_{i\bar{\sigma}}}}. \tag{A.5}$$

The mean-field solution at a given value of the density n is obtained by assuming translation invariance (i.e. $f_i^{(0)} = f_0$, $f_{i\sigma}^{(1)} = f_{1\sigma}$, $f_i^{(2)} = f_2$) and taking the saddle-point value for the Bose fields; for the paramagnetic homogeneous phase this corresponds to take $\langle e_i \rangle = e_0$, $\langle p_{i\sigma} \rangle = p_0$ and $\langle d_i \rangle = d_0$, but one can choose other phases, such as the staggered antiferromagnetic or the charge ordered one, by means of a proper choice of the saddle-point values of the bosonic fields and without any further approximation. The ground state energy reads:

$$\begin{aligned} \frac{E_0}{N} &= -|\varepsilon| \frac{4}{n(2-n)} |S|^2 + U d_0^2 - \lambda^{(1)} (1 - d_0^2 - e_0^2 - 2p_0^2) - \lambda^{(2)} (2d_0^2 + 2p_0^2 - n) \\ & + \alpha^2 \omega_0 \left[(f_0^2 + 2nf_0) e_0^2 + (f_1^2 - 2f_1 + 2nf_1) 2p_0^2 + (f_2^2 - 4f_2 + 2nf_2) d_0^2 \right] \end{aligned} \tag{A.6}$$

with

$$|S| = p_0 e_0 e^{-\frac{\alpha^2}{2}(f_0 - f_1)^2} + p_0 d_0 e^{-\frac{\alpha^2}{2}(f_1 - f_2)^2}. \tag{A.7}$$

We have now to minimize with respect to boson fields, Lagrange multipliers and variational phononic parameters. Minimization with respect to the slave-boson fields gives:

$$U + \lambda^{(1)} - 2\lambda^{(2)} + \alpha^2 \omega_0 \left(f_2^2 - 4f_2 + 2nf_2 \right) = \frac{4|\varepsilon|}{n(2-n)} |S| \left[\frac{2}{2-n} |S| + \frac{p_0}{d_0} e^{-\frac{\alpha^2}{2}(f_2 - f_1)^2} \right] \tag{A.8a}$$

$$\lambda^{(1)} + \alpha^2 \omega_0 \left(f_0^2 + 2nf_0 \right) = \frac{4|\varepsilon|}{n(2-n)} |S| \left[\frac{2}{n} |S| + \frac{p_0}{e_0} e^{-\frac{\alpha^2}{2}(f_0 - f_1)^2} \right] \tag{A.8b}$$

$$2\lambda^{(1)} - 2\lambda^{(2)} + 2\alpha^2 \omega_0 \left(f_1^2 - 2f_1 + 2nf_1 \right) = \frac{4|\varepsilon|}{n(2-n)} |S|^2 \left[\frac{4}{n(2-n)} + \frac{1}{p_0^2} \right] \tag{A.8c}$$

while that with respect to the Lagrange multipliers reproduces the constraints. Finally minimization with respect to the f_i gives

$$f_0\left[1-\frac{|\varepsilon|}{\omega_0}\frac{4}{n(2-n)}|S|\frac{p_0}{e_0}\left(\frac{f_1}{f_0}-1\right)e^{-\frac{\alpha^2}{2}(f_0-f_1)^2}\right]=-n \tag{A.9a}$$

$$f_1\left\{1-\frac{|\varepsilon|}{\omega_0}\frac{4}{n(2-n)}|S|\left[\frac{e_0}{2p_0}\left(\frac{f_0}{f_1}-1\right)e^{-\frac{\alpha^2}{2}(f_0-f_1)^2}+\frac{d_0}{2p_0}\left(\frac{f_2}{f_1}-1\right)e^{-\frac{\alpha^2}{2}(f_1-f_2)^2}\right]\right\}=1-n \tag{A.9b}$$

$$f_2\left[1-\frac{|\varepsilon|}{\omega_0}\frac{4}{n(2-n)}|S|\frac{p_0}{d_0}\left(\frac{f_1}{f_2}-1\right)e^{-\frac{\alpha^2}{2}(f_1-f_2)^2}\right]=2-n. \tag{A.9c}$$

By manipulating the above equations one easily notices that they can be reduced to a two-equation system. Introducing $F_{01}=f_0-f_1, F_{21}=f_2-f_1$ one gets:

$$F_{01}\left[1+\frac{|\varepsilon|}{\omega_0}\frac{4}{n(2-n)}|S|\left(\frac{p_0}{e_0}+\frac{e_0}{2p_0}\right)e^{-\frac{\alpha^2}{2}F_{01}^2}\right]+F_{21}\frac{|\varepsilon|}{\omega_0}\frac{4}{n(2-n)}|S|\frac{d_0}{2p_0}e^{-\frac{\alpha^2}{2}F_{21}^2} = -1 \tag{A.10}$$

$$F_{21}\left[1+\frac{|\varepsilon|}{\omega_0}\frac{4}{n(2-n)}|S|\left(\frac{p_0}{d_0}+\frac{d_0}{2p_0}\right)e^{-\frac{\alpha^2}{2}F_{21}^2}\right]+F_{01}\frac{|\varepsilon|}{\omega_0}\frac{4}{n(2-n)}|S|\frac{e_0}{2p_0}e^{-\frac{\alpha^2}{2}F_{01}^2} = 1 \tag{A.11}$$

These are coupled self-consistent equations that allow to determine completely the values of f_i, through Eq. (A.9b), that can be rewritten as:

$$f_1=1-n+\frac{|\varepsilon|}{\omega_0}\frac{4}{n(2-n)}|S|\left[\frac{e_0}{2p_0}F_{01}e^{-\frac{\alpha^2}{2}F_{01}^2}+\frac{d_0}{2p_0}F_{21}e^{-\frac{\alpha^2}{2}F_{21}^2}\right]. \tag{A.12}$$

Eventually, one can exploit the constraints and introduce the standard notations $x=e_0+d_0$, $n=1-\delta$, which allow to express the mean-field value of the bosonic fields as follows:

$$d_0^2 = \frac{(x^2-\delta)^2}{4x^2} \tag{A.13}$$

$$e_0^2 = \frac{(x^2+\delta)^2}{4x^2} \tag{A.14}$$

$$p_0^2 = \frac{2x^2-x^4-\delta^2}{4x^2}. \tag{A.15}$$

where x^2 has to satisfy the following equation, coming from the combination of Eqs. (A.8a), (A.8b), (A.8c):

$$U+\alpha^2\omega_0\Big(F_{01}^2+F_{21}^2+2(n+f_1)(F_{21}+F_{01})-4F_{21}\Big)=\frac{2|\varepsilon|}{1-\delta^2}\left(e^{-\frac{\alpha^2}{2}F_{01}^2}+e^{-\frac{\alpha^2}{2}F_{21}^2}\right)^2$$
$$\left\{\frac{x^4}{x^4-\delta^2}(1-x^2)-\delta\tanh\frac{\alpha^2(F_{21}^2-F_{01}^2)}{4}\left[1+\frac{\delta}{x^2}\frac{x^2-\delta^2}{x^4-\delta^2}\tanh\frac{\alpha^2(F_{21}^2-F_{01}^2)}{4}\right]\right\}. \tag{A.16}$$

Eventually the complete mean-field analysis for the paramagnetic case can be carried out by considering the three mean-field equations (A.10), (A.11) and (A.16), implemented by Eq.

(A.12). In general they cannot be solved analytical and need to be handled numerically. They suggest that one needs at least two independent variational parameters in order to include properly phonon effects in a slave-boson framework, in such a way that exploitation of the capability of the slave operators to account for local charge states and for the relevant hopping processes is allowed. Within this formulation F_{01}, F_{12} represent a measure of the overlap between displaced harmonic oscillators associated to the different charge states involved in electronic hopping, meaning large overlap when they are small (electron mobility weakly affected by e-ph coupling) and small overlap when they are approximatively equal to one, with strong exponential suppression of the electron kinetic energy. On the other hand f_0, f_1, f_2 measure the amount of displacement of local phonons.

However in the highly symmetric half-filling regime it can be shown that only one variational parameters survives, measuring at the same time the displacement of the phonon and the amount of renormalization of the electronic kinetic energy. As a consequence, even if the properties of the small doping regime are likely to be descibed by the variational LFT of chapter 3 in an accurate enough manner, generalization to any finite value of doping should be considered in the context here defined. We conclude this appendix by showing the connection of the present mean-field equations with that derived in the half-filling and the doped large$-U$ limit by means of the variational LFT discussed in chapter 3.

Half-filling mean-field equations

Exploiting the particle-hole simmetry of the model for zero doping, one can put $e_0 = d_0$ inEqs.(A.10), (A.11) and find that they coincide provided $F_{01} = -F_{21}$; furthermore, replacing this result in Eq.(A.12) it is readily seen that f_1 must be zero, hence $f_2 = -f_0$. We can identify $f = f_2 = -f_0$ and express the ground-state energy as:

$$\frac{E_0}{N} = -|\varepsilon_0| q\, e^{-\alpha^2 f^2} + d_0^2 \Big[U + 2\alpha^2 \omega_0 (f^2 - 2f) \Big] \tag{A.17}$$

where $q = z_0^2 = 8d_0^2(1 - 2d_0^2)$ is the reduction of the kinetic energy due to the electronic correlation. The variational LF mean-field equations previously discussed in chapter 3 are therefore easily recovered.

Infinite$-U$ mean-field equations

In the limit of infinitly large Hubbard repulsion, it is known that one has to restore electron mobility by doping the system and introducing some vacancies ($\delta > 0$). It is convenient then to recast Eqs.(A.10), (A.11) as follows:

$$\begin{aligned}
-(1-\delta) &= -d_0^2 F_{21} + F_{01} \left[1 - e_0^2 + \frac{|\varepsilon|}{\omega_0} \frac{4p_0^2}{1-\delta^2} e^{-\alpha^2 F_{01}^2} \left(1 + \frac{d_0}{e_0} e^{-\frac{\alpha^2}{2}(F_{21}^2 - F_{01}^2)} \right) \right], \\
-(1+\delta) &= e_0^2 F_{01} - F_{21} \left[1 - d_0^2 + \frac{|\varepsilon|}{\omega_0} \frac{4p_0^2}{1-\delta^2} e^{-\alpha^2 F_{21}^2} \left(1 + \frac{e_0}{d_0} e^{\frac{\alpha^2}{2}(F_{21}^2 - F_{01}^2)} \right) \right].
\end{aligned}$$

Taking the limit of vanishing δ and plugging $d_0^2 = 0, e_0^2 = \delta$ and $p^2 = (1-\delta)/2$ in these equations we obtain for F_{01}:

$$F_{01} = -\frac{1}{1 + \frac{2|\varepsilon_0|}{\omega_0} e^{-\alpha^2 F_{01}^2}} \tag{A.18}$$

while F_{21} must be zero. Alternatively one can put $d_0 = 0$ from the outset in the energy Eq. (A.6), obtaining at leading order in δ

$$\frac{E_0}{N} \approx -\delta \left[2|\varepsilon_0| e^{-\alpha^2 F_{01}^2} - \alpha^2 \omega_0 (F_{01}^2 + 2F_{01}) \right] \tag{A.19}$$

and obtain the variational LFT self-consistency condition upon substitution $f = -F_{01}$.

Appendix B

Antiferromagnetic solution at half-filling

We discuss here the possibility to include antiferromagnetic ordering in the Hubbard-Holstein model by means of a variational treatment of the phononic degrees of freedom. We start from the generalization of the variational slave-boson approach described in appendix A. The antiferromagnetic phase can be implemented in this approach introducing a staggered magnetization $m(-1)^{\mathbf{R}} = n_{\mathbf{R}\uparrow} - n_{\mathbf{R}\downarrow}$ and assuming that $p_{\mathbf{R}_A\uparrow} = p_{\mathbf{R}_B\downarrow} = p_+$ and $p_{\mathbf{R}_B\uparrow} = p_{\mathbf{R}_A\downarrow} = p_-$, where A, B label the two sublattices of the bipartite lattice. Similarly one can label the other parameters associated with these operators (i.e. $\lambda_\sigma^{(2)}$ and $f_\sigma^{(1)}$). After a standard Bogolyubov transformation, the ground-state energy at zero temperature reads:

$$\begin{aligned}\frac{E_0}{N} &= \frac{2}{N}\sum_{k,\eta=\pm}\theta(-E_k^\eta)\eta\sqrt{(q\varepsilon_k)^2+h^2} + Ud_0^2 - hm + \alpha^2\omega_0\Big[(f_0^2+2nf_0)\,e_0^2 + \\ &\quad (f_-^2-2f_-+2nf_-)p_-^2 + (f_+^2-2f_++2nf_+)p_+^2 + (f_2^2-4f_2+2nf_2)d_0^2\Big] \\ &\quad +\lambda^{II}(n-2d_0^2-p_-^2-p_+^2) + \lambda^{(1)}(e_0^2+d_0^2+p_-^2+p_+^2-1) \end{aligned} \tag{B.1}$$

where $h = [\lambda_+^{(2)} - \lambda_-^{(2)}]/2$, $\lambda^{II} = [\lambda_+^{(2)} + \lambda_-^{(2)}]/2$, $m = p_+^2 - p_-^2$, ε_k is the dispersion of free electrons and

$$\begin{aligned} E_k^\eta &= \lambda^{II} - \mu + \eta\sqrt{(q\varepsilon_k)^2+h^2} \\ q &= G\left(p_+e_0e^{-\frac{\alpha^2}{2}(f_0-f_+)^2} + p_-d_0e^{-\frac{\alpha^2}{2}(f_2-f_-)^2}\right)\left(p_-e_0e^{-\frac{\alpha^2}{2}(f_0-f_-)^2} + p_+d_0e^{-\frac{\alpha^2}{2}(f_2-f_+)^2}\right) \\ G &= \frac{4}{\sqrt{[(1+\delta)^2-m^2][(1-\delta)^2-m^2]}} \end{aligned}$$

For the sake of simplicity we analyze here just the half-filling case. This allows us to consider only the lower (full) subband E_k^-, which is relevant for the kinetic term, and to obtain from

the minimization with respect to $\lambda^{(1)}, \lambda^{II}$:

$$e_0^2 = d_0^2 = \frac{x^2}{4} \tag{B.2}$$

$$p_\pm^2 = \frac{1}{2}\left(1 - \frac{x^2}{2} \pm m\right) \tag{B.3}$$

From the minimization with respect to the phononic variational parameters one finds four equations, but it is easy to demonstrate, after some tedious calculation, that in analogy with the paramagnetic case $f_+ = f_- = 0$ and $f_2 = -f_0 = f$. We can consider then only one equation:

$$f = \frac{1}{1 + \frac{2|K|}{\omega_0}\frac{qp^2}{1-m^2}e^{-\alpha^2 f^2}} \tag{B.4}$$

where $p = p_- + p_+$, $q = 4d_0^2 p^2 e^{-\alpha^2 f^2}/(1-m^2)$ and $|K| = \frac{2}{N}\sum_k \frac{\varepsilon_k^2}{\sqrt{(q\varepsilon_k)^2 + h^2}}$.

Togheter with Eq. (B.4) one obtains three mean-field equations, i.e.

$$m = -h\frac{2}{N}\sum_k \frac{1}{\sqrt{(q\varepsilon_k)^2 + h^2}} \tag{B.5}$$

$$h = 4d_0^2 q\frac{|K|}{2}\frac{m}{1-m^2}e^{-\alpha^2 f^2}\left[\frac{1}{p_+p_-} - \frac{4p^2}{1-m^2}\right] \tag{B.6}$$

$$U = -2\alpha^2\omega_0(f^2 - 2f) + 4p^2 q|K|\frac{1}{1-m^2}e^{-\alpha^2 f^2}\left[1 - \frac{d_0^2}{p_+p_-}\right] \tag{B.7}$$

Let's consider now the large-U limit. By assuming that $h \propto U$ one can expand $|K|$ and find $m \approx -1 + \left(\frac{q}{h}\right)^2|\varepsilon^2|$, where $|\varepsilon^2| = \frac{1}{N}\sum_k \varepsilon_k^2$; provided that the dominant energy scale is determined by U, it is easy to find $U + 2\alpha^2\omega_0(f^2 - 2f) = 2h$ and $q = e^{-\alpha^2 f^2}$, hence:

$$f \approx \frac{1}{1 + \frac{U}{\omega_0}} \tag{B.8}$$

that means that the present approach predicts a less effective e-ph coupling in the antiferromagnetic rather than in the paramagnetic regime. On the other hand, if one considers the opposite limit of very small U and neglects corrections of order m^2, the mean-field equation for f reduces to the paramagnetic one (Eq. (3.22) in the text).

Bibliography

[1] N. W. Ashcroft and N. D. Mermin, *Solid State Physics*, ed. by Cornell University (1976).

[2] L. N. Cooper, Phys. Rev. **104**, 1189 (1956).

[3] J. G. Bednorz and K. A. Müller, Z. Phys. B **64**, 189 (1986).

[4] C. Y. Chen, R. J. Birgeneau, M. A. Kastner, N. W. Preyer and T. Thio, Phys. Rev. B **43**, 392 (1991).

[5] J. G. Bednorz and K. A. Müller, Rev. Mod. Phys. **60**, 585 (1988).

[6] B. K. Chakraverty, J. Phys. Lett. **40**, L99 (1979).

[7] X. J. Zhou, T. Cuk, T. Deveraux, N. Nagaosa and Z.-X. Shen, cond-mat/0604284 (2006) and references therein.

[8] E. Dagotto, T. Hotta and A. Moreo, Phys. Rep. **344**, 1 (2001).

[9] M. Imada, A. Fujimori and Y. Tokura, Rev. Mod. Phys. **70**, 1039 (1998).

[10] H. W. Kroto, J. R.Heath, S. C. O'Brien, R. F. Curl and R. E. Smalley, Nature **318**, 162 (1985).

[11] O. Gunnarson, Rev. Mod. Phys. **69**, 575 (1997) and references therein.

[12] A. B. Migdal, Sov. Phys. JETP **7**, 996 (1958).

[13] M. Capone, M. Fabrizio, C. Castellani and E. Tosatti, Science **296**, 2364 (2002).

[14] J. von Delft and D. C. Ralph, Phys. Rep. **345**, 61 (2001).

[15] J. Park *et al.*, Nature (London) **417**, 722 (2002); W. Liang *et al.*, Nature (London) **417**, 725 (2002); S. Kubatkin *et al.*, Nature (London) **425**, 698 (2003); P. S. Cornaglia. D. R. Grempel and H. Ness, Phys. Rev. B **71**, 075320 (2005).

[16] C. E. Gough *et al.*, Nature **326**, 855 (1987).

[17] C. C. Tsuei and J. R. Kirtley,, Rev. Mod. Phys. **72**, 969 (2000) and references therein. *(da controllare)*

[18] For a review, see T. Timusk aand B. Statt, Rep. Prog. Phys. **62**, 61 (1999).

[19] E. Dagotto, Rev. Mod. Phys. **66**, 763 (1994).

[20] S. Uchida, T. Ido, H. Takagi, T. Arima, Y. Tokura and S. Tajima, Phys. Rev. B **43**, 7942 (1991).

[21] J. Hubbard, Proc. R. Soc. London A **276**, 238 (1963); M. C. Gutzwiller, Phys. Rev. Lett. **10** 159 (1963); J. Kanamori, Prog. Theor. Phys. **30** 275 (1963).

[22] A.-M.S. Tremblay, B. Kyung and D. Sénéchal, Fizika Nizkikh Temperatur (Low Temperature Physics) **32**, 561 (2006).

[23] M. L. Cohen and P. W. Anderson, *Superconductivity in d and f metals*, AIP Conference Proceedings (ed. D. H. Douglass) New York, p17 (1972).

[24] B. Batlogg *et al.*, Phys. Rev. Lett. **58** 2333 (1987).

[25] M. Gurvitch and A. T. Fiory, Phys. Rev. Lett. **59**, 1337 (1987); S. Martin *et al.*, Phys. Rev. B **41**, 846 (1990).

[26] G. M. Zhao, K. Conder, H. Keller and K. A. Müller, J. Phys: Condens. Matter **10**, 9055 (1998); T. Schneider and H. Keller, Phys. Rev. Lett. **86**, 4899 (2001).

[27] R. Khasanov *te al.*, J. Phys: Condens. Matter **15**, L17 (2003); R. Khasanov *te al.*, Phys. Rev. Lett. **92**, 057602-1 (2004).

[28] J. Bardeen, L. N. Cooper and J. R. Schrieffer, Phys. Rev. B **108**, 1175 (1957).

[29] For a recent review, see L. Pintsschovius, Phys. Stat. Sol.(b) **242**, 30 (2005); see also T. Egami and S. J. L. Billinge, in *Physical Properties of High Temperature Supercondutors V*, ed. D. Ginsberg (World Scientific), p265 (1996).

[30] E. Altendorf *et al.*, Phys. Rev. B **47**, 8140 (1990); S. Sugai *et al.*, Phys. Rev. B **68**, 184504 (2003).

[31] A. Lanzara *et al.*, Nature **412**, 510 (2001).

[32] G.-H. Gweon *et al.*, Nature **430**, 187 (2004).

[33] X. J. Zhou *et al.*, Nature **423**, 398 (2003).

[34] F. C. Zhang and T. M. Rice, Phys. Rev. B **37**, 3759 (1988).

[35] T. Tohyama and S. Maekawa, Supercond. Sci. Technol. **13**, R17 (2000).

[36] K. M. Shen *et al*, Phys. Rev. Lett. **93**, 267002 (2004).

[37] A. S. Mishchenko and N. Nagaosa, Phys. Rev. Lett. **93**, 036402 (2004).

[38] O. Rösch and O. Gunnarson, Eur. Phys. J. B **43**, 11 (2005).

[39] A. Georges, G. Kotliar, W. Krauth and M. J. Rozenberg, Rev. Mod. Phys. **68**, 13 (1996).

[40] E. Jeckelmann and H. Fehske, in *Proceedings of the International School of Physics 'E. Fermi', course CLXI*, ed. G. Iadonisi, J. Ranninger and G. De Filippis, p247 (2006).

[41] R. Peierls, Proc. Phys. Soc. London A**49**, 72 (1937).

[42] N. F. Mott, Proc. Phys. Soc. London A**49**, 416 (1949).

[43] J. Ranninger, in *Proceedings of the International School of Physics 'E. Fermi', course CLXI*, ed. G. Iadonisi, J. Ranninger and G. De Filippis, p1 (2006).

[44] T. Holstein, Ann. Phys. **8**, 325 (1959);**8**, 343 (1959)

[45] L. D. Landau, Phys. Z. Sowjetunion **3**, 644 (1933).

[46] M. Grilli and C. Castellani, Phys. Rev. B **50**, 16880 (1994).

[47] M. L. Kulić and R. Zehyer, Phys. Rev. B **49**, 4395 (1994); R. Zehyer and M. L. Kulić, Phys. Rev. B **53**, 2850 (1996).

[48] E. Cappelluti, B. Cerruti and L. Pietronero, Phys. Rev. B **69**, 161101(R) (2004).

[49] E. Koch and R. Zehyer, Phys. Rev. B **70** 094510 (2004).

[50] G. Aprea, C. Di Castro, M. Grilli and J. Lorenzana, cond-mat/0601374 (2006).

[51] Z. B. Huang, W. Hanke, E. Arrigoni and D. J. Scalapino, Phys. Rev. B **68**, 220507(R) (2003).

[52] F. Becca, M. Tarquini, M. Grilli and C. Di Castro, Phys. Rev. B **54**, 12443 (1996).

[53] V. Cataudella, G. De Filippis, G. Iadonisi, A. Bianconi and N. L. Saini, Int. J. Mod. Phys. **14**, 3398 (2000).

[54] M. Capone, G. Sangiovanni, C. Castellani, C. Di Castro and M. Grilli, Phys. Rev. Lett. **92**, 106401 (2004).

[55] W. Koller, D. Meyer, Y, Ōno and A. C. Hewson, Europhys. Lett. **66**, 559 (2004).

[56] G. S. Jeon, T.-H. Park, J. H. Han, H. C. Lee and H.-Y. Choi, Phys. Rev. B **70**, 125114 (2004).

[57] G. Sangiovanni, M. Capone, C. Castellani and M. Grilli, Phys. Rev. Lett. **94**, 026401 (2005).

[58] W. Koller, D. Meyer and A. C. Hewson, Phys. Rev. B **70**, 155103 (2004).

[59] W. Koller, A. C. Hewson and D. M. Edwards, Phys. Rev. Lett. **95**, 256401 (2005).

[60] G. Sangiovanni, M. Capone and C. Castellani, Phys. Rev. B **73**, 165123 (2006).

[61] C. A. Perroni, V. Cataudella, G. De Filippis and V. M. Ramaglia, Phys. Rev. B **71**, 113107 (2005).

[62] S. Fratini and S. Ciuchi, Phys. Rev. B **72**, 235107 (2005).

[63] G. Sangiovanni, O. Gunnarson, E. Koch, C. Castellani and M. Capone, Phys. Rev. Lett. **97**, 046404 (2006).

[64] J. E. Hirsch, Phys. Rev. B **31**, 4403 (1985).

[65] J. C. Slater, Phys. Rev. **82**, 538 (1951).

[66] E. Lieb and F. Y. Wu, Phys. Rev. Lett. **20**, 1445 (1967).

[67] W. F. Brinkman and T. M. Rice, Phys. Rev. B **2**, 4302 (1970).

[68] M. C. Gutzwiller, Phys. Rev. Lett. **10**, 159 (1963); Phys. Rev. **134**, A923 (1964); **137**, A1726 (1965).

[69] T. Ogawa, K. Kanda and T. Matsubara, Prog. Theor. Phys. **53**, 614 (1975).

[70] D. Vollhardt, Rev. Mod. Phys. **56**, 99 (1984).

[71] W. Metzner and D. Vollhardt, Phys. Rev. Lett. **59**, 121 (1987).

[72] F. Gebhard and D. Vollhardt, Phys. Rev. Lett. **59**, 1472 (1987); Phys. Rev. B **38**, 6911 (1988).

[73] W. Metzner and D. Vollhardt, Phys. Rev. Lett. **62**, 324 (1989); W. Metzner, Z. Phys. B **77**, 253 (1989).

[74] J. Bünemann, W. Weber and F. Gebhard, Phys. Rev. B **57**, 6896 (1998).

[75] C. Attaccalite and M. Fabrizio, Phys. Rev. B **68**, 155117 (2003).

[76] F. Gebhard, Phys. Rev. B **41**, 9452 (1990).

[77] S. E. Barnes, J. Phys. F **6**, 1375 (1976).

[78] N. Read and D. News, J. Phys. C **16**, 3273 (1983).

[79] P. Coleman, Phys. Rev. B **29**, 3035 (1984).

[80] G. Kotliar and A. E. Ruckenstein, Phys. Rev. Lett. **57**, 1362 (1986).

[81] Z. Zou and P. W. Anderson, Phys. Rev. B **37**, 627 (1988).

[82] M. Lavagna, Phys. Rev. B **41**, 142 (1990).

[83] R. Raimondi and C. Castellani, Phys. Rev. B **48**, 11453 (1993).

[84] R. Micnas, J. Ranninger and S. Robaszkiewicz, Rev. Mod. Phys. **62**, 113 (1990).

[85] A. Toschi, P. Barone, M. Capone and C. Castellani, New J. of Phys. **7**, 7 (2005).

[86] S. Ciuchi, F. de Pasquale, S. Fratini and D. Feinberg, Phys .Rev. B **56**, 4494 (1997).

[87] S. Engelsberg and J. R. Schreffer, Phys. Rev. **131**, 993 (1963).

[88] J. Ranninger and U. Thibblin, Phys. Rev. B **45**, 7730 (1992).

[89] P. B. Allen and R. C. Dynes, Phys. Rev. B **12**, 905 (1975).

[90] S. Robaszkiewicz, R. Micnas and K. A. Chao, Phys. Rev. B **23**, 1447 (1981).

[91] J. K. Freeriks, M. Jarrell and D. J. Scalapino, Phys. Rev. B **48**, 6302 (1993).

[92] A. J. Millis, R. Mueller and B. I. Shraiman, Phys. Rev. B **54**, 5389 (1996).

[93] D. Meyer, A. Hewson and R. Bulla, Phys. Rev. Lett. **89**, 196401 (2002).

[94] M. Capone and S. Ciuchi, Phys. Rev. Lett. **91**, 186405 (2003).

[95] M. Capone, P. Carta and S. Ciuchi, Phys. Rev. B **74**, 045106 (2006).

[96] S. Ciuchi, G. Sangiovanni and M. Capone, Phys. Rev. B **73**, 245114 (2006).

[97] A. A. Abrikosov, L. P. Gorkov and I. E. Dzyaloshinski, *Methods of Quantum Field Theory in Statistical Physics* (Dover Publications, 1963).

[98] A. S. Alexandrov, V. V. Kabanov and D. K. Ray, Phys. Rev. b **49**, 9915 (1994).

[99] P. Benedetti and R. Zeyher, Phys. Rev. B **58**, 14320 (1998).

[100] J. P. Hague and N. d'Ambrumenil, cond-mat/0106355 (2001).

[101] M. Capone, W. Stephan and M. Grilli, Phys. Rev B **56**, 4484 (1997).

[102] I. G. Lang and Yu. A. Firsov, Zh. Eksp. Teor. Fiz. **43**, 1843 (1962) [Sov. Phys. JETP **16**, 1301 (1963)].

[103] G. D. Mahan, *Many-Particle Physics* (Plenum Press, New York, 1990).

[104] A. S. Alexandrov and J. Ranninger, Phys. Rev. B **45**, 13109 (1992).

[105] A. C. Hewson and D. M. Newns, J. Phis. C: Solid State Phys. **12**, 1665 (1979); **13**, 4477 (1980).

[106] D. Ihle and H. Fehske, J. Phys. A: Math. Gen. **28**, L275 (1995).

[107] V. Cataudella, G. De Filippis, G. Iadonisi, A. Bianconi and N. L. Saini, Int. J. Mod. Phys. B **14**, 3398 (2001).

[108] V. Cataudella, G. De Filippis, G. Iadonisi and C. A. Perroni , in *Proceedings of the International School of Physics 'E. Fermi', course CLXI*, ed. G. Iadonisi, J. Ranninger and G. De Filippis, p119 (2006).

[109] A. H. Romero, D. W. Brown and K. Lindenberg, J. Chem. Phys. **109**, 6540 (1998).

[110] D. Vollhardt, P. Wolfle and P. W. Anderson, Phys. Rev. B **35**, 6703 (1987).

[111] H. Löwen, Phys. Rev. B **37**, 8661 (1988).

[112] P. Paci, M. Capone, E. Cappelluti, S. Ciuchi, C. Grimaldi and L. Pietronero, Phys. Rev. Lett. **94**, 036406 (2005).

[113] G. Sangiovanni, private communication.

[114] P. Barone, R. Raimondi, M. Capone and C. Castellani, Phys. Rev. B **73**, 085120 (2006).

[115] P. Barone, R. Raimondi, M. Capone, C. Castellani and M. Fabrizio, cond-mat/0606717 (2006).

[116] M. Capone, private communication.

[117] A. Ramšak, P. Horsch, and P. Fulde, Phys. Rev. B **46**, R14305 (1992).

[118] G. Sangiovanni, A. Toschi, E. Koch, K. Held, M. Capone, C. Castellani, O. Gunnarson, S.-K. Mo, J. W. Allen, H.-D. Kim, A. Sekiyama, A. Kamasaki, S. Suga and P. Metcalf, Phys. Rev. B **73**, 205121 (2006).

[119] J. Bünemann, F. Gebhard, K. Radnòczi and P. Fazekas, J. Phys.: Condens. Matter **17**, 3807 (2005).